Theses and Dissertations--Chemistry   Chemistry

2021

Investigation of Multidrug Efflux Transporter AcrB in *Escherichia coli*: Assembly, Degradation and Dynamics

Prasangi Irosha Rajapaksha
University of Kentucky, prasangi88@gmail.com
Author ORCID Identifier:
https://orcid.org/0000-0002-3596-9386
Digital Object Identifier: https://doi.org/10.13023/etd.2021.275

Right click to open a feedback form in a new tab to let us know how this document benefits you.

Investigation of Multidrug Efflux Transporter AcrB in *Escherichia coli*: Assembly, Degradation and Dynamics

_____

DISSERTATION
_____

A dissertation submitted in partial fulfillment of the
requirements for the degree of Doctor of Philosophy in the
College of Arts and Sciences
at the University of Kentucky

By
Prasangi Irosha Rajapaksha
Lexington, Kentucky
Director: Dr. Yinan Wei, Professor of Chemistry
Lexington, Kentucky
2021

ABSTRACT OF DISSERTATION

Investigation of Multidrug Efflux Transporter AcrB in *Escherichia coli*: Assembly, Degradation and Dynamics

The Resistant Nodulation Division (RND) super family member, tripartite AcrA-AcrB-TolC efflux pump, is a major contributor in conferring multidrug-resistance in *Escherichia coli*. The structure of the pump complex, and drug translocation by functional rotation mechanism have been widely studied. Despite of all these data, the dynamics of the assembly process of the pump and AcrB during functional rotation in the process of drug efflux remains poorly understood. My thesis focuses on understanding the pump assembly process, dynamics of AcrB in functional rotation mechanism, and also investigate the mechanism of degradation of AcrB facilitated by a C-terminal ssrA tag.

In the first project, I studied the impact of relative flexibility at the inter-subunit interface utilizing disulfide bond crosslinking, minimum inhibitory concentration (MIC), and EtBr efflux assay. Six inter-subunit disulfide links were inserted into the periplasmic domain of AcrB using site-directed mutagenesis. Based on results from MIC measurement, the double Cys mutants tested led to equal or higher susceptibility to AcrB substrates compared to their corresponding single mutants. EtBr accumulation assays was conducted utilizing Dithiothreitol (DTT) as the reducing agent. In two cases, the activities of the double Cys-mutants were partially restored by DTT reduction, indicating the importance of relative inter-subunit movement in the respective location for function. In addition, crosslinking at the other 4 sites did not have such an effect.

In the second project, I tested the effect of over-expressing functionally defective pump components in wild-type *E. coli* cells to probe the pump assembly process. The incorporation of defective components is expected to reduce the complex's efflux efficiency and lead to the so-called "dominant negative" effect. The study examined two groups of mutants defective in different aspects and found that none of them demonstrated the expected dominant-negative effect, even at concentrations many folds higher than their genomic counterpart. Based on the data, the assembly of the AcrAB-TolC complex appears to have a proof-read mechanism that effectively eliminated the formation of the futile pump complex.

Moreover, I utilized a novel tool- transposons library creation in studying the possible other proteases that contribute to the degradation of the AcrB-ssrA. Using the next-generation sequencing, I identified the already known *clpX* gene, and MIC and western blot analysis confirmed the results. While this result demonstrated the effectiveness of the strategy, the current library size is too small and does not yield novel genes related to AcrB-ssrA degradation.

Prasangi Irosha Rajapaksha

06/25/2021

Investigation of Multidrug Efflux Transporter AcrB in *Escherichia coli*: Assembly, Degradation and Dynamics

By
Prasangi Irosha Rajapaksha

Dr.Yinan Wei
Director of Dissertation

Dr.Yinan Wei
Director of Graduate Studies

06/25/2021

DEDICATION

Dedicated to,

My Parents and My teachers

For making me who I am today, for being the role models of my life, for giving me wings of freedom to achieve my dreams, for being the best motivators and advisers in my life

My Brother and My Friends

For not letting me give up when life was difficult, for the unconditional love and support, for bringing the warmth of happiness and sounds of laughter in my life

ACKNOWLEDGMENTS

Last but not least, I want to express my gratitude to my parents, brother, sister-in-law, and my niece Tenu for their unwavering support and contributions to my achievements.

TABLE OF CONTENTS

LIST OF TABLES

LIST OF FIGURES

CHAPTER 1.   Introduction

1.1   Discovery and history of Antibiotics

Human life expectancy during the middle ages was low, and one main reason for this was infectious diseases. During this time, infectious diseases were one of the primary causes of mortality, and bacterial infections were among the common causes of these infectious diseases[1]. Tuberculosis, bubonic plague, anthrax, and cholera, for example, were all widespread infections[2]. However, with the discovery of antibiotics, this all changed. Mycophenolic acid isolation by Bartolomeo Gosio in 1893 was regarded as the first pure isolation of an antibiotic agent[3]. Following this initial impetus, the enormous efforts from scientists worldwide led to the discovery of a vast array of antimicrobial agents, which has been a great boon in improving human life expectancy and the quality of life.

Antibiotic is derived from an antonym to symbiosis: "antibiose." Selman Waksma first used the term "antibiotic" in 1942[3, 4]. In 1890, Paul Vuillemin used this word to describe the relationships between different microbes such as bacteria vs. protozoa, fungi, and bacteria. Antibiotics or antibacterials are natural secondary metabolites produced by bacteria and fungi, consisting of inhibitory or lethal/killing properties against bacteria.

Natural anti-fungal, anti-viral, and antibacterial substances have been used as remedies for a long time[5]. For example, in Jordan, red soils are utilized as antibiotics, and several herbals are exploited in traditional Chinese medicine as antimicrobial agents. Qinghaosu (artemisinin), a traditional Chinese medicinal, was later revealed to be a potent anti-malarial drug. This was isolated from Artemisia plants in the 1970s [6]

The emergence of the organic synthesis of antibiotics in the 19th century ushered in the discovery of numerous antibacterial drugs. The first man-made antibacterial agent was arsphenamine synthesized by Alfred Bertheim, which was approved as a drug in 1910. Later, in 1928, Alexander Fleming observed a *Staphylococcus aureus* plate had been contaminated with the fungus *Penicillium notatum*, (now *P. chrysogenu*m). He observed an intriguing pattern on the plate. Closer to the fungus, the bacteria were not growing, marked by clear areas on the plate[7]. The extract from *P. notatum* was later named penicillin in 1929 and has been used to treat infection by several pathogenic bacterial strains, mainly

Gram-positive ones, ever since[7]. In 1940, commercial production of penicillin began and was used to treat soldiers injured in World War II. The X-ray crystallographic structure of penicillin was analyzed by Dorothy et al., who categorized it as the first member of the β-lactam family[8].

The discovery of penicillin ushered in a new era of antibiotics. With the development of techniques and accessibility, scientists developed various antibiotics by adding different functional groups. The timeline of antibiotic development is shown in Figure 1.1. The period between 1940 to 1960 is considered the golden era of antibiotics development. Over 100 novel antibiotics have been introduced to the market during this period due to the rapid identification and characterization of compounds with antibacterial activities. The subsequent significant antibiotic discovery was the sulfonamide groups. After that, another milestone was achieved in 1943 by the discovery of the aminoglycoside antibiotics streptomycin. This antibiotic group exhibited activity against both Gram-positive and Gram-negative strains. The majority of these antibiotics were produced through fermentation methods except chloramphenicol which was synthesized.
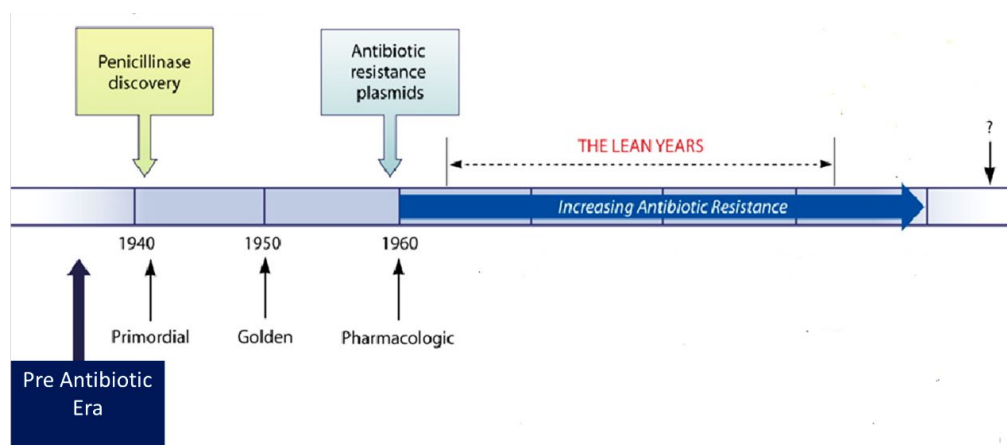
Figure 1.1 The timeline of antibiotic discovery and development of antibiotic resistance[5]. Copyright © 2010, American Society for Microbiology.

Based on the mechanism of action, antibiotics can be divided into two major groups. i) bacteriostatic; these inhibit bacterial growth by interrupting the major cellular processes such as DNA replication, protein biosynthesis, and cellular metabolism (e.g., tetracycline, sulfonamides).

ii) bactericidal- these antibiotics kill bacteria by disturbing cell membrane permeability, disrupting cell wall synthesis, and essential bacterial enzymes (e.g., penicillin, cephalosporin). The major groups of antibiotics and their mechanism of action are summarized in Table 1.

1.2   Antimicrobial resistance, the current development, and challenges

Scientific knowledge and technology have immensely contributed to the fight against microbes and benefited human and animal health. The use of antimicrobial drugs has been one of the most successful therapies in human and veterinary medicine[9]. Even though antibiotics are powerful in treatments, they lose their efficiency over time. This loss leads to the survival of a subpopulation of bacteria that evolve to be resistant to the drugs. Antimicrobial Resistance (AMR) occurs when bacteria, viruses, fungi, and parasites change over time and no longer respond to the antimicrobial drugs. The overuse of antimicrobial agents in healthcare and veterinary, agriculture, and the poorly regulated antibiotic market has significantly contributed to developing resistant strains against antibiotics[10-12]

The first antibiotic-resistant strain was found soon after the discovery of penicillin. A *Staphylococcu*s strain was found to be resistant to penicillin, and as an alternative, methicillin was developed[13]. Later, with the increase of antibiotic usage, more resistant strains emerged.

At present, AMR is one of the major threats to global health. The continuous evolvement of pathogenic microbes against the developed and available drugs is menacing humanity by causing deadly infections[14-16]. The efforts by the scientific community to characterize and develop new antibiotics had helped us reduce the impact of resistant strains temporarily. However, as new strains of resistant bacteria emerge, the battle proves to be a difficult one[17]. Currently, there are resistant bacteria to all the available antibiotics, causing a huge problem in treating bacterial infections. According to the Centers for Disease Control and Prevention (CDC) and World Health Organization (WHO), about 2.8

million people are infected with antibiotic-resistant bacteria or fungi. As a result, more than 35,000 people lose their lives each year in the United States[15, 16].

Bacteria develop resistance to antibiotics through a variety of mechanisms. Horizontal gene transfer during cell divisions, overexpression of specific genes, decreased membrane permeability and increased efflux, antibiotic inactivation, modification of the drug target site, and creation of by-pass reactions to prevent inhibitory effects are a few such mechanisms [18]. Among the drug-resistant bacteria, more problematic ones are placed in a group called ESKAPE, named as an acronym for six bacteria; Enterococci, Staphylococcus aureus, Klebsiella pneumoniae *Acinetobacter baumannii, Pseudomonas aeruginosa, Enterobacter spp*.

There are several approaches that we can consider in fighting against the pathogenic bacteria, i) Reduction in the spread of bacterial pathogens through the maintenance of personal hygiene and public health awareness ii) Development of new antibiotics as well as novel anti-virulence strategies to slow down bacterial evolution and resistance iii) Proper regulation of the antibiotics use[17]. Apart from reducing the spread of resistant strains, there is a huge requirement to develop new antibiotics. However, the period after the 1960s is called the lean years in antibiotic development. This is because the number of new antibacterial drugs developed and approved is rapidly declining. Since then, only four new classes of antibiotics have been approved and are available commercially[19]. Most recently, in 2015, teixobactin was developed and approved as a new antibiotic. Teixobactin acts by inhibiting bacterial cell wall synthesis and exhibited a high efficiency against Gram-positive bacteria[20].

Breakthroughs in genomics and proteomics have brought new possibilities to antimicrobial research[21-23]. The first complete bacterial genome sequence became available in 1995[24, 25]. However, even with such developments, the development of new antibiotics has lagged far behind. Antimicrobial drug discovery is a complex process mainly due to the inefficient penetration of compounds into bacterial cells[26]. Moreover, other major problems associated with developing new antibiotics are i) traditional and nontraditional methods have already identified the low hanging fruits of the antibiotics ii) it takes about 8-12 years from the discovery of an antibiotic to the point of commercial availability. iii)

drugs need to be safe and effective, optimization process needs to consider the suitability of its use in near future iv) cost of production is high[19].

From an industrial perspective, most of the early companies have stopped or significantly downsized their focus on antimicrobial drug research[27]. In the progress of commercial drug development, industrial research focuses on identifying broad-spectrum drug targets and novel inhibitors, determining the molecular mode of actions, and developing combination drug therapy modes[28]. However, there are resistance mechanisms against these commercial antibiotics, which raises the need to establish new inhibitors[29]. For example, studies are being conducted to produce novel inhibitors for the β-lactam antibiotics, which are considered the most produced and used antibiotics[30].

For acceleration of antibiotic production, in 2016, Combating Antibiotic-Resistant Bacteria Biopharmaceutical Accelerator (CARB-X) was launched by USA[31]. It is a non-profit partnership dedicated to the rapid innovation of antibacterial agents and other products to combat drug-resistant bacteria. It is the world's most prominent early development pipeline of antibiotics.

Even with the development of new drugs, there is always the possibility that bacteria will eventually develop resistance against them. Hence, regulation of antibiotic use is eassential[6]. For example, the European Union (EU) recommends the cautious use of antimicrobial agents in medicine[32]. They have regulations in monitoring the sales and usage of antibiotics and assessing the risk of developing drug resistance by using antibiotics on animals.

1.3   Multidrug resistance in bacteria (MDR)

Some bacteria become resistant to a broad range of antibiotics, creating multidrug-resistant bacteria (MDR)/"superbugs." Drug resistance to all the major antibacterial classes in Gram-negative and Gram-positive bacteria is prevalent [33]. Multidrug-resistant bacteria are more concerning due to their impact on available effective therapies against bacterial infections[34]. An estimated seven million deaths occur due to infections by MDR bacteria worldwide each year, and this number could increase to 10 million by 2050[15, 16].

As mentioned above, multidrug-resistant bacteria have become one of the major global problems by hindering the ability to cure infectious diseases using currently available antibiotics[35]. For example, in 1991, an MDR strain of *M. tuberculosis* was isolated in the USA, which was resistant to isoniazid, rifampin, ethambutol, streptomycin, kanamycin, ethionamide, and rifabutin. Due to this extreme situation, a new antibiotic, Bedaquiline received fast-track FDA approval to treat MDR tuberculosis. According to the reports by the CDC, bacterial strains have developed resistance against "last resort" antibiotics such as carbapenems and colistin [36]. Hence, the requirement for designing drugs against MDR is crucial at present. Glycopeptides, quinolones, oxazolidinones, and antibacterial cationic peptides are being studied to see if they can be improved to be more effective against MDR bacteria. [37, 38].

Drug-resistant bacteria develop resistance mechanisms due to selective pressure, and the acquired genetic alterations pass from generation to generation, creating a whole population of resistant bacteria. There are several mechanisms from which microbes develop drug resistance, i) genetic mutation or enzymatic alteration, e.g., production of MRSA by the acquisition of *mecA* gene ii)inactivation of drugs by enzymatic degradation, e.g., production of β-lactamase that hydrolyze the β-lactams antibiotics iii)antibiotic modification, e.g., aminoglycosides iv) Loss of porin and changes in membrane permeability, e.g., polymyxin resistance v)alteration of the drug target site, e.g., quinolones vi) overexpression of specific group proteins such as multidrug efflux pumps, e.g., tetracycline resistance (Figure 1.2)[39, 40]. Different classes of antibiotics have different mechanisms of drug resistance depending on their mechanism of action. These are summarized in Table 1.1
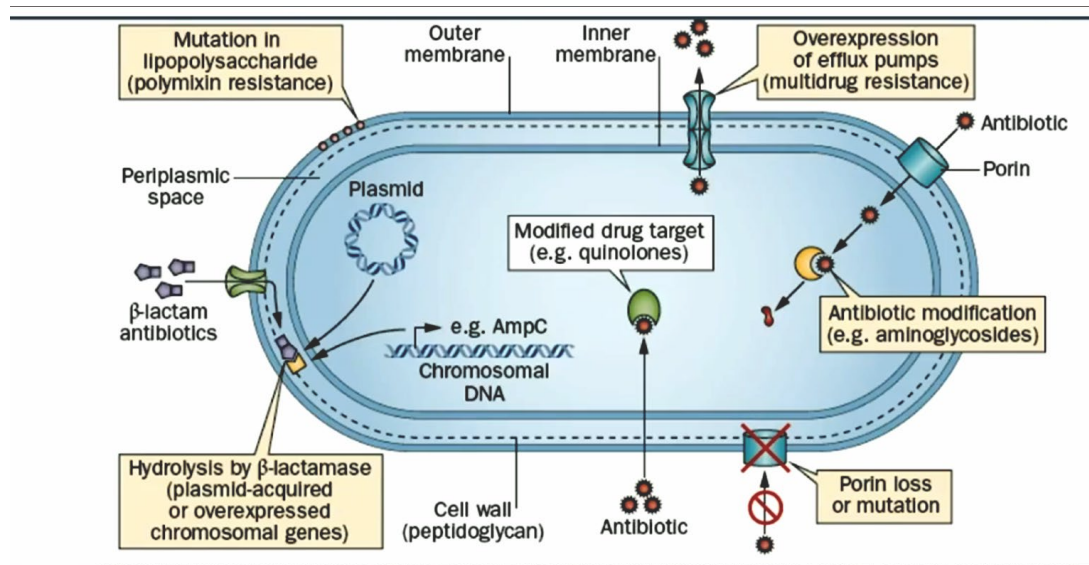
Figure 1.2 The figure illustrates different mechanisms bacteria use to acquire drug resistance. The figure belongs to [39].

The overexpression of efflux pumps is the most prevalent multidrug resistance mechanism, while other mechanisms lean towards single drug resistance. Efflux pumps expel out a broad range of molecules, including antibiotics, dye, detergents, and salt in Gram-negative and Gram-positive bacteria.[18, 41] Overexpression of efflux pumps reduces the concentration of the drug within the bacterial system by exporting it into the external environment, thereby contributing to intrinsic resistance[42].

Table 1.1 Class of antibiotics, mode of action, and resistance mechanisms. [5, 6, 9, 29]

Class of Antibiotics/ Year of first introduction/examples	Mechanism of action	Drug resistance mechanism
β-lactam (1929) Penicillin, Methicillin, Carbapenems	Inhibition of bacterial cell wall synthesis.	Production of the β lactamase Alteration of the penicillin-binding protein (PBP)
Sulfonamides (1935) Sulfadiazine	Inhibition of folate synthesis	Enhanced efflux and alteration of targets

Table 1.1 (Continued)

Polypeptides (1939) Bacitracin, Colistin	Disruption of the Gram-negative bacterial outer membrane and membrane permeability by associating with anionic lipopolysaccharides	Genetic mutations
Aminoglycosides (1943) Gentamicin, Kanamycin, Tobramycin, Neomycin, Spectinomycin	Inhibition of protein synthesis and disruption of the bacterial cell membrane	Phosphorylation, acetylation, nucleotidylation, efflux ,and target modification
Tetracyclines (1945) Tetracycline, Doxycycline, Tigecycline	Inhibition of protein synthesis	Overexpression of efflux mechanism. Synthesis of alternative elongation factor to prevent ribosomal binding enzymatic degradation of tetracycline
Lipopeptides (1947) Daptomycin, Polymixin B	Disruption of the bacterial membrane, inhibition of protein, DNA, and RNA synthesis	Alteration of drug target
Chloramphenicol (1948)	Inhibition of protein synthesis by binding to the ribosome	Enzymatic inactivation by acetylation, via different types of chloramphenicol acetyltransferases, target mutations, and efflux of chloramphenicol,

Table 1.1 (Continued)

Macrolides (1950) Erythromycin, Clarithromycin, Azithromycin	Inhibition protein synthesis	Modifications in target Enhanced efflux
Oxazolidonones (1952) Linezolid, Torezolid	Inhibition of protein synthesis	Enhanced efflux and alteration of targets
Glycopeptides (1953) Vancomycin, Teicoplanin	Inhibition of peptidoglycan synthesis in bacterial cell wall	Target alteration by genetic mutations (*vanA, vanB*) Reprogramming peptidoglycan biosynthesis
Quinolones (1962) Ciprofloxacin, Ofloxacin	Inhibition of DNA replication and transcription.	Target modification, acetylation, and efflux
Lincosamides (1963) Lincomycin, Clindamycin	Inhibition of protein synthesis	Nucleotidylation, efflux, altered target

1.4   Multidrug resistance mechanisms

Among the severe bacterial infections, the majority of them are related to the MDR Gram-negative bacterial species[43]. Gram-negative bacteria have three main layers in their cell walls: the outer membrane, inner membrane, and peptidoglycan cell wall. Gram-positive bacteria have two principal layers: the peptidoglycan cell wall and the inner membrane. These multi-layers provide an extra barrier for the drugs and other influx compounds. One of the multidrug resistance mechanisms in Gram-negative bacteria is efflux pumps. Most of these are located in the inner membrane. These pumps transport substrates from the inner membrane and periplasm through an outward channel. The

detailed analysis of these pumps in Gram-negative and Gram-positive bacteria has revealed they have versatile, functional roles in regulating compounds during infections, cell-to-cell communications, and the formation of biofilms[44].

Based on the sequence, structural, and functional analysis, efflux pumps are categorized into five major superfamilies. These are known as Resistance nodulation division (RND), Small molecule resistance (SMR), ATP binding cassette (ABC), Multidrug and toxic compound extrusion (MATE), and Major facilitator superfamily (MFS)[45, 46] (Figure 1.3). Among these, ABC superfamily uses ATP as the energy source while other families use electrochemical gradient[47]. ATP- dependent ABC family is diverse in importing or exporting solutes and functions as modulators of ion channels. An example of an ABC transporter is MacAB-TolC.[48]

The MFS group is considered the largest and most diverse family of transporters. Moreover, it is known as the uniporter-symporter-antiporter superfamily; uniporters (move substrates across the lipid bilayer without any coupling ions); symporters (substrate transport is coupled with ion and transport in the same direction) and antiporters (ion and substrates are moved in opposite directions). E.g., glycerol 3-phosphate/phosphate exchanger GlpT belongs to the MFS group. Most of this superfamily functions as single, monomeric units. SMR family proteins are small transporters that show resistance against quaternary ammonium compounds and other lipophilic cations such as EmrE in *E.coli*. MATE family transporters utilize proton or sodium gradient to efflux substrates from the bacteria.[44]
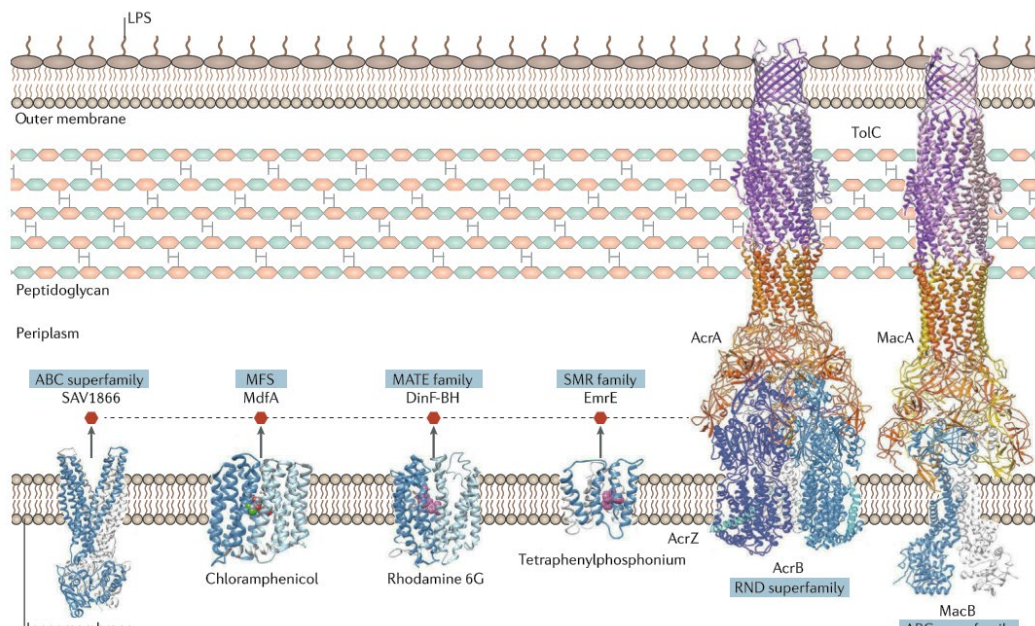
Figure 1.3 Different superfamilies of efflux pumps are represented in Gram-negative bacterial membrane.
Resistance nodulation division (RND), small molecule resistance (SMR), ATP binding cassette (ABC), Multidrug and toxic compound extrusion (MATE) and Major facilitator superfamily (MFS).[44] Reprinted with permission from Macmillan Publishers Ltd., Springer Nature.

1.4.1 AcrAB-TolC efflux pump system in *E. coli*

One of the most studied members of the resistance nodulation division (RND) family is the AcrAB-TolC (Acriflavin binding A and B- Tolerance Colecin) efflux system in Gram-negative bacteria[49, 50] (Figure 1.4). AcrA-AcrB-TolC efflux pump confers resistance to a broad range of antimicrobial compounds such as β-lactams, tetracycline, novobiocin, fluoroquinolones, and fusidic acids[51, 52]. The study into the efflux pump structure has evolved over the years through the work of many research groups. Mainly, it is a proton antiporter and has three distinct protein groups. This tripartite assembly consists of an outer membrane protein TolC, a plasma membrane-spanning protein that acts as the transporter -AcrB, and a periplasmic membrane fusion protein AcrA that connects the two trans-membrane components. The role of these has been debated over the years. The most recent finding summarizes that AcrB, the inner membrane-spanning trimer, acts as a drug

recognition transporter. AcrA, which is in the periplasm, supports the formation of the pump by anchoring AcrB and TolC. TolC is the outer membrane channel from where the drug is transported out of the cell. The recent crystal structure of the efflux pump supports the functional rotating mechanism of drug binding and extrusion of the pump[53-55].

Upon recognition of substrate, AcrB uses the energy from the proton-motive force derived from substrate/proton antiport. Substrates are recruited from the periplasmic space and outer leaflet of the inner membrane[56, 57]. In the periplasm, AcrA serves as a bridge between the inner and outer membranes to transfer the substrate to TolC in the outer membrane. [58, 59]. TolC, shared by many other efflux systems, exports the drug into the extracellular environment[60, 61] The individual crystal structures of AcrA, AcrB, and TolC have been solved[62-64]. The near-atomic resolution cryo-EM structure of the entire AcrAB-TolC complex solved by Wang et al.; reveals the intricate interacting interfaces between components of the pump[65]. The compositional stoichiometry of the complex was postulated to be AcrB: AcrA: TolC interaction in a 3:6:3 ratio to facilitate the transport of molecules across the double-membrane bacterial cell[66-68].
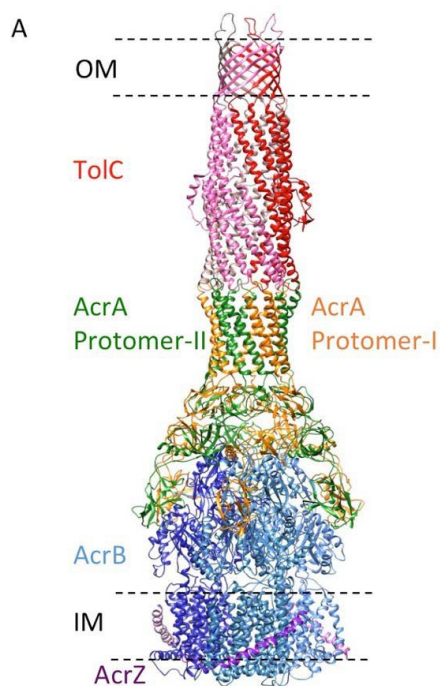
Figure 1.4 Structure of asymmetric AcrABZ-TolC pump visualized inside view.
OM-outer membrane, IM-inner membrane. The text color represents the respective section of the pump. E.g.: AcrB-Blue[65]. Reprinted with permission from Elife Sites.

1.4.2 The deep interpenetration and the Tip-to-tip Models of the AcrAB-TolC Efflux Assembly

AcrA -AcrB-TolC is a tripartite protein complex theworking together to transport substrate through the periplasm and membranes out of the bacteria system.[65, 69]. Initially, by utilizing X-ray crystallography and electron microscopy and recently by novel techniques like cryo-EM, numerous studies have been conducted to elucidate the structure of these efflux pumps[65, 70]. The first interpreted model of the pump assembly was referred to as the deep interpenetration model (Figure 1.5). This model shows that AcrB and TolC have direct interactions with each other, with each hairpin of AcrA contacting each groove on TolC surface, necessary to the functional rotation mechanism[71]. This was revealed from 74 different *in vivo* cysteine cross-linking studies between AcrA and AcrB.

However, another model has been recently postulated called "the tip-to-tip model." The AcrA hairpin in a barrel-like conformation contacts TolC in a tip-to-tip arrangement, as exemplified by Wang and coworkers in their published near-atomic resolution cryo-EM structure of the AcrAB-TolC complex assembly.[65]
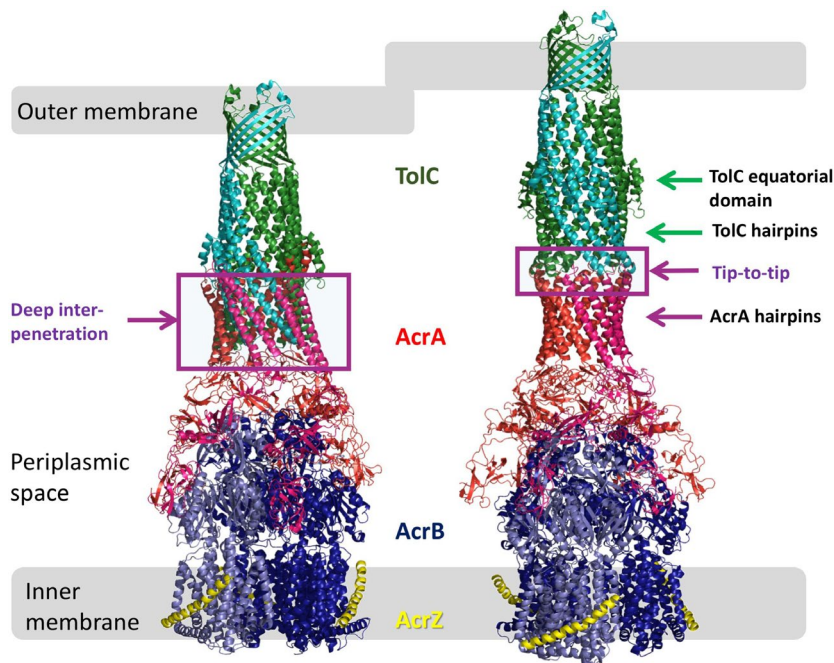
Figure 1.5 The comparison of two different proposed models for the AcrAB-TolC pump assembly.
The left side shows the deep inter-penetration model, and the rights side exhibits the tip to tip model.[72] Copyright © 2020 Marshall and Bavro, Frontiers in Molecular Biosciences.

1.4.3 Exit duct of the efflux pump- Tolerance to Colicin (TolC)

The outer membrane protein (OMP) of the AcrAB-TolC complex is TolC, which has a primary role in the expulsion of the molecules, toxins, and drugs from the cell. Many different biological processes share TolC in *E. coli* in the cell. Trimeric TolC is a 12 stranded β-barrel composed of 493AAs in each protomer. It spans through the outer membrane and periplasmic space. TolC is 140 Å in length and has a funnel/tube shape with a tight constriction at the periplasmic end. Once a complex recruits it for assembly, it translocates the molecules into the external environment.[73] The TolC tube is small, with a diameter of 3.9 Å. The two major domains, the channel domain, and the tunnel domain, are a 40 Å β-barrel and a 100 Å α-helical barrel, respectively.[51] TolC consists of protomers with structural repeats, forming a six-fold symmetry. It has three docking domains that include a central funnel leading to the TolC lumen. It creates trimers with structural regions such as periplasmic helical barrel, transmembrane barrel, and folds in the periplasm[74, 75].

14

1.4.4 Adaptor protein- Acriflavine resistance protein A (AcrA) Structure

AcrA can undergo large-scale conformational changes because of its flexibility. AcrA comprises of four domains with flexible linkers: the α-helical hairpins, lipoyl, the β-barrel, and the proteolytically labile membrane-proximal (MP) domains.[59] The other domains interact with AcrB except for the α hairpin that docks to TolC.[61, 76-78] The functional relevance of AcrA has been revealed through mutational studies. These studies have shown that deletion of the gene locus of AcrA led to the total abrogation of the efflux pump activity.[79, 80] AcrA or other PAPs are attached to the membrane through an acylated cysteine residue at position 25 or via a transmembrane residue at the N terminus. This attachment to the membrane is not relevant to the efflux function because even when the attachment is removed, the soluble AcrA retains its activity.[59]

1.4.5 Acriflavine resistance protein B (AcrB) as a transporter

AcrB is a homo-trimeric protein, of which each protomer is contains 1049 amino acids. AcrB is a very crucial protein for the effective functioning of the efflux pump. Hence, a vast majority of the studies to find efflux pump inhibitors have focused on AcrB. The first crystal structure of AcrB was resolved in 2002[63].The symmetric and asymmetric crystal structures of AcrB protein in the apo and substrate-bound states have been determined through various studies.[53, 63, 81-85] Each subunit of the antiporter AcrB has 12 transmembrane -helices that make up the transmembrane domain (TMD) and a large periplasmic domain (Figure 1.6).[65] The TMD is necessary in proton transport and thereby energy production through proton motive force. Two periplasmic loops reside between TM1 and TM2 and TM7 and TM8, respectively. The periplasmic domain, which is further divided into the porter domain and the funnel/docking domain, functions in substrate recognition and binds to the specific drug binding pockets. Previous studies have indicated several drug binding sites located in the AcrB (central cavity, periplasmic site), which facilitates the broad range of recognition and binding capability of AcrB transporter.[86] In the transmembrane domain, charged residues such as Asp407, Asp 408, Lys940 are involved in the proton translocation.
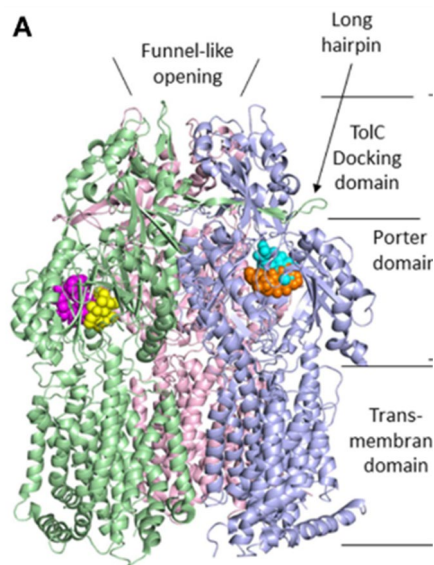
Figure 1.6 The crystal structure of AcrB. Each protomer represents in different colors AcrB has two major domains, a transmembrane domain and the periplasmic head domain. The assembly of each monomer creates a jellyfish-like structure with a funnel-like opening[57]. Copyright © 2015 Yamaguchi et al. Frontiers in Molecular Biosciences.

AcrB porter domain further divides into four major subdomains known as PN1, PN2, PC1, and PC2. The N terminal subdomains PN1 and PN2 are positioned between transmembrane helices TM1 and TM2. The C terminal subdomains PC1 and PC2 are located between TM7 and TM8. These subdomains have been revealed to have a significant role in the drug transport mechanism. Furthermore, PN1 and PC2, PN2, and PC1 subdomains form a rigid β- sheet structure comprising two structural subunits called PN1-PC2 and PN2-PC1. The funnel domain has two major subdomains, DC and DN (Figure 1.7). [51, 87-89]
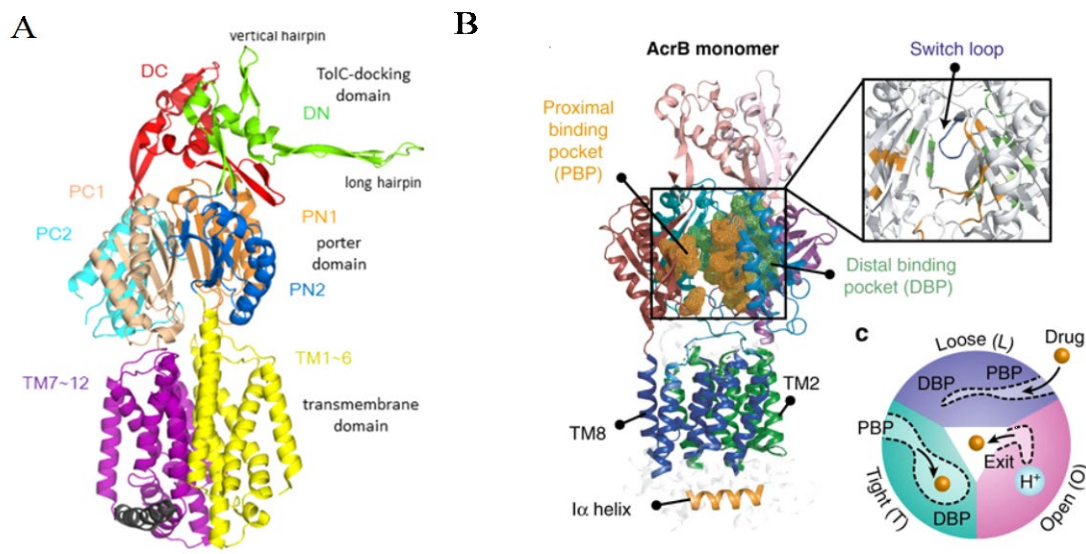
Figure 1.7 This figure shows the enlarged structure of one of the AcrB monomers A) represent the monomer with all the subdomains and subunit structures, B) shows the enlarge illustrations of drug binding pockets and switch loop[57]. Copyright © 2015 Yamaguchi et al. Frontiers in Molecular Biosciences

It was previously reported that there are two major drug-binding sites in AcrB. The access pocket (AP) or proximal binding pocket (PBP) is a cleft formed by subdomains PC1 and PC2 at the bottom of the periplasmic domain. The deep pocket (DP)/ distal binding pocket (DBP) located in the PN2-PC1 unit of the efflux pump is responsible for recognizing the low molecular mass compounds. The AP and DP sites are separated by a flexible, 11 amino acid residue known as a "switch loop," which is essential for drug transport.[87, 90] These drug binding sites have unique characteristics to facilitate different substrate-binding, contributing to the broad range of drug specificity. It has been reported that AP prefers larger substrates like erythromycin while DP favors smaller substrates like minocycline.[87, 91-93]

The central pore is formed by associating the subdomains and is located close to the periplasm and recognizing high molecular mass compounds (Channel (CH)1,2,3). More recently, some studies suggest that certain substrates could gain access from the cytoplasm through the central cavity or the transmembrane-embedded external surface of

the trimer.[94, 95] Therefore, the AcrB has 3 major entrance pathways for drugs; i) CH1-membrane surface channel entrance, ii) CH2- periplasmic entrance, and iii) CH3- central cavity entrance. The drugs entering these 3 pathways have different characteristics, allowing multidrug recognition by AcrB (Figure 1.8). Due to multiple entry pathways, drug efflux from the cell is significantly efficient.[46]
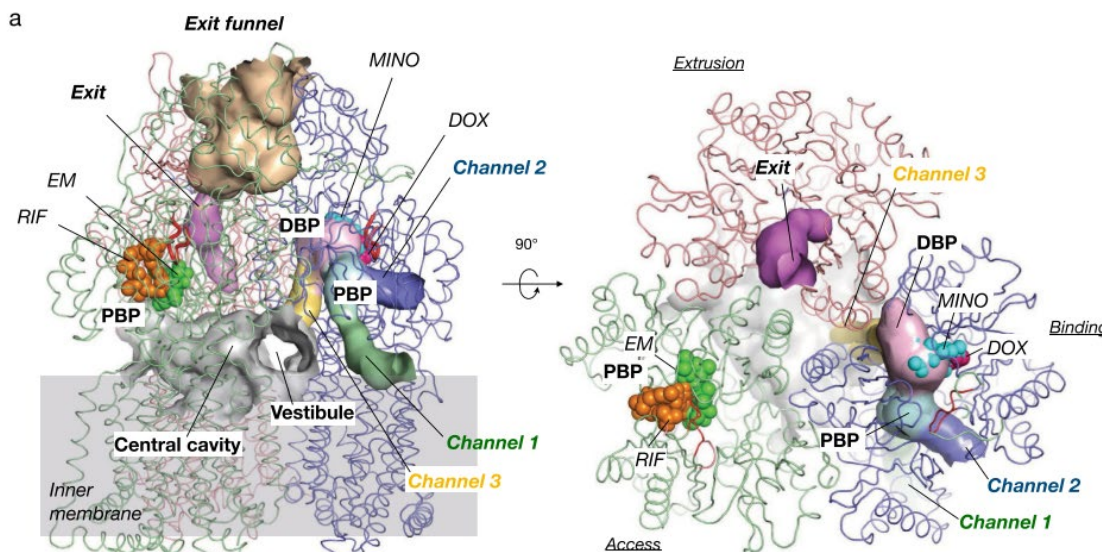
Figure 1.8 Side and a top-down view of AcrB showing the three main intramolecular entry channels in each monomer.Binding (blue) exit (pink) and extrusion (red)[46]. Reprinted from[46], Copyright (2018), with permission from Elsevier.

1.4.6 Functional Rotation mechanism of AcrB

The drug binding and extrusion mechanisms in AcrB have been highly studied. They have continuously been modified with new findings, providing insight into how the efflux pump causes multidrug resistance in bacteria. The AcrB transporter's structural asymmetry shows three conformations in each protomer, reflecting a different stage of the drug transport cycle. This was explained by the peristaltic functional rotation mechanism (Figure 1.9)[53-55, 96-99].These three different stages are termed open access (Loose-L), drug binding (Tight-T), and drug extrusion (Open-O) cycles.[53, 55, 97, 100]

The AcrB has high structural homogeneity, and the protomers exhibit characteristics protonation states in the transmembrane domain.[101] According to the

functional rotation mechanism, in the access conformation, the open and close activity of the external cleft between the PC1 and PC2 subdomains changes the distances between the protomers at the periplasmic domain. Substrates bind to AP/ PBP at the first stage. In the binding conformation, the cleft opens wide, whereas in the extrusion conformation, movement of the PC1 and PC2 subdomains causes the closure of PC2. Substrates that enter to AP/PBP move to DP/DBP during the transition from binding to extrusion. Thereafter, due to the movement of DBP, the substrate is expelled to the central funnel in TolC. The proton translocation across the transmembrane domain and drug binding to the porter domain initiate these conformational changes[53]. The new cryo-EM model study showed that ligand binding is allosterically coupled with the channel-opening. The channel remains open through the drug transport cycle, thus offering a dynamic mechanism of efflux.[65]
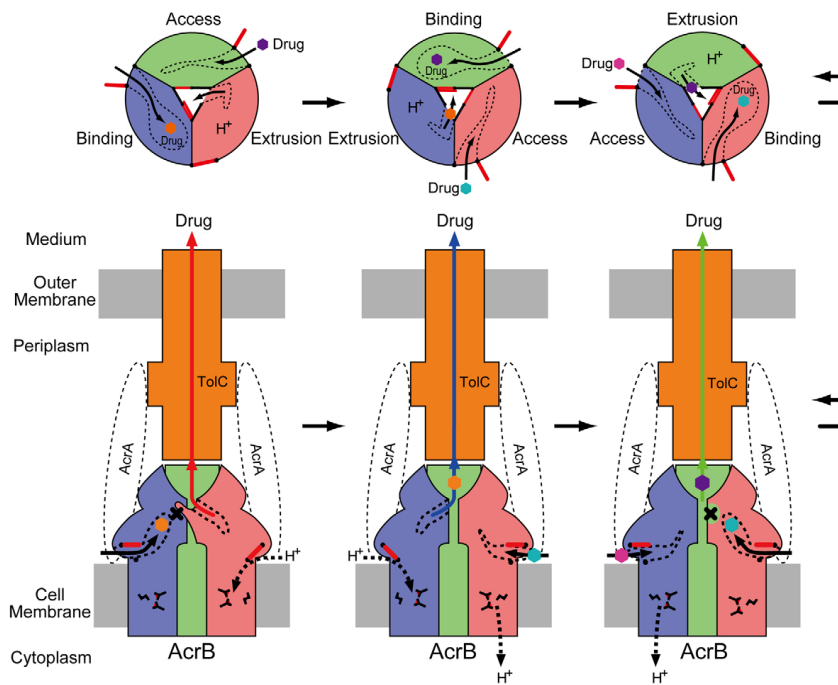
Figure 1.9 Illustration of the functionally rotating ordered multidrug binding change mechanism mediated by AcrB[82]. . Reprinted from[82] Copyright (2008), with permission from Rightslink® Service and Elsevier.

19

1.5   Protein degradation in bacteria

The biological networks are modulated through a series of protein expression, function, and degradation processes. Protein degradation in cells is an important process in regulating homeostasis and quality control of the cells. There are two major groups of proteins; ATPases associated with various cellular activities (AAA+) proteases and Heatshock protein70 (HSP70)[102]. AAA+ proteases use the energy from ATP hydrolysis to unfold, modify, degrade, and transport proteins. These are essential for the regulations of the proteome in cells ranging from bacteria to humans[103].

The proteolytic complexes consist of proteases and peptidases. In prokaryotes, the proteins are degraded by the ATP-dependent pathway involving proteases including ClpAP, ClpXP, FtsH and, Lon[104, 105]. Two well-studied examples in prokaryotic protein degradation are AAA+ proteases ClpAP and ClpXP. The ClpXP complex consists of two proteins. ClpXP has a vital role in the association, unfolding, and translocation of proteins into ClpP for degradation. The ClpX protease consists of six AAA + subunits and a ring-shaped motor structure. ClpP is a 14 subunits barrel-shaped peptidase (Figure 1.10). The six motor subunits coordinate ATP hydrolysis, and the translocation of the protein substrate through the central pore is mediated by the conformational changes within a single subunit. These conformational changes in one subunit subsequently drive the motions of the other subunits[106]. Bacterial proteins are degraded by including a degradation peptide tag in the coding region.
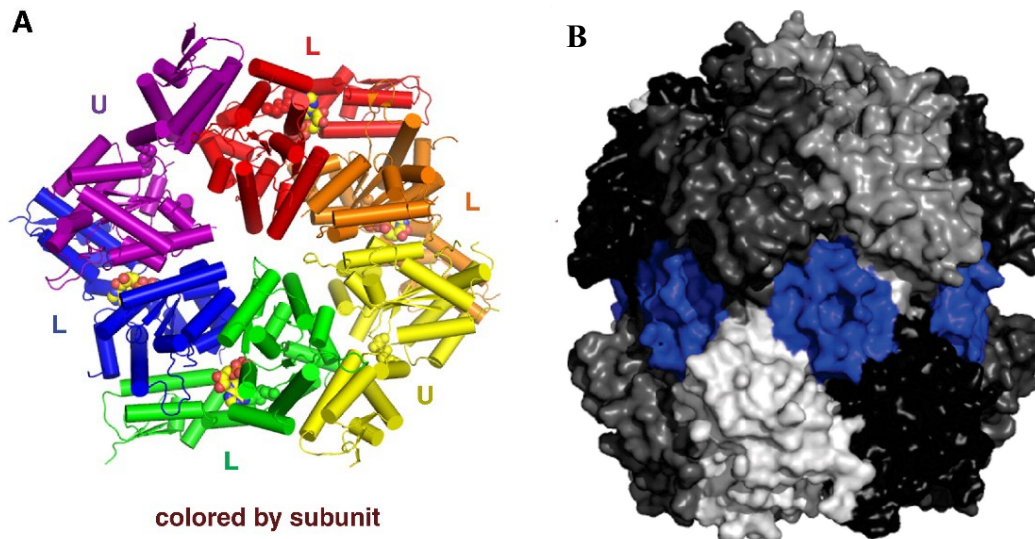
Figure 1.10 The structures of ClpX protease and ClpP peptidase. A) Top-down view of the ClpX protease arranges in hexameric ring. B) The side view of the ClpP arrange with 14 subunits[104]. . Reprinted from[104] Copyright (2012), with permission from Rightslink® Service and Elsevier.

The protein is flagged for degradation by five major peptide motifs. These are categorized into two main types of peptides: C-terminal and N-terminal[107]. For instance, in *E. coli* the C-terminal peptide ssrA, an 11 amino acid residue (AANDENYALAA), facilitates the rapid degradation of soluble proteins. Furthermore, degradation signals can be sent via the N-rule pathway through the N-terminal tagging of the protein[108].

In general, the function of ssrA lies in the rescuing of stalled ribosomes (Figure 1.11). The stalled ribosome is rescued by a mechanism called *trans*-translation. Through trans-translation ssrA peptide tag is added to bacterial proteins that do not have in-frame stop codons. Trans-translation is a crucial step in preventing negative impacts on cellular functions from the stalled ribosomes.
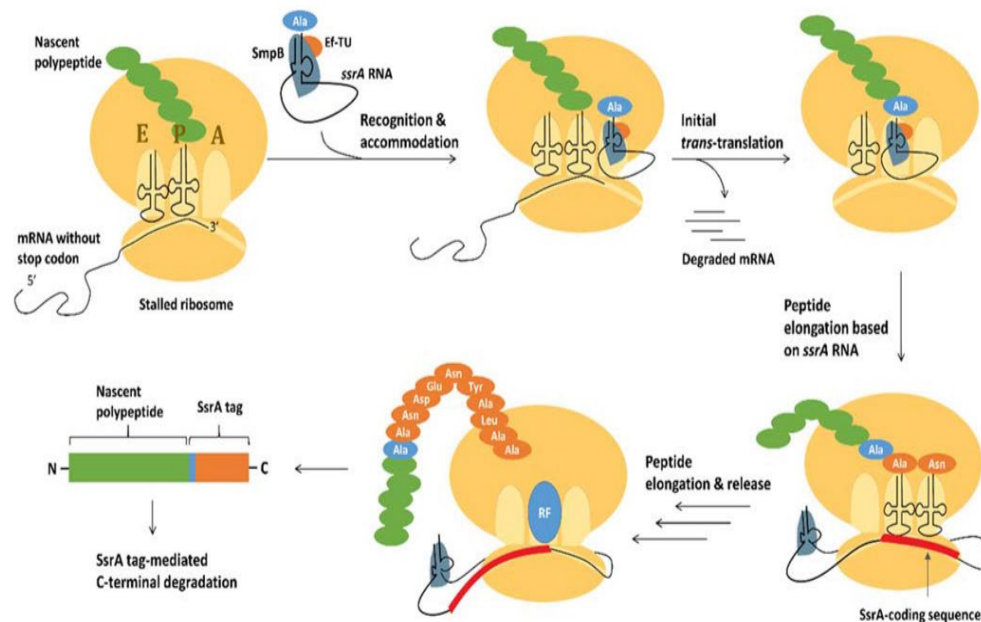
Figure 1.11 The pathway of ssrA tag added to the C-terminus of incompletely synthesized protein. Reprinted by permission from[109]. Copyright © 2020 Springer Applied Microbiology and Biotechnology

Stringent starvation protein B (SspB) is a highly specific dimeric delivery/adaptor protein that delivers ssrA- tagged proteins to ClpXP. The SspB adaptor binds to the ssrA tag's first seven amino acids (AANDENY), anchoring it to the ClpXP protease, while ClpX detects the last three amino acids (LAA), and unfolds the protein substrate (Figure 1.12). [110] This process enhances the degradation of ssrA-tagged proteins by ClpXP. Nyquist et al. used different peptide tags and demonstrated that adaptor-mediated proteolysis of the peptide-tagged protein substrates is comparatively efficient due to the increase in strength of protease-substrate contacts.[111] However, it was reported that the ssrA tagged protein degradation in *E. coli* occurs even in the absence of SspB.

ClpX protease recognizes and binds to the peptide tag during the degradation process, then unfolds the attached protein substrate, followed by translocating the polypeptide into the proteolytic compartment ClpP, which performs the degradation of the unfolded polypeptide into small peptide fragments (Figure 1.12).[105] Chaperone rings have a significant role in recognizing protein substrates by identifying specific tag sequences and hydrophobic motifs of some proteins (Figure 1.13).[112] The peptide-tagged protein degradation happens through more than one protease complex (e.g., ClpAP). Hence, the

efficient regulation of protein degradation is difficult[104]. In our attempt to study the lifetime of AcrB in *E. coli*, we discovered that the introduction of a small peptide tag, the ssrA, leads to the complete degradation of AcrB.[113]
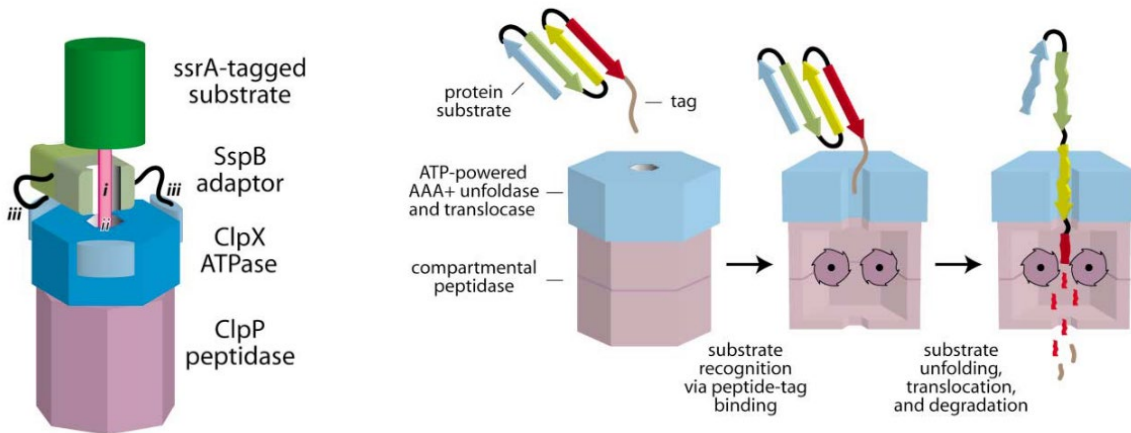
Figure 1.12 Protein degradation by ClpXP protease.
A) Model for Adaptor-Mediated Delivery of a Tagged Substrate to a AAA+ Protease complex B) Schematic representation of substrate recognition and degradation by AAA+ protease[105]. Reprinted with permission from © 2004 Cell Press. Published by Elsevier Inc.
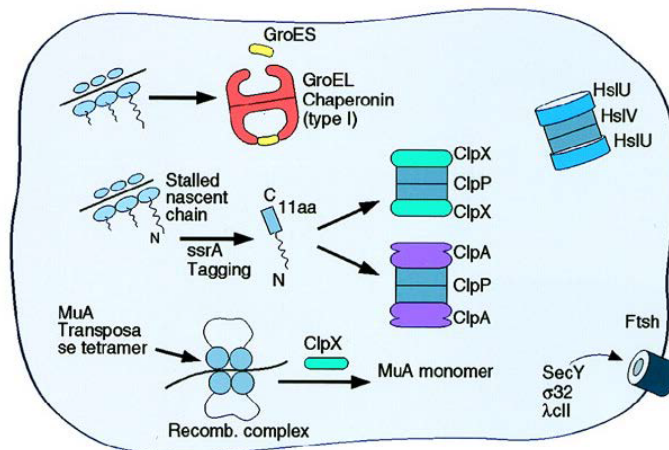
Figure 1.13 Schematic illustration of the roles of chaperone rings in ATP-dependent protein degradation in bacteria Protein folding chaperons, ATPases are shown in the figure[114]. © 2015 Venter, Mowla, Ohene-Agyei and Ma. Frontiers in Microbiology.

1.6 Transposons (Mobile genetic elements/"jumping genes") as a robust tool

The advent of genomics has paved the way for improved and robust phenotyping, structural, and biochemical analytical methods. As one of the applications, molecular genetics in bacterial phenotypic studies provides greater insight into the molecular processes which are beneficial in medical and industrial applications. Transposons have become one of the most versatile tools in the molecular genetic analysis of bacteria which are widely applicable in the study, construction, and manipulation of different phenotypes in bacteria. One of the major advantages of transposons over the traditional mutagenesis approaches is their ability to produce mutated genes with a meager chance of multiple insertions.

Transposons were first discovered by geneticist Barbara McClintock using the maize genome, for which she won the Nobel Prize in 1983. Transposable elements are generally known as "jumping genes/selfish genes".[115-117] These DNA sequences move from one place to another in the genome. Furthermore, these are capable of moving from one genome to another, which is known as "Horizontal gene transfer" [117, 118]. These events are widely found in eukaryotes and in some of the prokaryotes as well. For instance, 90% of the maize genome has been made up of transposons, and about 50% of the human genome consists of Transposable Elements (TE) [118]. Transposons insertion is a random process.[119] It is important to understand the definition of terms that explain the transposons (Table 1.2).

Table 1.2 Definition of transposons related terms.[120]

Term	Definition
Transposase enzyme -(i.e.Tn5),	Catalyzes the transposition reaction
Transposon	Transposable DNA sequence containing transposase recognition sequences
Transposome	It consists of the transposon complexed with the transposase.
Transpositions	The reaction, where the transposon is inserted into the target DNA
Transposed DNA-	Target DNA with a transposon insertion

There are two major classes of transposons; i) Class I, known as retrotransposons, uses RNA as a mediator to complete the transposition; ii) Class II are the DNA transposons flanked by terminal inverted repeats (TIR) (Figure 1.14). Furthermore, depending on the mode of action, they are further divided into conservative and replicative groups. In bacteria, there are a few types of transposons: i) IS element- insertion sequence transposons, transposase gene is flanked by inverted repeats (IR); conservative or replicative, ii) Composite transposons; conservative (Figure 1.15), iii) Transposable bacteriophages such as Mu phage, iv)Tn3 class transposons.

Figure 1.14 A representation of Class I and Class II transposons. The image belongs to [116]

DNA transposons which are prevalent in bacteria, allow DNA rearrangement, crucial for genomic evolution. DNA transposons have a mode of action that enables transferring a gene from one site to another, known as the "cut and paste" mechanism. However, these insertions mostly happen close to the parental insertions, which is called "local hopping." The transposase encoded by the IS binds at or near the IR of DNA; the transposition reaction follows this. In composite transposons phenotype responsible/resistance gene, DNA region is flanked by two IS elements. These IS elements are responsible for the encoding of transposase (Figure 1.15). Our studies have used the Tn5 transposons system, which comes under the group of composite transposons.[121]

a) **Insertion Sequence (IS)**

| IR | Transposase Gene | IR |

b) **Composite Transposon**

IS

IS

Antibiotic resistance gene   Transposase Gene   IR
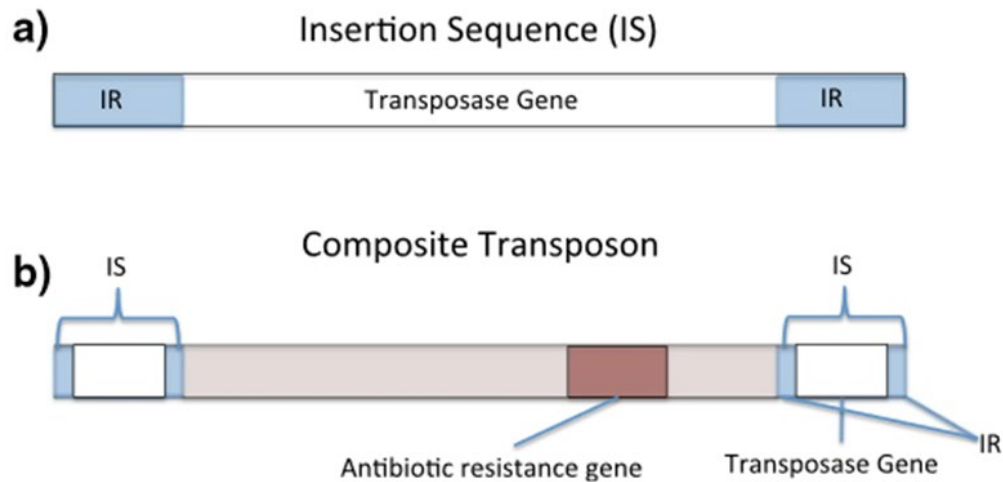
Figure 1.15 A comparison between two major types of bacterial transposons, a)IS element and b) Composite transposons.[122]

1.6.1 The applications of transposons in genomic studies

The identification of transposons has led to significant discoveries in various scientific aspects.[116, 118] The main problem associated with genome studies in terms of sequencing large DNA segments is sequencing an insert within the interior of a DNA. Alternative techniques such as genome walking/primer walking and shotgun subcloning have been developed to circumvent this limitation. Transposons, on the other hand, have proven to be an effective approach.

One of the most prominent uses of transposons in bacteria is the generation of recombinant plasmids, which helps with DNA sequencing and mapping.[123] Transposon insertions range from yeast to human DNA. These customized transposons are used as priming sites in the sequencing process. Advantages of using transposons include: 1) it can be designed to contain specific features, 2) assembly of a large number of transposons insertions is easy, and 3) the unique flanking sites of transposons allows rapid identification of insertion sites. The introduction of certain antibiotic resistance genes into bacteria (such as *E. coli*, Salmonella typhimurium, and others) in vivo is another use. Similarly, the insertion of replication origins into bacteria facilitates molecular cloning. Furthermore, *in vivo* DNA transposition plays a critical part in insertional mutagenesis, which is used to

create gene "knockouts." Integrating retroviral DNA and sequencing bacterial genomic DNA directly from transposon insertions without cloning, as well as guiding molecular cloning by providing genetic landmarks, are a few other examples (Figure. 1.16).[124]
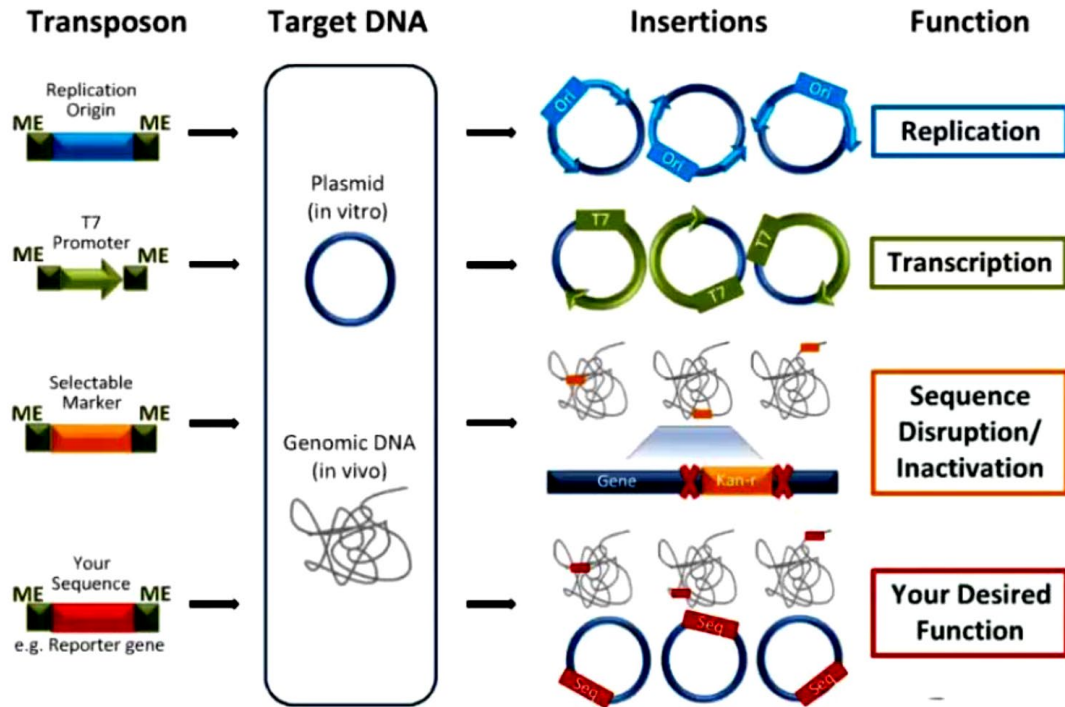
Figure 1.16 A summary of different applications of transposons[120]. . The images belong to Lucigen Inc.

1.6.2 The EZ-Tn5™ <KAN-2>Tnp Transposome™ system

The Tn5 transposons system, which has the cut and pastes mechanism, has been widely used by researchers in different studies. Transposons library creations have facilitated the identification of genes involved in virulence as well as non-essential processes.[125] A conjugative transposons process used in lactic acid bacteria is explained in detail in the review by Fitzgerlad et al. [126]

The EZ-Tn5™ <KAN-2>Tnp Transposome™ available through Lucigen Inc. (Middleton, WI) is based on the stable complex interaction between the EZ-Tn5 transposase enzyme and the kanamycin-2 transposon. It provides an efficient method for *in vivo* mutagenesis and target identification, allowing rescue cloning from the expected

mutant. This system includes the antibiotic resistance gene- kanamycin. Also, the ends of transposons are flanked by 19 bp repeats known as Mosaic Ends (ME). ME act as the EZ-Tn5 Transposase recognition sequences (Figure 1.17).[120]

The transposome system is incorporated into the cells via electroporation, and once inside, the Tn5 enzyme is activated by cytosolic Mg^{2+}. [127, 128] This activation leads to the random insertion of transposons into the host genome, resulting in gene disruption, inactivation, random mutations, and ultimately functional changes. The modified EZ-Tn5 transposase is highly reliable and more efficient than the wild-type Tn5 transposase.[129]

The transposon insertion happens in the genomic DNA. The primers included in the kit can be used for bi-directional DNA sequencing to determine the insertion site. The Tn5 transposition process involves the binding of transposase monomers to the 19 bp mosaic ends and oligomerization of the end-bound transposase monomers. The blunt end cleavage is subsequently performed, resulting in the formation of a transposome complex that requires Mg^{2+} ions from the host cell. The next step binds to the target DNA; followed by strand transfer of the transposon 3′ ends into a 9 bp target sequence.[124] The insertion process results in small gaps which are filled by host enzymes. These gaps create short duplications of sequences that are called target site duplications (TSD).[130] This process of transposition is summarized in Figure 1.17.
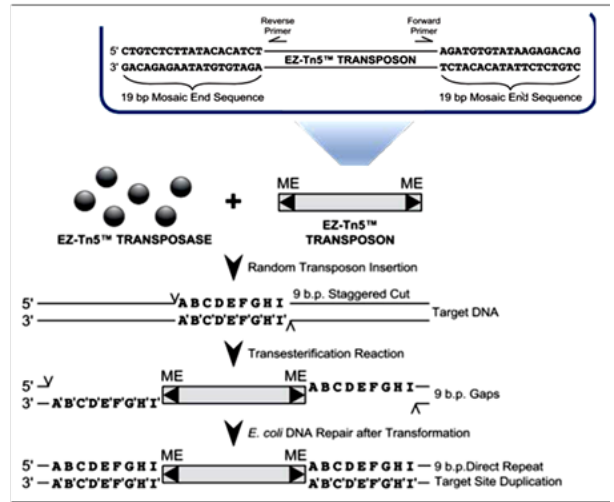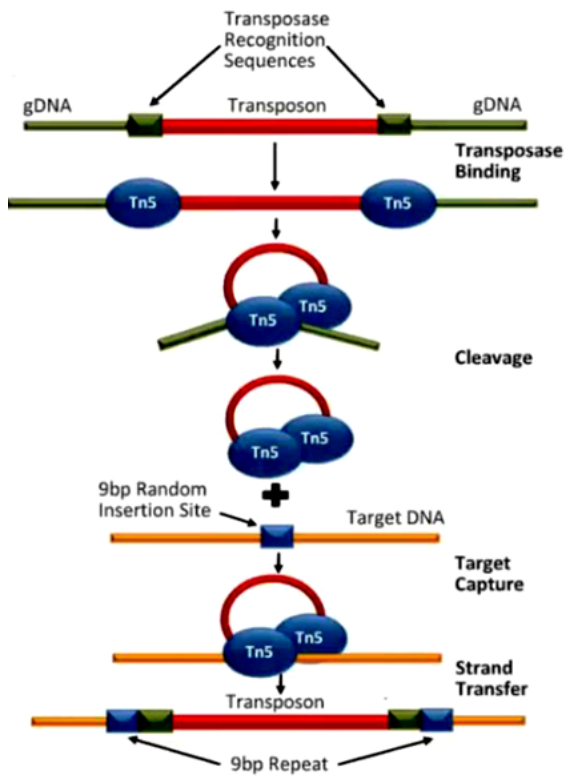
Figure 1.17 A schematic representation of the transposition process.

A) Shows tranposition by Tn5 Transposons binding cleavage and integration followed by the gap repair by host enzymes. Figure B)shows the enlarged version of the process that happens in the gap repair process [120]. The images belong to Lucigen Inc.

CHAPTER 2.   Probing the dynamics of AcrB through disulfide bond formation

2.1   Introduction

The multidrug resistance in bacteria has become one of the major threats in global health. Bacteria have developed a mechanism to evade the attack of most commercially available drugs. In gram-negative bacteria such as Escherichia coli, multidrug efflux systems are a major mechanism that confers intrinsic and increased drug resistance to a broad spectrum of antimicrobials.[132] The overexpression of resistant-nodulation- division (RND) superfamily member AcrAB-TolC, a tripartite complex that spans through the outer membrane and the inner membrane, has been identified as an important mechanism leading to multidrug resistance.[133-135] AcrAB-TolC is one of the major efflux systems contributing to the multidrug resistance in *E. coli*.

This pump has an important role in transporting substances such as antibiotics, detergents, dyes, and free fatty acids out of the cell [46, 70, 94, 136]. In this protein complex, TolC is a homotrimeric outer membrane channel that enables the exit of drugs from the cell to the external medium. AcrA belongs to the membrane fusion protein (MFP) family and exists in the periplasm. AcrB is a homotrimer inner membrane antiporter that couples the inward proton transport with the outward substrate transport. The assembly of the AcrAB-TolC tripartite complex has a stoichiometry of 3:6:3 for TolC:AcrA:AcrB, respectively.[49, 70]

The assembled structure of the AcrAB-TolC pump complex has been revealed in several scanning electron microscopy studies,[70, 137] and more recently through cryoEM studies, which provides insight into the molecular mechanism of transport by this pump.[65, 138] Moreover, symmetric and asymmetric crystal structures of AcrB in the apo and substrate-bound states has been determined.[53, 63, 81-85] The antiporter AcrB functions as a trimer, with 12 transmembrane α helices and a large periplasmic domain in each subunit.[65] AcrB plays a pivotal role in the recognition and binding of substrates and harvests the

proton motive force to energize drug efflux. In the periplasmic domain of each subunit, there are multisite drug- binding pockets, which enable a broad range of drugs to enter and bind, and subsequently exit through efflux.[74, 91]

The asymmetric structure of AcrB revealed novel insight into the drug binding and transport mechanism of the pump. The AcrB periplasmic domain divides into two domains, the porter (pore) domain and the funnel (previously known as "docking") domain (Figure 2.1). Porter domain is further categorized into four subdomains as PN1, PN2, PC1, and PC2. The funnel domain has two major subdomains, DC and DN. PN1 and PC2 subdomains together form a rigid β- sheet structure, in a similar way PN2 and PC1 form a β-sheet.

Hence, in previous reports, the porter domain has been divided into two structural subunits called PN1−PC2 and PN2−PC1.[87, 88] The substrate access and transport pathway is formed between these two structural units. The analysis of crystal structures has revealed that a distal/deep binding pocket is located in the PN2−PC1 unit. Subdomains PC1 and PC2 form the cleft in the bottom of the periplasmic domain, which is another drug-binding pocket termed the proximal binding site. PN1 and PN2 form the drug exit pathway connecting to the central pore.[53, 88, 139]

Substrates can access the AcrB binding pocket from the periplasm or the outer leaflet of the inner membrane, through entry points/vestibules near promoters.[53] More recently, some studies suggest that certain substrates could gain access from the cytoplasm through the central cavity or the trans- membrane-embedded external surface of the trimer.[46, 95] In the asymmetric AcrB structure, each protomer exhibits conformational differences representing each stage of the drug transport cycle, open access (loose-L), drug binding (tight-T), and drug extrusion (open-O)[53, 55, 97]. This proposed mechanism is termed the peristaltic functional rotation mechanism [53-55, 96-99].According to the functional rotation mechanism, the external cleft between the PC1 and PC2 subdomains opens and closes, thus changes the distances between the protomers at the periplasmic domain. In the binding conformation, the cleft opens wide. Also, in the extrusion conformation, the cleft closes through the movement of the PC1 and PC2 subdomains. These conformational changes are due to proton translocation across the trans- membrane domain and drug binding to the porter domain.

Disulfide bond trapping is an effective method in studying the conformational changes in proteins. Cysteine residues are introduced into the desired locations through site-directed mutagenesis, and then disulfide bond formation is monitored. For proteins in gram-negative bacteria, sites located in the periplasmic domain are normally chosen for mutation since disulfide bonds form readily in this cellular compartment[140]. In this study, we introduced inter-subunit disulfide bonds in the periplasmic domain of AcrB. Through ethidium bromide (EtBr) accumulation assays and drug susceptibility assays, we have investigated how the Cys mutation and disulfide bond introduced at each specific location affected the function of AcrB.
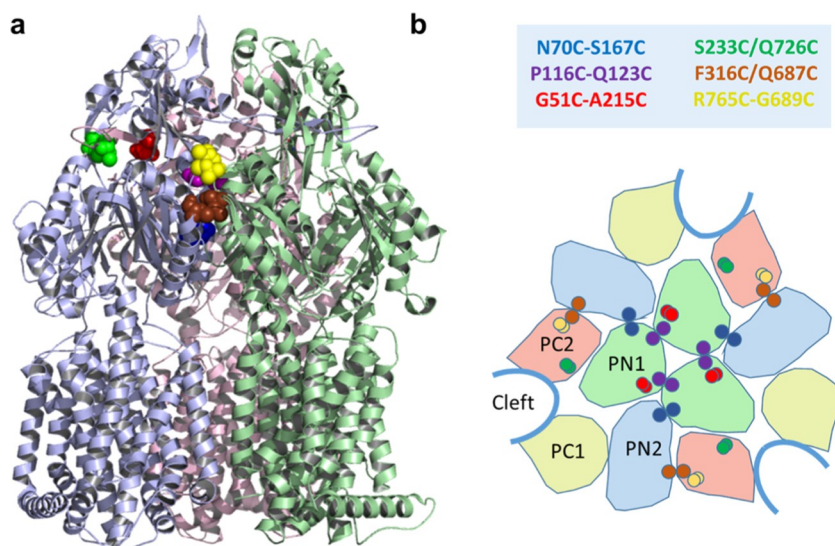
Figure 2.1 Locations of the six Cys pairs in the structure of AcrB
a) Structure of an AcrB trimer showing the color-coded Cys pairs. Only mutated residues in the light purple subunit and their partners are shown for clarity. (b) Organization of the subdomains in the porter domain. The locations of disulfide bonds are shown as dots. Structure image is rendered with pymol (https://pymol.org/2/) using the asymmetric structure 2HRT.pdb.[55]

2.2   Materials and Methods

2.2.1 Bacterial Strains, Plasmids, and Growth Conditions

Plasmid pQE70-CLAcrB, which encodes a cysless AcrB, was used as the template to create AcrB double cys mutations[141] The two intrinsic cysteines in CLAcrB were both replaced by alanine to reduce the potential of nonspecific disulfide bond formation. The cysless AcrB is fully functional[142, 143].Mutations were introduced using the Quikchange site-directed mutagenesis kit following the manufacturer's instruction (Agilent, Santa Clara, CA). Primers used in the study were listed in Table 2.1. *E. coli* strain BW25113 and BW25113Δ*acrB* were obtained from Yale *E. coli* genetic resources. Bacteria were cultured at 37 °C with shaking at 250 rpm in Luria broth (LB) media unless otherwise noted.

Table 2.1 Primers used in this study

Construct	Primer (5'-3')
AcrB_G51C_F	CCTCCTACCCCTGTGCTGATGCGAAAAC
AcrB_G51C_R	GTTTTCGCATCAGCACAGGGGTAGGAGG
AcrB_A215C_F	GAACGCCCAGGTTTGTGCGGGTCAGCTC
AcrB_A215C_R	GAGCTGACCCGCACAAACCTGGGCGTTC
AcrB_Q123C_F	CGCAAGAAGTTTGTCAGCAAGGGGTG
AcrB_Q123C_R	CACCCCTTGCTGACAAACTTCTTGCG
AcrB_P116C_F	CAGCTGGCGATGTGTTTGCTGCCGCAAGAAG
AcrB_P116C_R	CTTCTTGCGGCAGCAAACACATCGCCAGCTG
AcrB_S167C_F	GAAAGATGCCATCTGTCGTACGTCGGGC
AcrB_S167C_R	GCCCGACGTACGACAGATGGCATCTTTC
AcrB_N70C_F	GAACAGAATATGTGCGGTATCGATAACC
AcrB_N70C_R	GGTTATCGATACCGCACATATTCTGTTC
AcrB_F316C_F	GAAGATGGAACCGTGTTTCCCGTCGGG
AcrB_F316C_R	CCCGACGGGAAACACGGTTCCATCTTC
AcrB_Q687C_F	GAGCTGATTGACTGTGCTGGCCTTGGTC
AcrB_Q687C_R	GACCAAGGCCAGCACAGTCAATCAGCTC

33

Table 2.1 (Continued)

AcrB_Q726C_F	GAAGATACCCCGTGCTTTAAGATTGATATCG
AcrB_Q726C_R	CGATATCAATCTTAAAGCACGGGGTATCTTC
AcrB_S233C_F	CAGCTTAACGCCTGCATTATTGCTCAG
AcrB_S233C_R	CTGAGCAATAATGCAGGCGTTAAGCTG
AcrB_R765C_F	CGACTTTATCGACTGTGGTCGTGTGAAG
AcrB_R765C_R	CTTCACACGACCACAGTCGATAAAGTCG
AcrB_G689C_F	GATTGACCAGGCTTGCCTTGGTCAC
AcrB_G689C_R	GTGACCAAGGCAAGCCTGGTCAATC
AcrB Seq2_R	GTGTTGCACGCATGGTAATC
AcrB Seq3_R	CCATTGCTTCACCGGTACTT

2.2.2 Drug Susceptibility Assay.

The MIC was determined for erythromycin, novobiocin, ethidium bromide (EtBr), and tetrapheynlphosphonium chloride (TPP) following the CLSI guidelines.[144] Briefly, overnight cultures of the indicated strain were diluted to a final concentration of 10^5 CFU/mL in fresh Muller Hinton Broth 2 (cation adjusted) media (Millipore Sigma, St. Louis, MO) in a 48-well microtiter plate containing the indicated compounds at two-fold serial dilutions. Plates were incubated at 37 °C with shaking at 200 rpm for 17 h, and the absorbance at 600 nm (OD_{600}) were measured to identify the lowest concentrations with no observable cell growth.

2.2.3 Protein Purification, Sodium Dodecyl Sulfate Polyacrylamide Gel Electrophoresis (SDS-PAGE), and Western Blot Analysis.

Five milliliters of cells were cultured overnight at 28 °C with shaking at 250 rpm. The next morning, cells were pelleted and resuspended in 1 mL of phosphate buffer containing 10 mM iodoacetamide (IAM) and phenyl- methylsulphonyl fluoride (PMSF) (1:1000 dilution of a saturated ethanol solution),and sonicated for 1 min followed by centrifugation for 10 min at 15 000 rpm. The supernatant was removed, and cell pellets

were resuspended in 0.2 mL of phosphate-buffered saline (PBS) + 2% Triton-X100 containing 10 mM IAM. The samples were incubated at room temperature with shaking for 45 min and centrifuged again for 10 min. The supernatant was used for SDS-PAGE and Western blot analysis.

For Western blot analysis, a disulfide bond was reduced either by incubating with 10% β-mercaptoethanol (BME) for 10 min or 50 mM dithiothreitol (DTT) for 1 h as indicated. After transferring to the poly(vinylidene difluoride) (PVDF) membrane, protein bands were detected using an anti-AcrB polyclonal (Rabbit) antibody raised to recognize a C-terminal peptide corresponding to residues number 1036−1045[145].The membrane was then washed and incubated with an alkaline phosphatase-conjugated Goat anti-Rabbit secondary antibody. The BCIP/NBT (5-bromo-4-chloro-3′-indolyphosphate and nitro-blue tetrazolium) solution was used to stain the membranes.

2.2.4 EtBr Accumulation Assay.

The EtBr assay was performed following the established procedure with slight modi*fi*cation.[146] Briefly, cells were grown in 15 mL of LB media until the mid-log phase (OD_{600} of 0.6−0.8). The bacteria were then centrifuged at 3000g for 15 min and washed, the cell suspension was loaded into a cuvette and monitored using a *fl*uorescence spectrometer (Perkin-Elmer LS 550), at excitation and emission wavelengths of 520 and 590 nm, respectively. After ∼40 s, 1 mL of EtBr was added to a *fi*nal concentration of 10 μM and to make *fi*nal OD_{600} of cell suspension 1.0, and the emission was monitored for an additional 600 s. For the samples with DTT treatment, cells were incubated with 50 mM freshly prepared DTT for 1 h at room temperature before loading into the cuvette.

2.3 Results and discussion

2.3.1 Inter-Subunit Disulfide Cross-Linking Construction.

The functional rotation mechanism proposed first in 2006 highlighted the importance of AcrB conformational change during substrate efflux.[53, 55] During this three-step mechanism, each protomer of the AcrB trimer adopts a distinct conformation. The

conformational changes are driven by the proton translocation into the cytoplasm from the periplasm through a pathway along the transmembrane domains of AcrB. As discussed above, the relative locations of the periplasmic subdomains change during the functional rotation. This cycling mechanism suggested that AcrB acts as a peristaltic pump through the opening and closing of the drug-binding pockets and access to the TolC. Furthermore, it has been speculated that the conformational changes caused by substrate binding and proton motive force may transfer through AcrA bound to the cleft.[53] Using the online server of "Disul*fi*de by Design 2.0" (http://cptweb.cpt.wayne.edu/DbD2/),[147] we identified six sites on the inter-subunit interface to introduce Cys pairs and used these pairs to study the flexibility and relative conformational change at the corresponding locations.

The locations of the six cys pairs are shown in Figure 2.1. Residues G51, N70, Q123, and P116 are located in the PN1 subdomain. S167 and F316 are in the PN2 subdomain. Q687 and G689 are in the PC2 domain. A215 and S233 exist in the long-extended loop that penetrates deep into the neighboring subunit. R765 exists at the tip of a long loop formed by the C- terminal half of AcrB, which is equivalent to the extended loop in the N-terminal half of AcrB. Q726 is located at the boundary between PC2 and the DC domain. These introduced cysteine pairs were expected to form crosslinks at the inter-subunit interface between the PN1−PN2 subdomains (N70C/ S167C), PN1−PN1 subdomains (P116C/Q123C), PN2−PC2 subdomains (F316C/Q687C), the loop and DC subdomain (S233C/Q726C), the loop and PN1 subdomain (G51C/ A215C), and the PC2-DC subdomains (G689C/R765C). From the four subdomains in the porter domain, PN1−PC2 and PN2−PC1 form the binding pockets. The proximal binding site involves PC1−PC2 interaction, and PN1−PN2 is important in the exit stage of the substrate.[87] Furthermore, V105C in the PN1 domain, which has been reported to form a disulfide bond in an AcrB trimer, was used as a control to reveal the migration position of a disulfide bond-linked dimer.[148] Cell lysate samples prepared from BW25113Δ*acrB* and BW25113Δ*acrB* transformed with plasmid pQE70-cLAcrB were used as the controls. In cLAcrB, two intrinsic Cys residues were replaced with Ala.
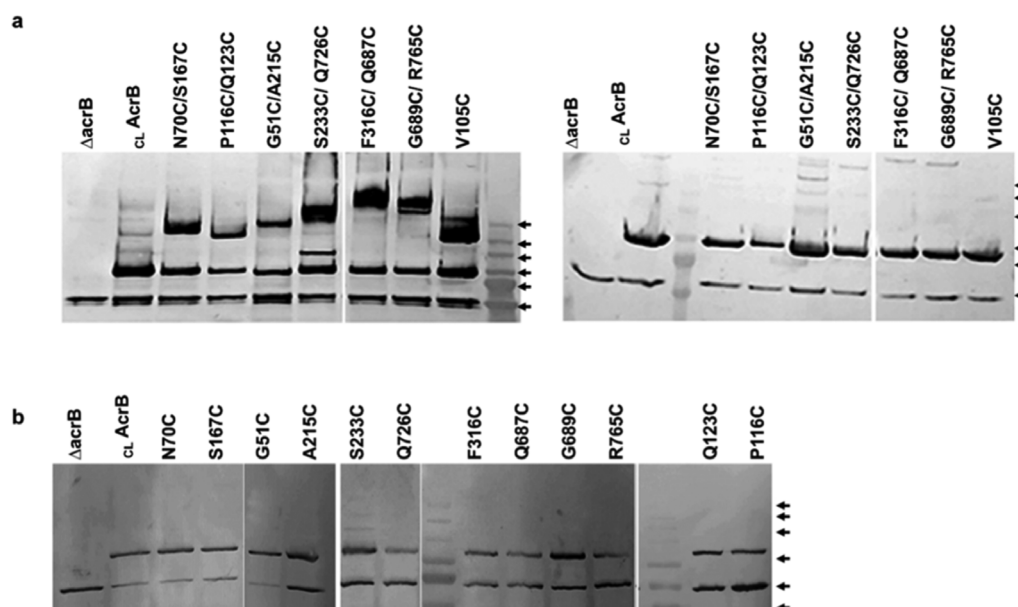
Figure 2.2 Western blot analysis of disulfide bond formation in AcrB mutants.
(a) Double-cysteine mutants, with nonreduced samples shown on the left and reduced
samples shown on the right. (b) Single-cysteine mutant samples without reduction. Bands
in the molecular weight marker are highlighted using black arrows. From top to bottom,
the arrows correlate with molecular weights of 245, 190, 135, 100, 80, and 58 kDa.

Table 2.2 Percentage of Oligomers in Mutants

AcrB mutants	N70C/ S167C	P116C/ Q123C	G51C/ A215C	S233C/ Q726C	F316C/ Q687C	G689C/ R765C	V105C
oligomer (%)	58.3 ± 5.4	53.2 ± 11.4	60.6 ± 6.8	69.1 ± 6.6	68.9 ± 6.4	74.9 ± 6.8	57.9 ± 13.2

2.3.2 Detection and Quantification of Disulfide Bond Formation.

The formation of disulfide crosslinks was analyzed using Western blot analysis
with an anti-AcrB antibody. In the absence of the reducing reagent, all six pairs formed

oligomers (Figure 2.2a). IAM was added before the lysis of the cells to prevent the formation of a disulfide bond during the cell lysis and analysis process. An unknown band close to the 58 kDa marker could be observed in all samples, including the negative control. This band has been observed in previous studies using the same antibody[149]. It could be an unknown protein that also contains a stretch of a similar peptide like the one used to raise the antibody. Since this nonspecific band is well separated from those of the AcrB band, it does not interfere with the interpretation of the data. The intensity of this nonspecific band also served as a loading control. Otherwise, the cell lysate prepared from BW25113Δ*acrB* did not have a protein band, confirming the good specificity of the antibody. The background construct $_{CL}$AcrB migrated with an apparent molecular weight of ~100 kDa, consistent with a monomer. The oligomers formed by other Cys pair constructs are likely dimer or trimers. The treatment with 10% *β*-mercaptoethanol led to a complete reduction of oligomers to monomers, further confirming that the high-molecular-weight bands were formed due to disulfide bonds. The expression level of most Cys pair constructs was similar to that of $_{CL}$AcrB, while the P116C/Q123C pair seemed to express significantly less.

Furthermore, Western blot analysis of single-cysteine mutations revealed that no high-molecular-weight oligomers were present, confirming that disulfide bonds were formed between the pair of cysteines (Figure 2.2b). The mobility of oligomers was different for different Cys pairs. In an AcrB trimer containing a Cys pair at each inter-subunit interface, there are four possible products: a circular trimer trapped with three disulfide bonds, a linear trimer trapped with two disulfide bonds, and a disulfide bond trapped dimer plus a monomer. We included V105C in this study as a mobility marker, as it would migrate as a monomer and a disulfide bond-linked dimer. Through comparison with the V105C dimer bands, it appeared that the mobility of P116C/Q123C, G51C/A215C, and N70C/S167C oligomers seemed to be closer to that of the V105C dimer with an apparent molecular weight of ~200 kDa, and the oligomer formed in F316C/Q687C, G689C/R765C, and S233C/Q726C constructs migrated slower than the V105C dimer and with apparent molecular weight larger than the highest band in the marker (245 kDa). Disulfide bond introduced at different locations has a clear impact on the mobility of the protein.

While all Cys pair mutants formed a significant portion of disulfide bond-linked oligomers, they all have a monomer population. We used the software ImageJ to analyze the percentage of crosslinked products in each of the mutants.[150] The percentage of crosslinked oligomers ranged from 53 to 75% (Table 2.2). Several factors may affect the level of disulfide bond formation between two residues in the structure of a protein, the distance between the residues, the compatibility of the geometry of the Cys pair to that of a disulfide bond, and the intrinsic flexibility of the relevant protein regions including both the backbone and the side chain (the B-factor).[147] We noted that one of the Cys pairs we created in this study, S233C/Q726C, have been reported in a previous study by Seeger et al.[151]. The previously reported cross-linking level of $17.0 \pm 0.4\%$ is significantly lower than our observation (69.1 ± 6.6). The difference could be due to differences in the cell culture and sample procession procedure. An extra band could be observed at $\sim$120 kDa, which disappeared upon reduction. We speculate that this could be a different protein conformation that was trapped by the disulfide bond. This band could also be observed, although at a lower concentration, in the study by Seeger et al. [151]

2.3.3 Functional Analysis of Cysteine Mutations through Drug Susceptibility Assay.

To evaluate the impact of the introduced Cys mutations and subsequent formation of disulfide bond on AcrB function, we measured the MIC of BW25113Δ*acrB* transformed with plasmids encoding each single or double Cys mutant. Four known AcrB substrates were used in the assay (Table 2.3). If relative movement at the respective sites is important for efflux, we expect the formation of disul*fi*de bonds at these sites would affect protein function.

Table 2.3 MIC (µg/mL) Values for *E. coli* Containing Single- or Double-Cysteine AcrB Mutants

Plasmid	novobiocin	erythromycin	EtBr	TPP
none	8	4	16	16
cLAcrB	128	128	256	512
S167C	64	64	128	512
N70C	128	64	128	512
N70C/S167C	64	64	128	512
Q123C	64	64	128	256
P116C	64	64	256	512
P116C/Q123C	32	64	128	256
G51C	64	128	128	256
A215C	128	128	256	512
G51/A215C	64	128	128	256
Q726C	64	128	256	512
S233C	128	128	256	512
S233C/Q726C	64	128	256	512
F316C	64	64	256	512
Q687C	128	128	256	512
F316C/Q687C	16	16	32	32
R765C	64	64	256	512
G689C	64	64	256	512
G689C/R765C	32	32	128	256
V105C	16	32	64	128
V105G	32	32	128	128

The behavior of the constructs could be clustered into two groups. In the first group, the Cys pair mutants behaved similarly as the less active single mutant for most of the substrates tested. Four out of the six constructs belonged to this group. Strains containing N70C, S167C, or the N70C/ S167C double mutant all had similar MIC values as the

positive control _{CL}AcrB for TPP, while the MIC of the other three compounds was reduced by half. The Q123C mutation reduced the MIC of all four drugs tested by half, while the P116C mutation only affected the MIC of novobiocin and erythromycin. The double mutant P116C/Q123C behaved similar to the single Q123C mutant except for novobiocin, for which the MIC was further reduced by 2-fold. The G51C single mutation led to a 2-fold reduction of the MIC of G51C/A215C double mutation had similar MIC as the G51C single mutant for all four test compounds. Strains containing Q726C, S233C, or the corresponding double mutant had similar MIC as the positive control for all substrates except for novobiocin. The Q726C single mutant and the double mutant displayed a 2- fold reduction in MIC for novobiocin.

The other two pairs belong to the second group. For the F316C/Q687C pair and the G689C/R765C pair, strains containing the double mutants displayed lower MICs for all four compounds tested than the corresponding single mutants. While the Q687C mutation did not lead to an observable reduction of activity, the F316C mutation led to a 2-fold reduction of MICs for novobiocin and erythromycin. The F316C/Q687C double mutant displayed an 8- to 16-fold reduction in MIC for all substrates. Similarly, R765C and G689C single mutants had similar activity as the positive control for EtBr and TPP, and a 2-fold reduction of MIC for erythromycin and novobiocin. The double mutant showed lower activity toward all four compounds with a reduction in MIC of 2- to 4-fold. For this group, there is a possibility that the observed higher susceptibility of the cysteine double mutants is due to the restriction of conformational change resulted from crosslinks, which impaired the efflux activity of AcrB. We have also included V105C and V105G mutants in this study. As expected, mutation of V105 led to a significant reduction of efflux activity as the MICs of all four compounds tested were reduced. For novobiocin and EtBr, the MICs of the strain containing V105C were 2-fold lower than that of the V105G.

2.3.4 Restoration of the Activity by Dithiothreitol (DTT) Detected Using EtBr Accumulation Assay.

If the previously observed higher drug sensitivity is a result of disulfide bond formation, the reduction of the disulfide bonds should restore the efflux activity. This was

investigated using the EtBr accumulation assay. We found that DTT at 10 mM could not fully reduce the disulfide bonds formed in our AcrB constructs, even with 4 h incubation (Figure 2.3). While the portion of monomers did increase after the treatment, clear oligomer bands could still be observed in all cases. And for some samples, multiple oligomer bands could be observed after this treatment, which are likely partially reduced oligomers. When incubated with 50 mM DTT, disulfide bonds could be completely reduced after 1 h incubation (Figure 2.3). Thus, this higher DTT concentration was used for the accumulation assay.
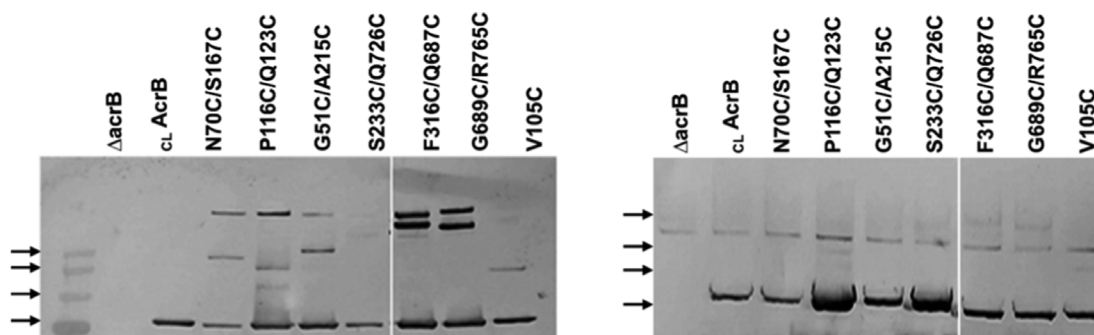
Figure 2.3 Anti-AcrB Western blot analysis of double-cysteine AcrB mutants under different reduction conditions.
Left: Reduced with 10 mM DTT and incubated for 4 h at room temperature. Oligomers are only partially reduced. Right: Reduced with 50 mM DTT and incubated for 1 h at room temperature. Oligomers are fully reduced. The bands in the molecular weight marker are highlighted by black arrows. From top to bottom, the molecular weights are 245, 190, 135, and 100 kDa.

Cells containing the indicated plasmids were prepared as described in Section 2.2.4 for the EtBr accumulation assay. We included all six pairs, as well as V105C, in the study for comparison. For four out of the six Cys pair constructs, the DTT treatment did not lead to a significant difference in the rate of EtBr accumulation (Figure 2.4). However, for the other two pairs, F316C/Q687C and G689C/R765C, reduced samples exhibited notably lower accumulation of EtBr, indicating that the formation of a disulfide bond contributed significantly to the reduced activity. This indicated that the reduction of disulfide crosslinks by DTT at these two locations had partially restored the efflux activity (Figure 2.4d,e). In a previous study by Takatsuka and Nikaido, the introduction of the F316C/ Q687C double

mutant has also been shown to greatly reduce the efflux activity, consistent with our observation[97].
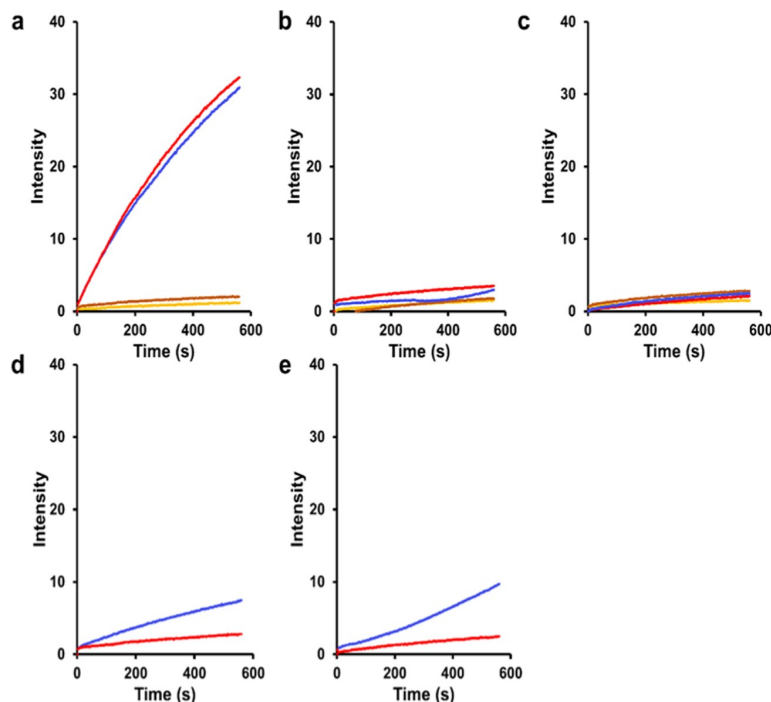
Figure 2.4 EtBr accumulation assay of all double-cysteine mutants with or without reduction.
(a) Negative control BW25113ΔacrB (blue no DTT, red with DTT) and positive control BW25113ΔacrB expressing plasmid-coded cLAcrB (orange no DTT, brown with DTT). (b) BW25113ΔacrB expressing AcrB mutants N70C/S167C (blue no DTT, red with DTT) or P116C/Q123C (orange no DTT, brown with DTT). (c) BW25113ΔacrB expressing AcrB mutants G51C/A215C (blue no DTT, red with DTT) or S233C/Q726C (orange no DTT, brown with DTT). (d) BW25113ΔacrB expressing AcrB mutant F316C/Q687C (blue no DTT, red with DTT). (e) BW25113ΔacrB expressing AcrB mutant G689C/R765C (blue no DTT, red with DTT).

2.5 V105 Mutations and Efflux.

V105C is located in a helix close to the threefold axis of the AcrB trimer and forms a disulfide bond.[148] It was speculated that the formation of a disulfide bond restricted the conformational changes to reduce the efflux activity. In our study, we observed low MIC

values (Table 2.3) for novobiocin and erythromycin, consistent with previous studies, indicating that the mutation significantly impacted AcrB activity.[148] However, the DTT treatment reduced the dimer but only led to a modest reduction of EtBr accumulation in BW25113*ΔacrB* expressing V105C (Figure 2.5). To further investigate the potential role of the disulfide bond in activity, V105 was mutated to Gly. Accumulation of EtBr in BW25113*ΔacrB* containing V105G was higher than that in the positive control, indicating that the replacement of Val itself is detrimental to function. This result is consistent with the MIC measurement. Accumulation of the strain containing V105C was higher than that in the strain containing V105G, suggesting that the formation of the disulfide bond further impaired efflux. Upon reduction, accumulation in the V105C strain was reduced to be more similar to the accumulation in the V105G strain.
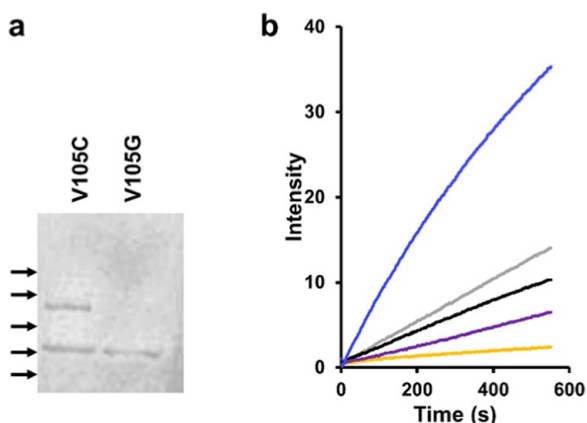
Figure 2.5 Analysis of V105C and V105G.
(a) Anti-AcrB Western blot analysis of V105C and V105G, showing the formation of a disulfide bond in V105C but not V105G. The molecular weight of bands in the marker is highlighted by black arrows. From top to bottom: 245, 190

2.4 Conclusions

The structure of the entire AcrABZ-TolC complex has been revealed using cryoEM.[65, 152] More recent studies illustrated the in situ structure of the complex in *E. coli* cells overexpressing the pump components.[138] While these structure insights have led to the answer of many questions related to the mechanism of efflux by the RND pumps, studies on the dynamic aspects of the pumps lag far behind. As any molecular machines,

the AcrAB-TolC system undergoes a conformational change to carry out efflux. While the combination of structures, which are snapshots of proteins, and computational simulation cast lights on how proteins move, experimental testing of the simulation movies is critical. Based on the crystal structure of AcrB, we designed and engineered six Cys pairs to examine the consequence of these structure staples on its efflux activity. We found that for four pairs, the formation of a disulfide bond did not seem to have much impact on efflux, as the double mutant behaved similarly as the less active single mutants. Relative inter-subunit movement at these sites does not seem to be required for efflux.

For the other two pairs, the double mutants are less active than the individual single mutants, which could be potentially due to the restriction effect from the disulfide bond that either restricted relative movement of neighboring subunits or locked the subunits in a conformation incompatible with substrate binding and/or translocation. While the activity of the efflux pump is most conveniently evaluated using the MIC assay, the effect of disulfide bond on activity could not be measured this way since the high concentration of reducing reagent that is necessary to effectively reduce the disulfide bonds would inhibit *E. coli* growth. Alternatively, EtBr efflux could be monitored using cells containing reduced or nonreduced AcrB Cys pair constructs. We found that for two pairs, F316C/Q687C and G689C/R765C, reduction of the disulfide bond significantly improved efflux, confirming the functional relevance of conformational flexibility at these sites. There appears to be a discrepancy between the apparent percentage of cross-linking with the level of reduced activities in these double mutants, which is most likely explained by the different growth phases the cells were harvested for the two types of experiments. For the activity (MIC) measurement, the proliferation of cells was monitored in the presence of test compounds. For the EtBr accumulation assay, mid-log phase cells were taken and used in the study, whereas for the cross- linking analysis, overnight cultures were taken, and those cells were in the stationary phase and took longer time for disulfide formation.

Apart from the interference by disulfide bond formation on the function of AcrB, the reduction of the activity of the Cys pairs could be due to an unfavorable conformation of the disulfide dimers that interfere with the substrate binding and transport activity. Interestingly, the two sites with high impact on activity are located close to each other, with one containing Q687C and the other containing G689C, just two residues apart (Figure 2.1,

brown and yellow dots). While F316C/ Q687C forms a disulfide bond at the interface between the PN2 and PC2 subdomain of the neighboring subunit (brown), G689C/R765C linked the PC2 subdomain to the tip of the long loop formed by the C-terminal half of the neighboring subunit.

Since each subunit in an AcrB trimer contains a separate and complete set of substrate binding residues and translocation pathway, a conformational change that is involved in substrate binding and extrusion should be localized more to the inside of a subunit. Yet, relative inter-subunit conformational change has been reported in several cases to be critical for AcrB function, likely due to the functional rotation mechanism in which the trimer needs to undergo conformational change simultaneously. Thus, some of the sites that are located at the inter- subunit interface are expected to be the "sensor" sites that need to play the role of coordinating the movement. While in other sites, including several sites described in this, and V225C/ A777C, R558C/E839C, V32C/A299C, and I235C/K728C reported in previous studies (Table 2.4), Cys substitution and disulfide bond formation do not have a clear impact on functions.[151] These could be sites that maintain close contact throughout the functional rotation mechanism to maintain AcrB as a tightly associated, integrated, functional trimer.

Table 2.4 Engineered Disulfide Bonds in AcrB[a]

Res1	Res2	oligomer (%)	activity level	citation
Inter-Subunit				
G51	A215	60.6 ± 6.80	+++	this study
Q123	P116	53.2 ± 11.4	++	
S167	N70	58.3 ± 5.4	+++	
F316	Q687	68.9 ± 6.4	−	
Q726	S233	69.1 ± 6.6	+++	
R765	G689	74.9 ± 6.8	−	
V105C	V105C	57.9 ± 13.2	+	
Q229	R586	46.4 ± 0.5	++	[151]
R558	E839	$-9.5 \pm 4.7e$	+++	

Table 2.4 (Continued)

S562	T837	15.4 ± 1.3e	+	
S132	A294	41.6 ± 0.6	+	
V32	A298	41.3 ± 1.2	+	
V32	A299	18.1 ± 1.0	+++	
Q726	S233	17.0 ± 0.4	+++	
I235	K728	23.8 ± 0.6	+++	
V225	A777	80.2 ± 1.3	+++	
Q229	T583	69.4 ± 0.5	+	
D566	T678	N/A	+	[97, 140]
F666	T678	N/A	−	
F666	Q830	N/A	+	
F316	Q687	N/A	++	[97]
F316	A688	N/A	+	
F316	G854	N/A	−	
Intra-Subunit				
V32	I390	82.5 ± 6.8	+++	[141]
T44	T91	100.7 ± 3.0	+++	
M184	V771	76.2 ± 4.9	+++	
T199	T749	82.7 ± 2.9	+++	
I335	A995	51.7 ± 0.8	+++	
T574	A627	102.9 ± 6.8	+++	
Q726	G812	97.7 ± 5.0	+++	
G570	A627		+++	
F572	A627		+++	
V576	A627		+++	
L578	A627		+++	

[a]+++: MIC equals to 50−100% of the wild-type MIC. ++: MIC equals to 25% of the wild-type MIC. +: MIC equals to 12.5% or less of the wild-type MIC. −: MIC close to the negative control MIC

CHAPTER 3.   Insight into the AcrAB-TolC complex assembly process learned from competition studies

Reproduced in parts with permission from[153], antibiotics; published by MDPI 2021.

3.1   Introduction

Antimicrobial resistance, especially multidrug resistance in bacterial pathogens, is among the top 10 global threats to humanity [15]. Among the large array of different defense mechanisms adapted by bacteria, the overexpression of efflux pumps has a significant role in conferring multidrug resistance. AcrAB-TolC is one of the most extensively studied efflux pump systems in Gram-negative bacteria, playing a crucial role in the multidrug resistance in bacteria such as *Eshcherichia coli* [57, 69, 154]. AcrAB-TolC is a member of the resistance nodulation division (RND) superfamily. AcrAB -TolC efflux pump confers resistance to a broad spectrum of antimicrobial compounds including β-lactams, tetracycline, novobiocin, and fluroquinolones [51, 52]. This tripartite efflux transporter consists of three major protein components [135, 136], an outer membrane channel TolC, a periplasmic adaptor protein (PAP) AcrA, and an inner membrane proton-driven antiporter AcrB [70, 74, 87, 137]. TolC forms a channel that spans the outer membrane and acts as the exit pathway of substrates translocated from the inner membrane and the periplasmic space. AcrA has function in stabilizing the connection between the two membrane components TolC and AcrB [58, 59]. The RND transporter protein AcrB is responsible for substrate recognition and energy transduction. Upon binding of a substrate, AcrB uses the energy from the proton flow down its concentration gradient through a proton translocation pathway in the transmembrane domain to drive the conformational change necessary to move the substrate upward toward the exit tunnel [56, 57]. TolC is shared by several efflux systems, hence *E. coli* strains deficient in TolC are more sensitive to a wider variety of chemicals (e. g. detergents, drugs, bile salts, and organic solvents) [60, 61].

With the dedication of many research groups, the structure and mechanism of drug efflux by the RND pumps have been brought to light. The first crystal structure of the pump component was determined for TolC by Koronakis et al. [64] in 2000. TolC is a trimer with

an overall length of 140 Å with 40 Å in the β-barrel domain mainly composed of β strands, and 100 Å in the periplasmic domain mainly composed of α-helices. The periplasmic end of the TolC tunnel is sealed at the resting state, which likely opens by an allosteric protein–protein interaction mechanism [138]. In 2002, Murakami et al. first reported the crystal structure of AcrB, followed by the proposal of the functional rotation mechanism [53, 63, 96]. Later in 2006, Mikolosko and coworkers determined the crystal structure of AcrA. In contrast to the trimeric TolC and AcrB, AcrA forms a hexamer in the pump assembly [62]. The assembled pump structure was first proposed as the "deep interpenetration model", which shows that AcrB and TolC have direct interactions with AcrA wrapped around on the outside to strengthen the interaction [71]. More recently, Wang et al. proposed a new model based on Cryo-EM studies, known as the "tip-to-tip model". In this model, AcrA hairpins form a barrel-like conformation, contacting TolC in a tip-to-tip arrangement [65, 72]. The recent determination of the complex structure first by cryo-EM, then by X-ray crystallography, confirmed the tip-to-tip model [55, 63, 82, 83, 91, 136, 138]. Energy does not seem to be required to assemble the AcrAB-TolC complex and AcrAB could interact with the TolC channel to form a AcrAB-TolC complex even in the absence of known substrate [77]. The dynamic process that leads to the formation of the complex is still elusive.

The dominant negative effect describes the phenomena in which an excess of a functionless mutant of a protein in the presence of its wild type counterpart, reduces the observed activity due to competition from the mutant for interaction with functional partners of the protein of interest. In the AcrAB-TolC complex, over-expression of functionless AcrB or AcrA mutant in wild type *E. coli* strains is expected to drastically reduce the assembly of functional efflux complex, and thus reduce the efflux activity and increase the sensitivity to substrate compounds. However, we tested the overexpression of several functionally defective mutants in the wild type *E. coli* strain, but did not observe the expected level of reduction. We speculate that the assembly of the AcrAB-TolC is a precisely controlled process involving delicate proof-reading procedures.

3.2 Materials and Methods

3.2.1 Bacterial strains, plasmids and growth conditions

Escherichia coli BW25113 and BW25113Δ*acrB* were obtained from Yale *E. coli* genetic resources. BW25113Δ*acrAB* was constructed using *E. coli* gene deletion kit (Cat #K006, Gene Bridge) following the manufacturer's protocol. Plasmids pBAD33-AcrB was created in our previous study[155]. To create the plasmid pBAD33-AcrAB, *acrAB* gene was amplified from genomic DNA of BW25113 and cloned into pBAD33 by following the fast cloning method described previously by Li et al.[156]. Plasmids pBAD33-AcrB, and pBAD33-AcrAB were used as the templates to create respective mutations discussed below. Mutations were introduced using the Quikchange Site Directed Mutagenesis Kit following manufacturer's instruction (Agilent, Santa Clara, CA). Primers used in this study mentioned in Table 3.1. Bacteria were cultured at 37°C with shaking at 250 rpm in Luria broth (LB) media unless otherwise noted.

Table 3.1 Primers used in this study

Construct	Primer (5'-3')
AcrB D408A-F	CATCGGCCTGTTGGTGGATGCCGCCATCGTTGTGGTAG
AcrB D408A-R	CTACCACAACGATGGCGGCATCCACCAACAGGCCGATG
AcrB K940A-F	CCATTGGGTTGTCGGCGGCTAACGCGATCCTTATCG
AcrB K940A-R	CGATAAGGATCGCGTTAGCCGCCGACAACCCAATGG
AcrB R971A-F	CTTGATGCGGTGCGGATGGCATTACGTCCGATCCTGATG
AcrB R971A-R	CATCAGGATCGGACGTAATGCCATCCGCACCGCATCAAG
AcrB T978A-F	CGTCCGATCCTGATGGCCTCGCTGGCGTTTATCCTC
AcrB T978A-R	GAGGATAAACGCCAGCGAGGCCATCAGGATCGGACG
AcrB F178A- F	GGGTGATGTTCAGTTGGCCGGTTCACAGTACGCGATG
AcrB F178A- R	CATCGCGTACTGTGAACCGGCCAACTGAACATCACCC
AcrB I278A-F	GGTGAGAACTACGACATCGCCGCAGAGTTTAACGGCCAAC
AcrB I278A-R	GTTGGCCGTTAAACTCTGCGGCGATGTCGTAGTTCTCACC
AcrB F610A -F	CAACGTTGAGTCGGTGGCCGCCGTTAACGGCTTCGGC

Table 3.1 (Continued)

AcrB F610A -R	GCCGAAGCCGTTAACGGCGGCCACCGACTCAACGTTG
AcrA P57C-F	CAG ATC ACA ACC GAG CTT TGT GGT CGC ACC AGT GCC TAC
AcrA P57C-R	GTA GGC ACT GGT GCG ACC ACA AAG CTC GGT TGT GAT CTG
AcrA T217C-F	CCG ATC GTT GAT GTG TGT CAG TCC AGC AAC GAC TTC
AcrA T217C-R	GAA GTC GTT GCT GGA CTG ACA CAC ATC AAC GTA GAT CGG
AcrB N191C-F	CGT ATC TGG ATG AAC CCG TGT GAG CTG AAC AAA TTC CAG
AcrB N191C-R	CTGGAATTTGTTCAGCTCACA CGG GTT CAT CCA GAT ACG
AcrB S258C-F	CTG AAA GTG CAG GAT TGT CGC GTG CTG CTG CGT TCC
AcrB S258C-R	GGA ACG CAG CAC GCG ACA ACC ATC CTG ATT CAG TTT CAG

3.2.2 Drug susceptibility assay

The minimum inhibitory concentration (MIC) was determined for erythromycin, novobiocin, ethidium bromide (EtBr), rhodamine 6G (R6G) and tetraphenylphosphonium chloride (TPP) following the CLSI guidelines.[144] Briefly, overnight cultures of the indicated strain were diluted to a final concentration of 10^5 CFU/mL in fresh Muller Hinton Broth 2 (cation adjusted) media (Millipore Sigma, St.Louis, MO) in a 48 well microtiter plate containing the indicated compounds at two-fold serial dilutions. Plates were incubated at 37°C with shaking at 160 rpm for 17 hrs the absorbance at 600 nm (OD_{600}) were measured to identify the lowest concentrations with no observable cell growth.

3.2.3 Protein expression, SDS-PAGE and Western blot analysis

For expression test, 5 mL of cells were cultured overnight at 37°C with shaking at 250 rpm. In the next morning, the cell was inoculated with a 100-fold dilution into a 5 ml fresh LB media supplemented with antibiotics and grow until ~ OD600 1.0. Cells were pelleted and resuspended in 1 mL phosphate buffer containing phenylmethylsulphonyl fluoride (PMSF) (1:1000 dilution of a saturated ethanol solution) and sonicated for 1 min followed by centrifugation for 10 mins at 15,000 rpm. The supernatant was removed, and cell pellets were resuspended in 0.1 mL PBS containing 2% Triton-X100. The samples were incubated at room temperature with shaking for 45 mins and centrifuged again for 10 mins. The supernatant was used for SDS-PAGE and Western blot analysis. For studies of disulfide bond formation, iodoacetamide (IAM) was added to a final concentration of 20 mM in all buffers. To reduce disulfide bond, β-mercaptoethanol (BME) was added to a final concentration of 2% followed by incubation at room temperature for 30 mins.

For Western blot analysis, after transferring to the PVDF membrane, protein bands were detected using an Anti-AcrB polyclonal (Rabbit) antibody raised to recognize a C-terminal peptide corresponding to residues number 1036-1045[145]. The membrane was then washed and incubated with an alkaline phosphatase conjugated Goat anti-Rabbit secondary antibody. The BCIP/NBT (5-bromo-4-chloro-3'-indolyphosphate and nitro-blue tetrazolium) solution was used to stain the membranes.

For AcrAB dissociation experiment, BW25113 or BW25113*ΔacrA* containing plasmid pBAD18-AcrA was cultured to the log phage (OD600 0.8) and arabinose was added to a final concentration of 0.2% (*w/v*) to induce the expression of AcrA for 50 min. The cells were then pelleted, washed, and resuspended with fresh LB. An aliquot of cell culture was collected, pelleted, and stored at −20 °C. The rest of the cell culture was returned to the shaker and cultured for 5 h, and another aliquot of sample was collected, pelleted, and stored at −20 °C. The last sample was collected at 17 h. OD600 of the samples were measured and used to adjust the sample volume collected to ensure that the same number of cells were used for each time point. All pellets were resuspended and sonicated to lyse the cells. After centrifugation, the pellet was extracted using PBS + 2% Triton for 2 h. The mixtures were centrifuged again and the supernatants were incubated with Ni beads for 40 min, followed by washing with the same buffer supplemented with 50 mM

imidazole, and finally eluted with the same buffer supplemented with 500 mM imidazole. For DSP crosslinking experiments, the cell pellet was washed and then resuspended in PBS buffer. DSP was added to a final concentration of 1 mM, and the mixture was incubated at room temperature for 30 min. To stop the reaction, a Tris-Cl buffer (pH 8.0) was added to a final concentration of 20 mM. Cells were then pelleted, and proteins were purified similarly as described above. To break the disulfide bond in DSP, DTT was added to the sample to a final concentration of 10 mM. For Western blot analysis, Anti-AcrB polyclonal (Rabbit) antibody or Anti-AcrA antibody used respectively. All experiments were repeated at least three times.

3.3   Results and discussion

3.3.1 AcrB mutants defective in proton transport

Several key residues have been identified in the AcrB transmembrane domain, forming the proton translocation pathway [55, 63, 88, 139, 157-161]. We have created single alanine replacement mutations at each of these sites to obtain mutants AcrB-D407A, AcrB-D408A, AcrB-K940A, AcrB-T978A, and AcrB-R971A [158, 160]. The plasmid encoding of these mutants was first transformed into the BW25113Δ*acrB* strain to examine their efflux activity (Table 1). As expected, the minimum inhibitory concentrations (MICs) of most examined substrates against the strains containing the mutants were the same as those against the strains without plasmids. The only mutant that displayed significant activity is T978A, which remained partially active. As a positive control, we showed that transformation with a plasmid encoding the wild type AcrB completely restored the efflux activity with MIC values similar to a wild type BW25113 strain. Next, we transformed these plasmids into the wild-type BW25113 strain and measured the MIC. We expected the AcrB mutants to compete with the genomic AcrB in binding and interaction with genomic AcrA and/or TolC, thus reduce the number of functional efflux complexes and subsequently the drug susceptibility. However, we observed a two-fold reduction of MIC value in some cases, and no reduction others, which is consistent with an earlier study reporting the modest reduction of substrate susceptibility when AcrB-D407A was over-expressed in a wild -type *E. coli* strain (Table 3.2) [145].

Table 3.2 MIC values (μg/mL) of BW25113 or BW25113ΔacrB strains containing the indicated plasmid encoding AcrB mutants defective in proton translocation pathway.

Substrate [1]	NOV	ERY	TPP	EtBr	R6G	NA
BW25113Δ*acrB* *c*ontaining						
/	4	4	4	8	8	1
WT	128	64	256	128	256	4
D407A	4	4	4	8	8	ND
D408A	4	4	4	8	8	ND
K940A	8	4	4	8	8	ND
R971A	8	4	4	8	16	ND
T978A	8	8	16	32	128	ND
BW25113 containing						
/	256	64	1024	512	1024	4
WT	512	128	1024	512	1024	4
D407A	128	64	1024	256	512	4
D408A	128	64	1024	512	1024	4
K940A	256	64	1024	512	1024	4
R971A	128	32	1024	512	1024	4
T978A	256	64	1024	512	1024	2

[1] NOV, novobiocin. ERY erythromycin, TPP tetraphenylphosphonium, EtBr ethidium bromide. R6G, rhodamine 6G, NA, nalidixic acid. ND, not determined.

We conducted the MIC assay under the basal expression condition without induction to avoid the potential artifact that may arise from over-expression. To examine how much of each mutant actually expressed under the basal condition, we prepared samples from BW25113 containing different plasmids, and compared the expression level from the plasmid to the level of genomic AcrB. Even without induction, under our experimental condition, the plasmid-encoded mutants were expressed at a much higher level (5–20 folds higher) compared to the level of the genomic AcrB (Figure 3.1a). This result indicates that the lack of impact on drug susceptibility is not due to the lack of

expression. Even presented at a large excess, the mutants were not effective in disrupting the normal efflux activity.

Single mutations on the proton relay pathway do not significantly affect the overall structure of AcrB. The crystal structure of a couple of these mutants have been determined using X-ray crystallography [158, 162]. All mutants form trimeric structures similar to those in the wild-type AcrB [158]. To examine if a mutant defective in proton translocation could still bind AcrA, we used two inter-subunit disulfide bonds as our yardsticks to probe the interaction between AcrA and AcrB. We first constructed a plasmid expressing both AcrA and AcrB (pBAD33-AcrAB), then introduced a pair of cysteines, one in AcrA and the other in AcrB: AcrA-P57C/AcrB-N191C, and AcrA-T217C/AcrB-S258C. These residues are predicted to be close to each other according to the "Disulfide by Design 2.0" (http:// cptweb.cpt.wayne.edu/DbD2/ (accessed on 06/01/2019))[147]. The formation of disulfide bond linked AcrA-AcrB complex was confirmed using anti-AcrA and anti-AcrB Western blot (Figure 3.1b). A high molecular weight complex could be detected in both blots, which disappeared upon incubation with β-mercaptoethanol (BME). The disulfide bond-linked species migrated slightly differently in the gel, likely due to differences in the conformations of the two complexes under the gel running condition. Mutation and disulfide bond formation did not significantly impair efflux activity, as revealed in the MIC measurement (Table 3.2). Next, we introduced the D408A mutation into both constructs to examine the effect of this additional mutation on the formation of disulfide bond linked AcrA-AcrB complex. If the D408A mutation had a significant impact on the interaction between AcrB and AcrA, we expect to see a reduction of the intensity of the high molecular weight AcrA-AcrB complex. As shown in Figure 3.1c, disulfide bond formation was to a similar level in both constructs, suggesting that the additional D408A mutation did not have a significant impact on AcrA-AcrB interaction.

To examine if the additional expression of AcrA from the same plasmid as the AcrB-D408A have any impact on the competition with the genomic AcrB, we introduced plasmid pBAD33-AcrAB-D408A into the wild type BW25113 strain and examined the MIC. Both AcrA and AcrB-D408A expressed at levels much higher than their genomic counterparts (Figure 3.1d), and yet, no dominant negative effect was observed (Table 3.3).
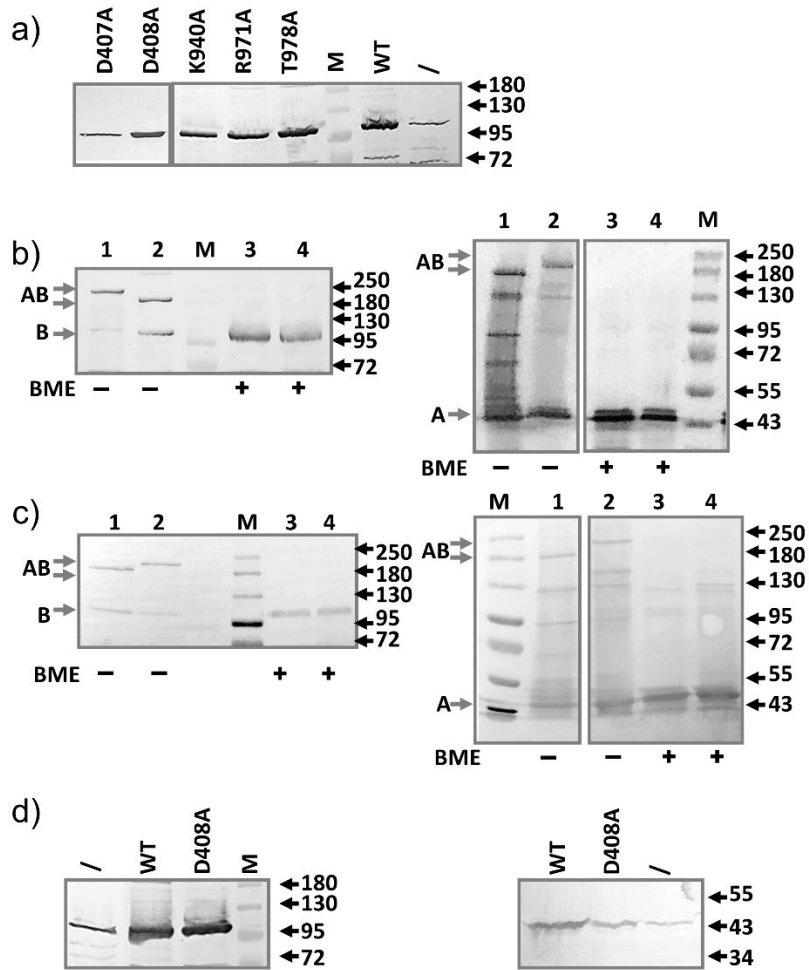
Figure 3.1 Characterization of mutants defective in the proton translocation pathway.

a) The point mutation did not affect expression level. Anti-AcrB Western blot analysis of the expression of all five mutants and the wild-type AcrB from plasmid transformed into BW25113. Sample prepared from plasmid-free BW25113 (\) was also prepared and loaded to serve as a control to highlight the difference in expression levels. (**b**) Anti-AcrB and Anti-AcrA Western blot analyses revealing the formation of disulfide bonded AcrA-AcrB complexes, which was reduced after incubation with BME. AcrA-P57C/AcrB-N191C (lane 1 and 3), AcrA-T217C/AcrB-S258C (lane 2 and 4). (**c**) Similar to b, with the additional D408A mutation introduced into the constructs. AcrA-P57C/AcrB-N191C/AcrB-D408A (lane 1 and 3), AcrA-T217C/AcrB-S258C/AcrB-D408A (lane 2 and 4). Molecular weight markers are labeled as "M" and the molecular weight of bands (kD) were indicated on the right. The expected bands for AcrA, AcrB, and disulfide bond linked AcrA-AcrB are marked on the left of the gels as A, B, and AB, respectively. (**d**) Anti-AcrB (left) and anti-AcrA (right) Western blot analysis of BW25113 expressing plasmid pBAD33-AcrAB (WT) or pBAD33-AcrAB-D408A (D408A). Samples prepared from BW25113 not containing plasmid was used as the control (/). For anti-AcrA Western blot, plasmid-containing samples were diluted 4-fold before being loaded into the gel.

56

Table 3.3 MIC values (µg/mL) of BW25113 and BW25113ΔacrAB strains containing the indicated plasmid encoding gene for both AcrA and AcrB.

Substrate	NOV	ERY	TPP	EtBr	R6G
BW25113Δ*acrAB* containing					
/	4	4	8	4	16
WT	32	32	128	128	32
AcrA/AcrB-D408A	4	2	8	8	8
AcrAP57C/AcrBN191C	32	16	64	64	32
AcrA-T217C/AcrB-S258C	64	16	128	128	32
BW25113 containing					
/	256	32	1024	512	512
AcrAB-WT	256	64	1024	512	1024
AcrAB-D408A	256	32	1024	512	512

3.3.2 AcrB Mutants Defective in Substrate Binding

One feature of the AcrAB-TolC complex that has drawn much research interest is their ability to efflux a large array of substrates ranging broadly in molecular weight, charge, and hydrophobicity. Many mutations have been introduced in the substrate binding pocket in AcrB to probe their impact on the efflux of different substrates [55, 100]. We chose three such mutants to include in this study, F610A, I278A, and F178A, since they were reported to have the most significant impact on efflux. First, plasmids containing single residue mutations at these sites were introduced into BW25113Δ*acrB* to examine their activities (Table 3.3). While the F610A mutant is largely inactive, both F178A and I278A remained partially active, which is consistent with previous reports [163]. It is clear that in general, single point mutations introduced at the substrate binding site are not as detrimental as mutations introduced in the proton translocation pathway. This is reasonable when considering several residues collectively form a substrate binding site, while the proton translocation pathway is more linear.

Next, plasmids encoding these mutations were transformed into BW25113 to determine their impact on efflux activity. Similar to proton relay pathway mutants, the MIC values of the strain were not significantly affected (Table 3.4). The presence of AcrB mutants defective in substrate binding does not display the dominant negative phenotype either.

Table 3.4 MIC values (μg/mL) of BW25113 and BW25113Δ*acrB* strains containing the indicated plasmid encoding AcrB mutants defective in substrate binding.

Substrate	NOV	ERY	TPP	EtBr	R6G	NA
BW25113Δ*acrB*						
containing						
/	4	4	4	8	8	1
WT	128	64	256	128	256	4
F610A	8	8	64	32	128	ND
F178A	64	8	128	128	256	ND
I278A	32	32	128	128	128	ND
BW25113 containing						
/	256	64	1024	512	1024	4
WT	512	128	1024	512	1024	4
F610A	512	64	1024	512	1024	2
F178A	512	64	1024	512	1024	4
I278A	512	64	1024	512	1024	4

Next, we examined the expression of these mutants under the basal condition (Figure 3.2a). Similar as described above, the plasmid-encoded mutants were expressed at a much higher level compared to the level of the genomic AcrB, indicating that the lack of impact on MIC is not due to the lack of expression.

To determine if a mutation in the substrate binding pocket of AcrB (F610A) affects interaction between AcrB and AcrA, we used the disulfide bond pairs as described above and introduced an additional AcrB F610A mutation (Figure 3.2b). Similar as in Figure 3.1b, AcrA-AcrB complexes were observed, similar as in samples without the F610A mutation, suggesting that the AcrB F610A mutant still binds with AcrA.
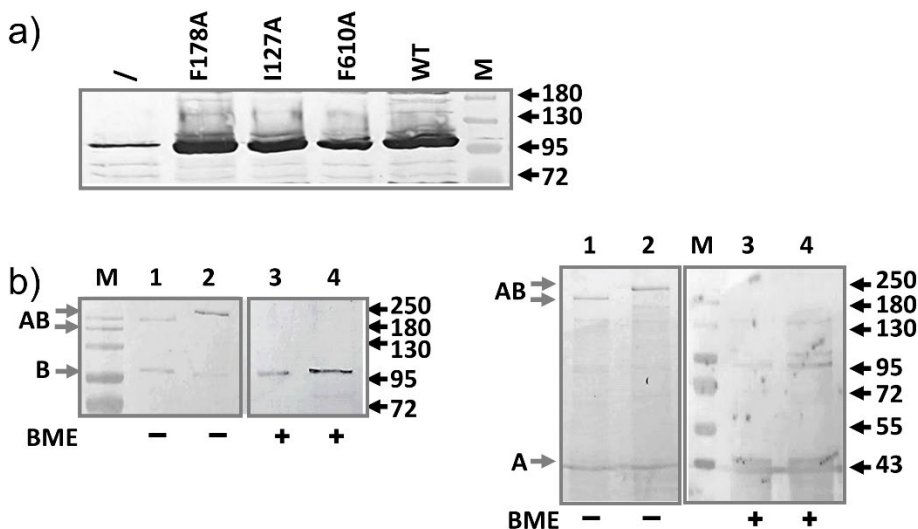
Figure 3.2 Characterization of AcrB mutants defective in substrate binding.

(**a**) The point mutation did not affect expression level. Anti-AcrB Western blot analysis of basal expression of all three mutants and the wild type AcrB from plasmid transformed into BW25113. Sample prepared from plasmid-free BW25113 (\) was also prepared and loaded to serve as a control to highlight the difference in expression levels. (**b**) Anti-AcrB and Anti-AcrA Western blot analyses revealing the formation of disulfide bonded AcrA-AcrB complexes, which was reduced after incubation with BME. AcrA-P57C/AcrB-N191C, F610A is in lane 1 and 3, and AcrA-T217C/AcrB-S258C, F610A in lane 2 and 4. Molecular weight markers are labeled as "M" and the molecular weight of bands (kD) were indicated on the right. The expected bands for AcrA, AcrB, and disulfide bond linked AcrA-AcrB are marked on the left of the gels as A, B, and AB, respectively.

3.3.3 Slow Dissociation of the AcrAB Complex

We speculate that the AcrAB complex, once formed, dissociates very slowly. To experimentally test this speculation, we introduced a plasmid encoding AcrA bearing a

histag at the C-terminus (AcrA-his) into a wild-type and the corresponding *acrA* knockout strains. We first confirmed that under our experimental condition, the genomic AcrB could not be purified using metal affinity chromatography (Figure 3.3a). In the absence of the plasmid, no AcrB could be detected in the eluate in anti-AcrB Western blot. In contrast, when AcrA-his was introduced into the cells, AcrB could be detected in the eluates, indicating that it was co-purified through interaction with AcrA-his. Interestingly, the AcrB band intensity was higher in the eluate prepared from the *acrA* knockout strain, indicating more AcrB were co-purified. Next, we examined the time course of co-purification. The rationale is, in the wild-type strain, genomic AcrB and AcrA form stable complexes. If the dissociation is fast, the introduced AcrA-his will quickly compete with genomic AcrA to form a complex with AcrB, and in turn enable purification of AcrB through metal affinity chromatography. Otherwise, if the dissociation is slow, then it takes much longer for the competition to happen. We monitored the formation of AcrAB complex between the genomic AcrB and plasmid-expressed AcrA-his at three-time points, right after the induction period, and 5 and 17 h after induction (Figure 3.3 b). We performed crosslinking right before protein extraction and purification to stabilize the complexes. As a control experiment, we also examined the formation of the AcrAB complex between the genomic AcrB and plasmid-expressed AcrA-his in an *acrA* gene knock-out strain. In this case, we do not expect competition from the genomic AcrA; thus complex should form faster. We found that the formation of the complex is plateaued much faster in the *acrA* knockout strain, as intensities of the eluates prepared from 5 and 17 h into incubation were very similar. In contrast, it took much longer for AcrB to interact with AcrA-his in the wild type strain, which is likely due to the requirement of an extra step of AcrAB dissociation between the genomic AcrA and AcrB.
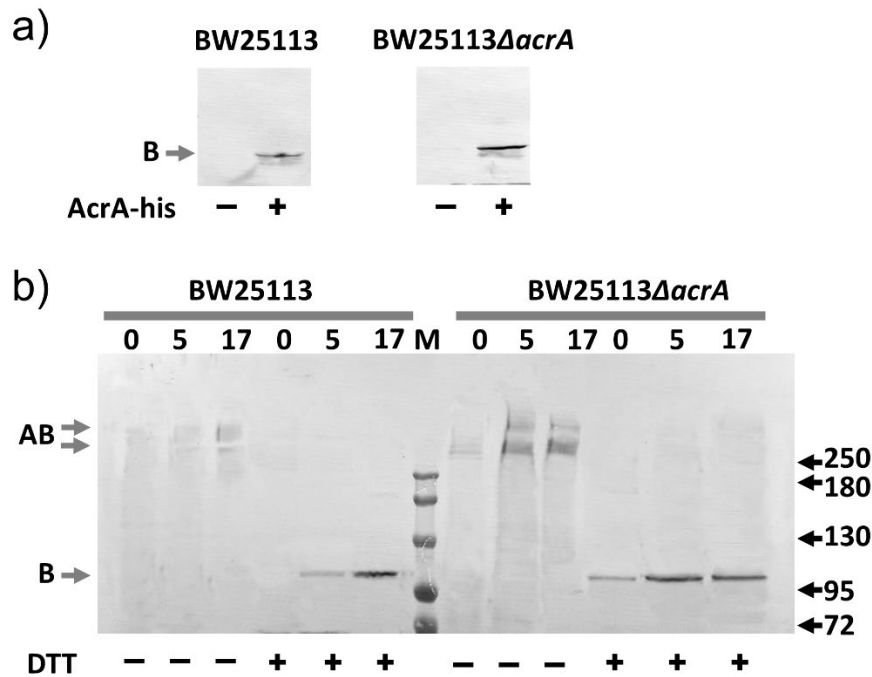
Figure 3.3 Co-purification of genomic AcrB with AcrA-his.

(**a**) Anti-AcrB Western blot analyses of samples prepared from BW25113 or BW25113Δ*acrA* with or without plasmid-encoded AcrA-his. (**b**) Anti-AcrB Western blot analyses of samples collected after 0, 5, or 17 h of incubation following the induction of AcrA-his production in BW25113 or BW25113Δ*acrA* strains. Dithiobis-(succinimidyl proprionate) (DSP) crosslinking was performed to stabilize the AcrAB complex before protein purification. Reduction using dithiothreitol (DTT) breaks the disulfide bond in the linker of DSP and the complex into AcrA and AcrB subunits. Molecular weight markers are labeled as "M", and the molecular weight of bands (kD) were indicated on the right. The expected bands for AcrB and DSP linked AcrA-AcrB are marked on the left of the gels as B and AB, respectively.

3.4   Discussion

The dominant negative effect describes the situation in which the phenotype is dominated by the negative impact of the functionless mutant. The observation of the dominant negative effect has been used in many studies to investigate the mechanism of protein–protein interaction, including the identification of protein–protein interactions interface [164], determination of enzymatic activity related to oligomerization [165], and the effect of mutations in genetic disorders [166, 167].

In the process of AcrAB-TolC assembly, there are many steps where the incorporation of a functionless AcrA or AcrB mutant would negatively impact the efflux activity. First, all three proteins in the system are oligomers. AcrB and TolC are obligate timers, while AcrA is believed to exist as a dimer or trimer in the free form and assembles into a hexamer in the pump complex [59, 168]. While AcrA and AcrB are believed to form a complex in the absence of substrate and efflux, TolC assembles with AcrAB during active efflux. When a functionless AcrB mutant is expressed in excess in a wild type *E. coli* cell containing genomic AcrB, we expect them to compete with their genomic counterpart to engage genomic AcrA, forming non-functional interactions to reduce the overall efflux activity. In addition, we expect the competition for genomic TolC will further enhance the dominant negative effect. For this competition to occur, we chose mutants that are defective due to mechanisms not directly related to the interaction between AcrA and AcrB. The structure of the AcrAB-TolC complex and location of mutants mentioned in this study are shown in Figure 3.4.

We determined the expression level of the mutants relative to their genomic counterpart. Using serial dilution and quantitative Western blot analysis, we found that the expression levels of the AcrB mutants were 10–20 folds of the level of the genomic AcrB. With this high level of excess, we expect to observe a strong dominant-negative effect if the mutants were actively involved in the pump assembly, competing for binding partners. We constructed two groups of AcrB mutants, defective in different aspects. We observed that the effect of certain mutations was not always the same for different substrates. For example, T978A mutation in AcrB is detrimental to all substrates tested except for R6G, while F178A mutation in AcrB drastically reduced the MIC for ERY, but not as much for other substrates tested. This difference in mutation effects has been observed in many studies characterizing AcrA and AcrB mutants, for example, [62, 100, 169]. We speculate that this difference could be due to differences in the binding and interaction of specific substrates with the pump complex. The substrates vary drastically in their size, shape, structure, and charged state. As a result, the subgroup of residues that they interact with on their way to be transported are not likely to completely overlap. Therefore, point mutations introduced in AcrA and AcrB could have different impacts on specific substrates.
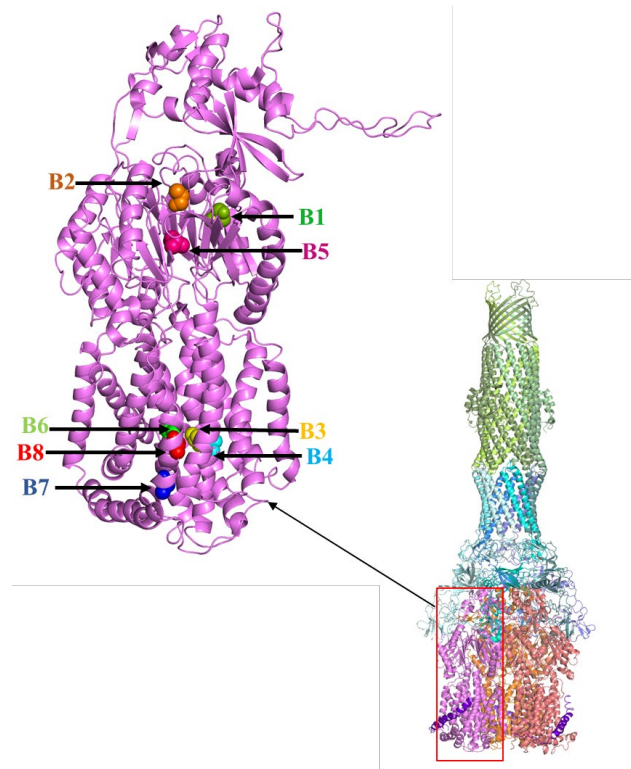
Figure 3.4 Structure of the AcrAB-TolC complex with the residues mutated in this study highlighted in AcrB structure.
AcrB mutations are labelled as; B1-F178A, B2-I278A, B3-D407A, B4-D408A, B5-F610A, B6-K940A, B7-R971A, B8-T978A. AcrAB crystal structure is created using pymol from 5N5G.pdb (https://pymol.org/2/)

Mutants defective in the proton translocation pathway still form trimers [158] and interact properly with AcrA (Figure 3.1c). Then, was why no dominant negative effect observed? One possibility is that the genomic AcrA and AcrB are transcribed together, sharing the same mRNA. Hence, the newly produced AcrA and AcrB could be clustered as well. As a result, the genomic AcrA and AcrB form a AcrAB complex as soon as they are translated and inserted into the membrane (AcrB) or secreted into the periplasm with lipid anchoring (AcrA). Since the local concentration of the genomic proteins are high, they associate with each other with a much higher chance than associate with a plasmid-encoded partner. Another requirement for the observed activity is that the AcrAB complex, once formed, should be resistant to dissociation. Otherwise, the high concentration of AcrB mutant in the cell membrane would be effective in competing with genomic AcrB to form a nonfunctional AcrAB complex.

CHAPTER 4.   Study of multi-drug efflux system protein degradation in *E.coli* using transposons library

4.1   Introduction

The pathogens have evolved different mechanisms for their survival. The antibiotic resistance in the pathogens is one such significant evolvement. Moreover, some pathogens have acquired the mechanisms to resist multiple drugs. These have created problems in the treatment of infectious diseases. There are several major mechanisms from which microbes develop drug resistance, including i) genetic mutation or enzymatic alteration ii) inactivation of drugs by enzymatic degradation, iii) antibiotic modification, iv) Loss of porin and changes in membrane permeability, v) alteration of the drug target, and vi) overexpression of efflux pumps[17, 170]. Our research work is mainly focused on studying a multidrug resistance mechanism known as active efflux. Our primary focus is on the Resistance-Nodulation-Division (RND) superfamily member AcrAB-TolC efflux pumps in *E. coli*. AcrAB-TolC forms a tripartite complex that spans the inner membrane, periplasmic space, and outer membrane of *E. coli* [137]. The pump assembles by inner membrane AcrB associating with periplasmic protein AcrA, and outer membrane channel TolC[44, 46, 171]. Inner membrane transporter AcrB plays a pivotal role in substrate recognition, binding, and translocation to the exit channel[70, 172]. Hence, the researchers focus on identifying methods to disrupt the AcrB either by targeting substrate binding sites, inhibiting pump assembly, or protein degradation methods[113, 157]. This chapter focuses on the identification of novel protease mechanisms important in AcrB degradation.

Protein degradation in both prokaryotes and eukaryotes require energy input, typically by hydrolysis of ATP. In prokaryotes, the proteins are degraded by an ATP-dependent pathway involving proteases including ClpAP, ClpXP, FtsH, and Lon[104, 112, 173]. Two well-studied examples are AAA+ proteases ClpAP and ClpXP. Protein degradation by ClpXP and ClpAP is initiated by recognizing the specific protein for degradation[105]. Signals for degradation include the C terminal tagging of the protein by the ssrA tag or N-terminal tagging via the N-rule pathway[108, 174].

In an effort to study the lifetime of AcrB in *E. coli* cells, Chai *et al.,* discovered that the introduction of a small peptide tag, the small stable RNA A (ssrA) tag introduced at the C terminus of AcrB facilitates complete degradation of AcrB[113]. The ssrA is a 11 amino acid residue tag (Amino Acid sequence-AANDENYALAA). The natural function of ssrA is to rescue the stalled ribosomes on truncated mRNA lacking the stop codon[110, 175]. The ssrA tag is added to the C-terminus of the incompletely synthesized proteins during translation. ClpP, ClpX, and a chaperon SspB have been identified to be involved in the degradation of ssrA tagged AcrB. However, partial degradation was observed when these genes were disrupted, indicating that other players were likely involved in the process[113].

The goal of the study described in this chapter is to discover novel proteases and protein degradation mechanisms that are involved in the destruction of AcrB. Specifically for this purpose, the transposons library has been created, which contains an extensive collection of strains with random gene knockouts. Transposable elements are generally known as "jumping genes/selfish genes." These DNA sequences move from one location to another in the genome[118, 126]. The identification of transposons has led to significant discoveries in various scientific aspects[116, 118]. The main problem associated with genome studies in sequencing large DNA segments is sequencing an insert within the interior of a DNA. Alternative techniques have been developed, such as genome walking/ primer walking and shotgun subcloning, to overcome these restrictions[118]. The Tn5 transposons system, which has the cut and pastes mechanism, has been widely used in different studies[120, 129]. Transposons library creations have facilitated the identification of genes involved in virulence and other non-essential processes[125]. Furthermore, to get insight into the essential gene, gene function, and genetic linkages, sophisticated deep DNA sequencing approaches have been influential in the use of transposon libraries. The Tn5 transposons system have been used in our study, which comes under the group of composite transposons[121]

Comparatively, an *E.coli* strain containing AcrB-WT has a higher tolerance to antibiotics than a strain containing AcrB-ssrA. Hence, in this study, the first goal was to establish a screening strategy to identify antibiotic concentrations under which strain containing AcrB-WT would grow but not those containing AcrB-ssrA. Next, plasmid encoding AcrB-ssrA was used to introduce the transposons using the Ez-Tn5 <Kan>

transposome system. The transposon has a kanamycin resistance marker, allowing mutants to be selected when the transposon is inserted into the recipient strain's genome. Insertion of the transposon is random, and thus we speculate there is an opportunity for it to disrupt genes important for the degradation of AcrB-ssrA. In this case, the expression level of AcrB-ssrA would be higher in the strain, and thus lead to higher tolerance of antibiotics that are substrates of AcrB. The elevated level of AcrB-ssrA expression was then confirmed using anti-AcrB antibody and Minimum inhibitory concentration assays. PCR-based sequencing methods and finally, the next-generation sequencing method (NGS) was used to determine the transposons inserted gene location. Data analyses revealed the *clpX* gene was disrupted in the strains with elevated levels of AcrB-ssrA expression.

4.2   Material and Methods

4.2.1 Knockout strain creation, competent cell preparation and Transformation

BW25113 wild-type strain was obtained from Yale *E. coli* genetic resources. BW25113Δ*acrB* was produced in the lab using *the E. coli gene deletion kit (Cat #K006, Gene Bridge).* The same kit was used to remove the kanamycin cassette to obtain the cells without kanamycin resistance (BW25113Δ*acrB*; K-). Next, to incorporate the ssrA into the system, competent cell preparation was done, followed by the transformation. *E. coli* BW25113Δ*acrB*; K- were transformed with the pQE70 AcrB -ssrA (ampicillin resistance-Amp+) plasmid and plated on Luria broth (LB)-Amp+ plate following the incubation at 37°C overnight. Furthermore, pQE70 AcrB WT was transformed into *E. coli* BW25113Δ*acrB*; K- and BW25113 WT cells; pQE70 AcrB WT and pQE70 AcrB ssrA into BW25113Δ*clpX* cells. These were later used in minimum inhibitory concentration (MIC) assay.

Preparation of BW25113Δ*acrB*; K- pQE70 AcrB- ssrA competent cells: A single colony was picked from the LB-Amp+ plate and used to inoculate 5 mL of fresh LB containing ampicillin (100 mg/mL; 1:1000 dilution). The culture was incubated at 37°C overnight. The next day 100 mL of liquid LB medium containing ampicillin was inoculated

using 500 µL of the overnight culture. The new culture was incubated at 37°C until its OD600 reached 0.5, which was used for the electrocompetent cell preparation. The culture was kept on ice for ~ 20 mins and then centrifuged at 2400rpm for 20 mins at 4°C followed by resuspension with ice-cold sterile distilled water (100 mL). Next, it was centrifuged at 2400rpm for 20 mins at 4°C. The washing step with ddH$_2$O was repeated. Then the cell pellets were resuspended in 10% ice-cold glycerol (40 mL) and centrifuged at the same conditions. The glycerol wash step was repeated one more time, and the supernatant was removed. The pellet was resuspended in 0.2mL of 10% glycerol.

The prepared BW25113Δ*acrB*; K- pQE70 AcrB -ssrA electrocompetent cells (Amp+) were used for the transposomes insertion and MIC assays described in the below sections.

4.2.2 The Minimum Inhibitory Concentration (MIC) LB agar plate assay and liquid assays to compare the growth of different *E. coli* strains.

The first step in creating the transposons library is to identify a reliable screening method to use after the insertion of transposomes. For our purpose, we need to identify a condition in which the BW25113Δ*acrB* containing pQE70 AcrB ssrA cells do not grow, while the BW25113Δ*acrB* containing pQE70 AcrB WT cells grow. The BW25113Δ*acrB* pQE70 AcrB WT strain, containing a higher level of AcrB, should be more tolerant to AcrB substrate than BW25113Δ*acrB* pQE70 AcrB ssrA, in which the expression of AcrB-ssrA was significantly reduced. The condition in which only the BW25113Δ*acrB* pQE70 AcrB WT strain, but not the BW25113Δ*acrB* pQE70 AcrB- ssrA strain grows, will be used to screen for new mutants that have gene disruptions that lead to functional loss of other proteins that are involved in AcrB-ssrA degradation. We expect to rediscover ClpX, ClpP, and SspB in our screening, which will serve as a positive control for the effectiveness of our screening method. In addition, we are looking for novel genes where the disruption will also lead to the survival of the strain. The following MIC assays were performed to find conditions of efficient screening assay. Two known AcrB substrates were tested, erythromycin (ERY), and novobiocin Sodium (NOV).

The LB agar plates with different antibiotic concentrations ranging from 100-20 µg/mL for novobiocin and erythromycin were prepared. To each plate 15 µg/mL of kanamycin was added as the second substrate. 5mL cultures at OD 0.5 was used for the experiment. We expect the concentration in the culture is 5×10^8 per mL. A dilution series was prepared from 10^9 to 10^4. After establishing a screening method, the next step was to create a random insertion library using a transposome system.

Liquid MIC assay was performed for the BW25113 Δ*acrB* pQE70 AcrB WT, BW25113 Δ*acrB* pQE70 AcrB ssrA, BW25113 pQE70 AcrB WT, BW25113 pQE70 AcrB ssrA, BW25113 Δ*clpX* pQE70 AcrB WT and BW25113 Δ*clpX* pQE70 AcrB ssrA strains using NOV and ERY.

4.2.3 Electroporation of BW25113 Δ*acrB* pQE70 AcrB ssrA electrocompetent cells with EZ-Tn5 <KAN-2>Tnp transposome and selection of transposed clones

The insertion of transposons to create the random mutations was achieved using the Lucigen Ez-Tn5™ <Kan-2> Tnp Transposome™ kit (Cat # TSM99K2). The transposons insertion was done by electroporation of the BW25113 Δ*acrB* pQE70 AcrB ssrA electrocompetent cells (Amp+) with one microliter EZ-Tn5 <KAN-2>Tnp Transposome. Electroporated at 2200 V, using a 2 mm cuvette, for ~5.7 ms using Eppendorf Eporator®, (Catalog #4309000019). The electroporated cells was immediately recovered after electroporation using Super Optimal broth with Catabolite repression (SOC) medium; (0.5% Yeast Extract, 2% Tryptone, 10 mM NaCl, 2.5 mM KCl, 10 mM MgCl₂, 10 mM MgSO₄, 20 mM Glucose). SOC medium was added to the electroporation cuvette to 1 mL final volume immediately after electroporation. The medium was pipetted gently to mix and then incubate on a 37°C shaker for 60 minutes to facilitate cell outgrowth (Figure 4.1)
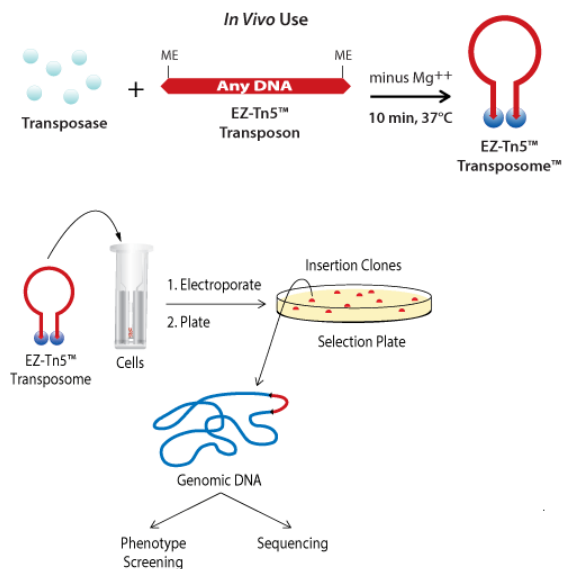
Figure 4.1 The schematic representation of the transposons library creation using electroporation method.
The image is belongs to Lucigen Inc. (https://www.lucigen.com/docs/slide-decks/Lucigen-EZ-Tn5-Transposon-Tools.pdf)

The control experiment was conducted using pET28a sfGFP plasmid (Kan+) electroporated in to the BW25113 Δ*acrB* pQE70 AcrB ssrA electrocompetent cells (*Amp+*). Then 100 μL aliquots of the recovered cells were plated on plates containing 50 μg/mL and 15 μg/mL kanamycin- for control and experimental samples, respectively. The transposome inserted sample was plated on kanamycin (15 μg/mL) included different antibiotic plates; NOV- 20 μg/mL, 40 μg/mL and ERY 20, 40 μg/mL. All the plates were incubated at 37°C incubators overnight (~16hrs). The rest of the recovered cultures were stored at 4°C. The next day, the plates were checked for colonies. Next, colonies were chosen from each plate and used to inoculate 3 mL cultures overnight; simultaneously, each colony chosen was streaked on a new plate, and a number was assigned for each colony. MIC assay was performed for the obtained colonies using NOV and ERY substrates.

4.2.4 Inhibition by Phenylalanine-Arginine-β-naphthylamide dihydrochloride (PAβN) Efflux pump inhibitor to confirm the elevation of MIC is due to AcrB activity

To confirm the observed effect on MIC depends on the AcrB expression, the efflux pump inhibitor PAβN (MCE; Cat# HY-101444A) was used to inhibit AcrB-mediated efflux using samples that have been selected from the previous MIC assays with ERY.

The antibiotic concentration for erythromycin was decided based on the previous MIC results. The assay with inhibitor was optimized by using a concentration range of PAβN (10, 20, 30, 40, and 50 µg/mL) with 1 mM Mg^{2+}. Magnesium was used to avoid the outer membrane disruption that can be caused by the high concentration of inhibitor. From the screening, 50 µg/mL of inhibitor was selected and used for the MIC assay. After overnight (~16 hrs) incubation, the plate reading was taken using the plate reader at OD 600 nm. The sample number finalized through this inhibitor assay, and the second phase of the MIC assay proceeded for the western blot analysis, genomic DNA extraction, and sequencing.

4.2.5 FLAG tag insertion, Western Blot analysis with Anti AcrB CT and FLAG antibody

The selected samples were used to prepare 5 mL overnight LB cultures. The next day these cultures were centrifuged to obtain the cell pellet. The cell pellet was resuspended in 50 µl of the lysis buffer (PBS (pH 7.5), 2.5 mM $MgCl_2$, 0.5mM $CaCl_2$, 10 µM DNase (Final pH 7.6) and 50 µl SDS loading dye (Tris-HCl, pH 6.8, 6%SDS, 48% glycerol, 0.03% bromophenol blue, 9% 2-Mercaptoethanol). The samples were incubated at 37°C for 30 mins, centrifuged at max speed (150,000 rpm) for 1 minute, and the supernatant was subjected to the SDS PAGE analysis. The SDS-PAGE electrophoresis was done at 220 V for 40 mins using 15% SDS gel. Then the gel was transferred to a Polyvinylidene difluoride (PVDF) membrane stack between the blotting papers. The transfer was done at 380 V for 25 mins, and then blot was proceeded for the western blot analysis. Briefly, the PVDF membrane was incubated in the blocking solution (5% skim milk powder+ Tris Buffered Saline (TBS) buffer; Tris-HCl, NaCl pH 8.0) for 1 hr. at room temperature on a shaker. Then the membrane was transferred to Anti AcrB CT (Rabbit)

antibody (1:5000 antibody in TBS buffer). The membrane was incubated for 1.5 hrs at room temperature. The membrane wash was performed using wash buffer (TBS + 1:1000 tween 20) 3 times, 10 mins each time. Then the membrane was transferred to a TBS buffer containing the Anti Goat to Rabbit secondary antibody (1:5000 in TBS buffer). The blot was Incubated for 45 mins with the antibody, followed by washing as described above. Then the BCIP/NBT (5-bromo-4-chloro-3'-indolyphosphate and nitro-blue tetrazolium) solution was used for staining the membranes and shake until the color is developed.

Another plasmid construct was created in which the FLAG tag was inserted at the N terminus of the pQE70 AcrB-WT and pQE70 AcrB-ssrA plasmids using the fast cloning method[156]. The BW25113 Δ*acrB* pQE70 FLAG AcrB WT and BW25113 Δ*acrB* pQE70 FLAG AcrB ssrA used for the Western blot analysis with anti- FLAG antibody. The same procedure was followed with Anti FLAG antibody (Santa Cruz Biotechnology).

4.2.6 Genomic DNA extraction and sequencing

Genomic DNA was extracted from colonies that show promising results from the MIC assay and processed for sequencing to identify the candidate genes. As the first step, 1.5 mL of overnight cultures were prepared from colonies identified through MIC assays. The PureLink™ Genomic DNA Mini Kit (Cat#:K182001, Thermofisher) was used in genomic DNA extraction. Briefly, the method is as follows:

The cells were harvested at 9000 rpm for 5 mins. Then those were proceeded to prepare the lysate using Pure link genomic Kit. First, 180 µl of the digestion buffer +20 µl of Proteinase K was added, vortexed briefly, and incubated at 55°C for 1 hr. with occasional vortexing (5s vortex). Then 20 µl of RNase was added, vortexed, and incubated at room temperature for 2 mins. After that, 200 µl of lysis buffer+200 µl of 99.5% Ethanol was added, followed by vortexing and mixing of samples. Next, the lysate was transferred to the spin column and centrifuged at 9,000 rpm for 1 min at room temperature. The next step was washing. First 1,500 µl wash buffer was added and centrifuged at 9000 rpm for1min, next 500 µl wash buffer was added and centrifuged at 15,000 rpm for 3 mins. Genomic DNA was eluted by adding 30 µl of elution buffer, incubating for 1 min at room temperature, and centrifuging at 15,000 rpm for 1 min. The elution step was repeated using

another collection tube with 30 µl of elution buffer. Agarose gel electrophoresis was performed to check the presence of DNA. Furthermore, a survey scan was done at wavelengths 260 nm and 280 nm to check the DNA quality.

4.2.7 Sequencing results analysis and identified gene verification

The samples were pooled and sent for Nest Generation Sequencing (NGS) (in collaboration with China). The extracted genomic DNA was sequenced using long-read MinION (Oxford Nanopore) and short-read Illumina MiSeq technologies. The long reads were generated by Oxford Nanopore MinION flowcell R9.4 with a depth more than 300 times and the 150 bp paired-end short reads were generated by Illumina MiSeq system (Illumina, San Diego, CA, United States) with a depth more than 100 times. The MinION reads were filtered using Filtlong (version 0.2.0) to remove any reads < 2000 bp, followed by removing the lowest 10% of reads by quality. Complete sequence assembly was performed with Canu version 1.5 using a combination of short and long reads, followed by error correction by Pilon version 1.12.

The sequences for each sample were used in the NCBI; nucleotide to nucleotide Blast (https://blast.ncbi.nlm.nih.gov/Blast.cgi). The sequence was entered in the FASTA format, and the reference sequence accession number for *Escherichia coli* str. K-12 substr. MG1655, complete genome *Escherichia coli* str. K-12 substr. MG16554,641,652 bp genomic sequence was given as U00096.3. As shown in the following image either the highly similar or somewhat similar sequence options were selected and performed the blast (Figure 4.2).

The gene sequence was checked using the ClustalX2 software to match up the regions aligning in the sample sequence and candidate gene sequence for further confirmation. This process was followed for all the samples to find out the disrupted genes. First, the verification of the kanamycin gene in the identified gene location was performed using primers to amplify the Kanamycin cassette. Next, further analyses were done to determine any other possible genes disrupted by Tn5 transposons insertion. The primers used for this process mentioned in Table 4.1
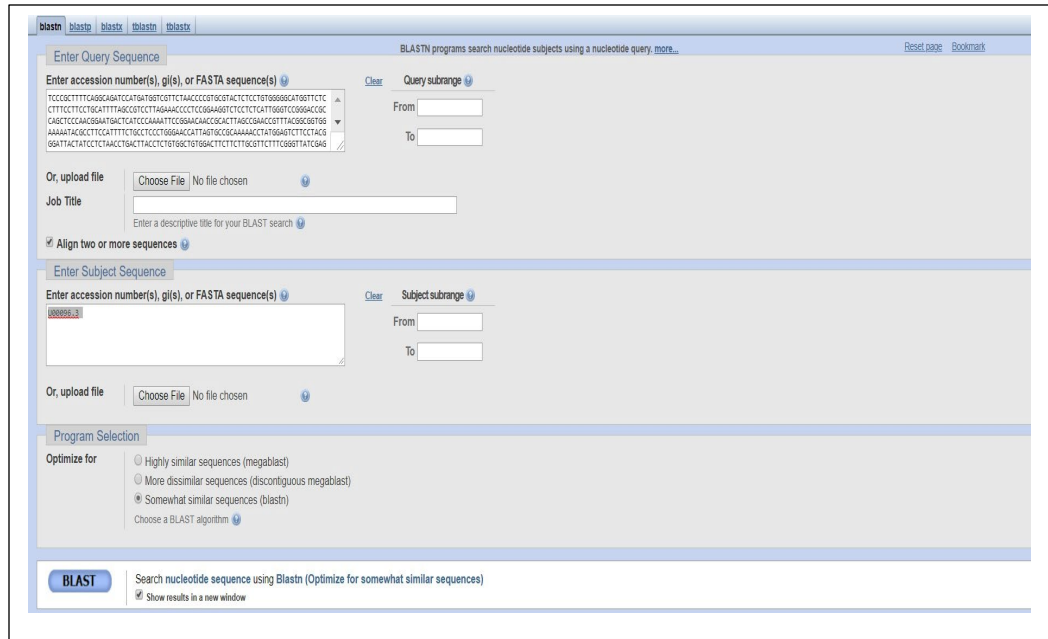
Figure 4.2 The figure illustrates the query and subject sequences entering and the parameters used for BLAST

Table 4.1 Primers used for the verification process

Primer	Primer sequence 5'-3'
KAN-verification-F:	AACACGTAGAAAGCCAGTCCG
KAN-verification-R:	CCCCTGATGCTCTTCGTCCA
Tn5-clpX-verification-F :	CGATTCGATTCTGACCCATC
Tn5-clpX-verification-R :	CGTCAGTATATGGGGATGTTTC
Clpp verification-F	ATGTCATACAGCGGCGAAC
Clpp verification-R	CAATTACGATGGGTCAGAATCG
SspB verification-F :	ATGGATTTGTCACAGCTAACAC
SspB verification-R :	TTACTTCACAACGCGTAATGC

4.3 Results and Discussion

4.3.1 Minimum inhibitory concentrations for pQE70 AcrB-ssrA and pQE70 AcrB WT strains in BW25113 ΔacrB

The identification of a proper condition is essential for the establishment of an efficient screening assay. As for the first step, we performed the MIC assay. This technique is used to determine the lowest concentration of an antibiotic that inhibits the growth of a bacteria. MIC assay is an easy method that can be done on a small scale. This assay can be performed either in a liquid medium or solid medium. However, the most prominent process is the liquid assay. During MIC measurement, serial dilutions of different antibiotics are added to the growth medium. In this experiment, we used two different antibiotics for liquid assay and solid assay. Table 4.2 summarizes the MIC values for each of the strains for different antibiotics for liquid assay. Figure 4.2 shows the differential growth of the wild type (WT) and ssrA strain to varying concentrations of novobiocin and erythromycin. During the actual screening, cells are be plated onto agar plates (solid assay). The liquid assay is used here to identify the proper concentration range. The rationale is that differences in protein expression level (AcrB-ssrA is less than WT AcrB) will lead to a smaller MIC for the strain containing AcrB-ssrA. Once we have identified a suitable substrate and a concentration, we will be able to select mutants containing gene deletions, enhancing the expression level of AcrB-ssrA. Thus, this gene/s is likely to be involved in the degradation of AcrB-ssrA.

Erythromycin is a macrolide antibiotic that participates in the inhibition of protein synthesis by binding to the 50S subunit of the ribosome during translation in bacteria. Novobiocin is an aminocoumarin that binds to DNA gyrase and acts as a competitive inhibitor of ATPase activity. A two-fold or four-fold difference in MIC values has been observed for strains containing either the WT or the ssrA tagged constructs. Thus, these two substrates could be used in the screening. The LB agar assay results facilitate identifying the proper concentration for the establishment of transposons library screening. As shown in Figure 4.2, at very low concentrations a (10 μg/mL) and very high concentrations d (100 μg/mL), the difference between WT and ssrA is insignificant. However, under conditions b (20 μg/mL) and c (40 μg/mL). a detectable difference could

be observed between the two samples. Therefore, those are suitable conditions for screening.

Table 4.2 The MIC values for pQE70 AcrB-ssrA and pQE70 AcrB WT strains in BW25113 Δ*acrB*, WT and Δ*clpX*

	NOV	ERY
BW25113 Δ*acrB* containing		
pQE70 AcrB WT	320	160
pQE70 AcrB ssrA	80	40
BW25113 containing		
pQE70 AcrB WT	640	320
pQE70 AcrB ssrA	160	80
BW25113 Δ*clpX*		
pQE70 AcrB WT	640	320
pQE70 AcrB ssrA	160	80
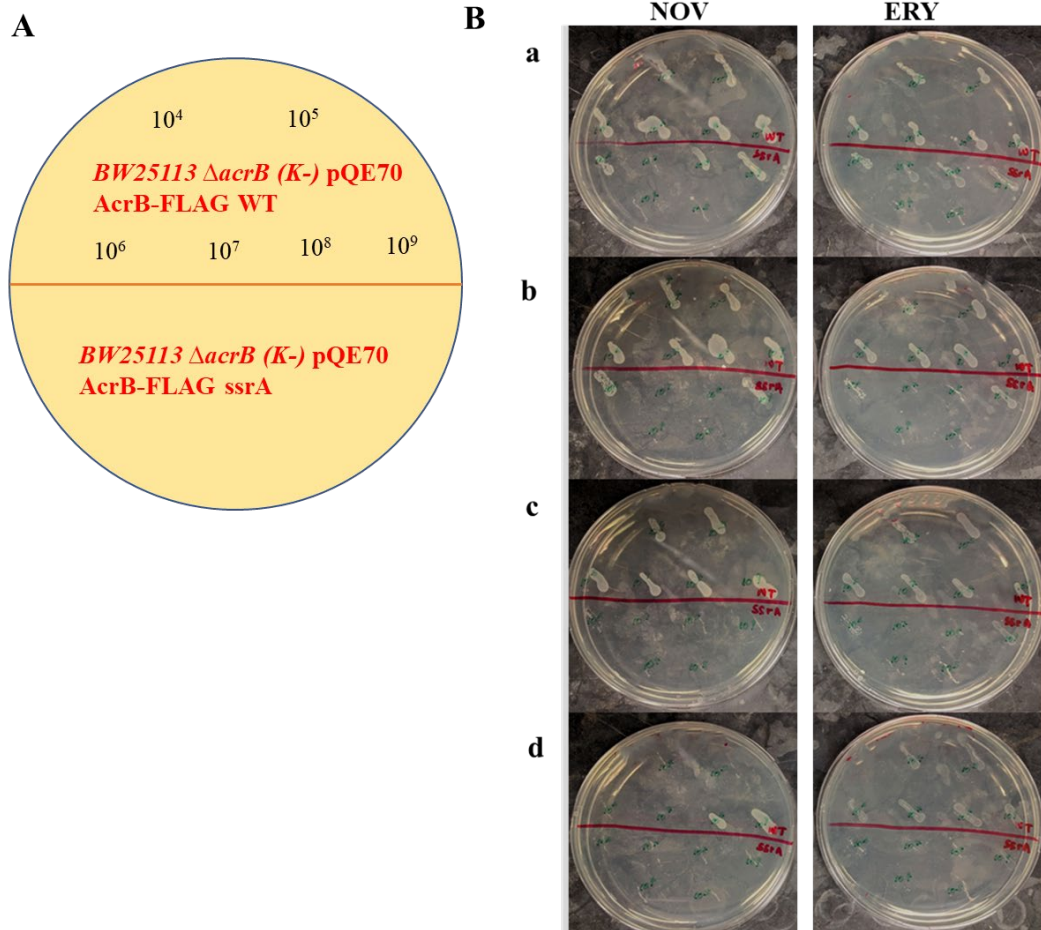
Figure 4.3 A representation of the streaking pattern on the LB agar plate used for the solid assay.

The dilution series ranges from 10^9 to 10^4. The top half of the plate was spotted using the WT strain, and the bottom half of the plate was spotted with ssrA strain. (the bottom should be labeled similarly as the top) B) This image shows the results obtained in a solid assay using NOV and ERY. All the plates contain 15 µg/mL concentration of kanamycin. Concentrations of NOV or ERY in each panel as; a) 10 µg/mL b) 20 µg/mL c) 40 µg/mL d) 100 µg/mL

4.3.2 The Ez-Tn5 transposons insertion by electroporation

The random insertion of the transposons was performed using the electroporation method. Figure 4.4 displays the colony growth of the control and the experimental strains with different concentrations of the antibiotics. In these experiments, different antibiotic concentrations were fine-tuned. The kanamycin 50 µg/mL control plate has many colonies; the pET28a sf-GFP control is intrinsically kanamycin-resistant (Figure 4.4 A). This result demonstrated that the electroporation transformation was successful. BW25113 Δ*acrB* pQE70-AcrB-ssrA with transposome insertion on kanamycin 15 µg/mL plate also has a higher number of colonies (Figure 4.4 B). The BW25113 Δ*acrB* pQE70-AcrB-ssrA cells do not have intrinsic resistance to kanamycin. Hence, this reveals transposons insertion is successful.

Plates containing LB-agar with different NOV, ERY concentrations, and kanamycin (15 µg/mL) allow for the selection of colonies with an expression similar to AcrB-WT. Because, under these low NOV or ERY concentrations, the BW25113 Δ*acrB* pQE70-AcrB-ssrA strain does not show significant growth. The growth at these concentrations will show that there might be a mutation of the genome of the strain containing AcrB-ssrA that increased its expression level (and thus drug tolerance) (Figure 4.4 C, D, E).

The colonies picked from these plates were subjected to further liquid MIC assays to confirm that they grow at higher antibiotic concentrations. The same two substrates were used for the liquid assay (Table 4.3). The samples show similar or higher MIC values than the WT strain, implying that the AcrB expression has increased despite ssrA. Hence, there could be a disruption in a gene responsible for the AcrB degradation.
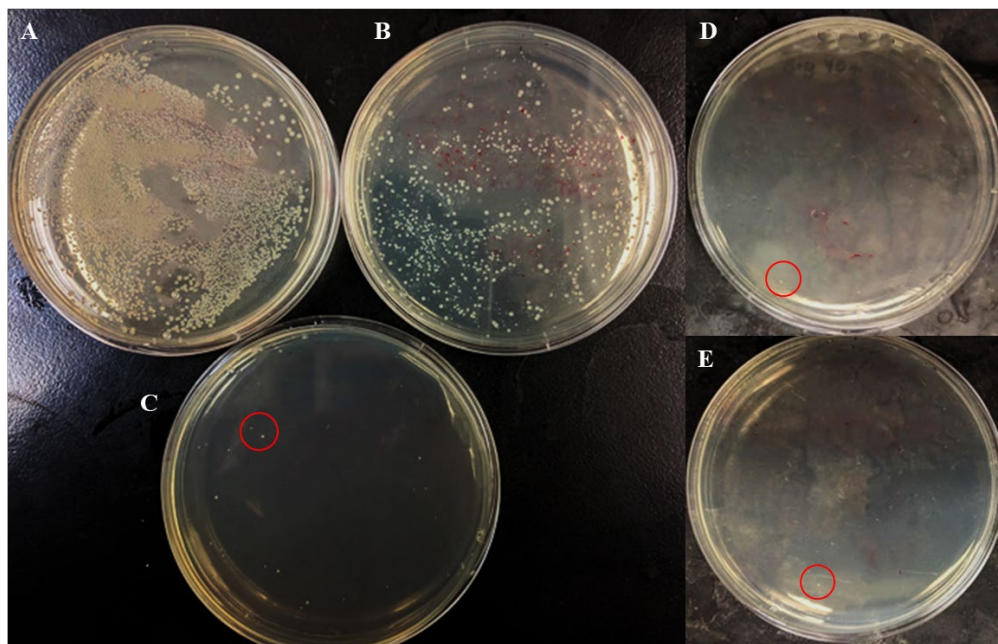
Figure 4.4 The colony growth of the experimental and control strains with transposome insertion plated in

(A) control pET28a sf-GFP in kanamycin 50 µg/mL (B) BW25113 Δ*acrB* pQE70-AcrB-ssrA with transposome insertion plated in kanamycin 15 µg/mL. (C), (D), (E) BW25113 Δ*acrB* pQE70-AcrB-ssrA with transposome insertion plated in Erythromycin 20 µg/mL+ kanamycin 15 µg/mL, Novobiocin 40 µg/mL+ kanamycin 15 µg/mL, Erythromycin 40 µg/mL+ kanamycin 15 µg/mL respectively. Red circle highlights the location of colonies.

Table 4.3 The MIC values for samples picked from the transposons library

Sample	ERY	NOV
S 1	320	80
S 2	160	320
S 3	320	320
S 4	320	320
S 5	320	320
S 6	320	320

Table 4.3 (Continued)

S 7	>320	160
BW25113 Δ*acrB*; K-	40	40
BW25113 Δ*acrB*; K- pQE70 AcrB WT	160	320

4.3.3 MIC assay with Phenylalanine-Arginine-β-Naphthylamide dihydrochloride (PAβN) Efflux pump inhibitor

Several inhibitors have been identified for RND family efflux pumps. These inhibitors increase antibiotics efficacy, reduce the pathogen's resistance occurrence, and reduce the pathogen's infection ability. Among available Efflux Pump Inhibitors (EPI), PAβN is a frequently studied efflux pump inhibitor. EPIs are essential in clinical use to inhibit the multidrug resistance of bacteria. We used this inhibitor in our experiment to confirm the increase of the MIC value for transposons inserted BW25113 Δ*acrB* pQE70-AcrB-ssrA strain was due to the activity of the AcrAB-TolC efflux pump.

The PAβN is capable of significantly reducing the antibiotic resistance of *E. coli* for selected compounds that are AcrB substrates. The combination of the antibiotics (pump substrate) and the inhibitor facilitate the study of efflux-mediated multidrug resistance. Under our experimental condition, we observed the inhibitor alone does not influence bacterial growth. All the tested colonies grow normally in the presence of the inhibitor. However, when it was added along with ERY the colonies had a four-fold decrease in MIC values. These observations explain that the previously observed higher MIC values are due to the efflux activity of AcrB-ssrA, likely a result of increased expression level due to a mutation in a gene that regulates the ssrA tagged protein degradation.

Table 4.4 shows the results obtained for some of the tested strains. The highlighted values show the growth in the examined antibiotic concentration and the strains that were selected for further analysis. ERY and 50 µg/mL of PAβN have been used in this experiment.

Table 4.4 The MIC values for the selected samples in the presence of an antibiotic and with or without inhibitors

Sample	Inhibitor PAβN (50 μg/mL)	
	(-)	(+)
S 1	320	80
S 2	160	80
S 3	>320	80
S 4	>320	80
S 5	>320	80
S 6	320	160
S 7	>320	80
BW25113 Δ*acrB*; K-	40	40
BW25113 Δ*acrB*; K- pQE70 AcrB WT	160	40

4.3.4 The selected colony analysis with western blot and sequencing

The above-discussed methods were used for the selection of the colonies that shows higher AcrB activity. We tested two vectors for AcrB-ssrA expression, pQE70 AcrB ssrA and pQE70- AcrB WT. Furthermore, we created pQE70 FLAG -AcrB- ssrA and pQE70 FLAG -AcrB WT and used those for initial testing for AcrB expression in BW25113 Δ*acrB* and BW25113 Δ*clpX* cells (Figure 4.5). The expression of AcrB-ssrA is significantly lower in the wt strain compared to the BW25113 Δ*clpX* strain. This confirms the role of ClpX in AcrB-ssrA degradation, as discussed in previous research.
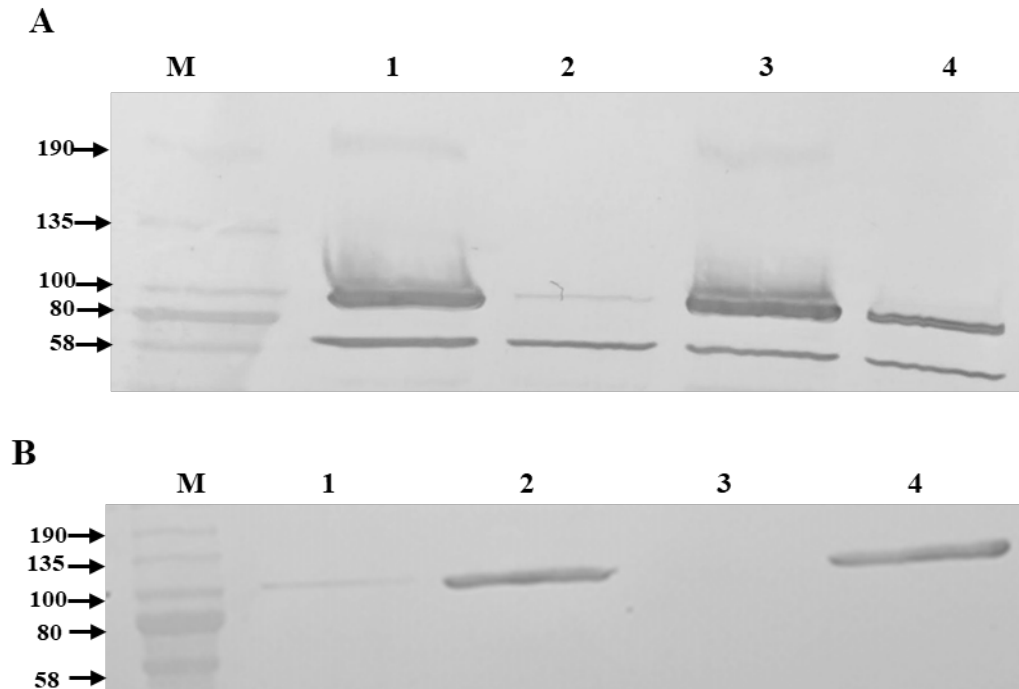
Figure 4.5 Western blot analysis with anti AcrB-CT and anti-FLAG antibodies.
(A)1. BW25113 ΔacrB- pQE70 AcrB WT, 2. BW25113 ΔacrB- pQE70 AcrB- ssrA, 3. BW25113 ΔclpX- pQE70 AcrB WT and 4. BW25113 ΔclpX- pQE70 AcrB -ssrA. (B) Western blot analysis with Anti FLAG antibody. 1. BW25113 ΔclpX- pQE70 AcrB- ssrA, 2. BW25113 ΔclpX- pQE70 AcrB WT, 3. BW25113 ΔacrB- pQE70 AcrB- ssrA, and 4. BW25113 ΔacrB- pQE70 AcrB WT.

To determine if the AcrB expression in the selected colonies were higher, we conducted Western blot analysis using Anti-AcrB antibody. The sample numbers are consistent with the numbers on the MIC plates used during selection. For several samples including 10,11,46,47,51, expression level was similar to AcrB WT (Figure 4.6).
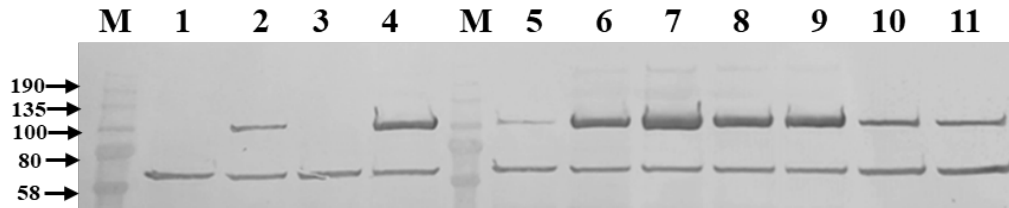
Figure 4.6 Western blot analysis with anti AcrB-CT antibody.
1) BW25113 ΔacrB; K-.2) BW25113 WT. 3) BW25113 ΔacrB pQE70 AcrB- ssrA. 4) BW25113 ΔacrB pQE70 AcrB WT. Lanes 5-11 are samples 1-7 (S1-S7) respectively.

4.3.5 Genomic DNA extraction and sequence analysis.

The genomic DNA was extracted from the selected colonies using the method described in material and methods. Then 1% agarose gel was used for the confirmation of the presence of genomic DNA. *E. coli* genomic DNA is ~4.4- 5.5mb. The samples were sent for NGS, and the received sequences were analyzed using NCBI and ClustalW methods as described in methods.

To confirm that transpositions was successful and the selected colonies contained the kanamycin cassette, we performed PCR to amplify the kanamycin resistance cassette (Figure 4.7 A). The agarose gel analysis shows all seven samples have the Tn5 kanamycin cassette. The presence of the Tn5 sequence in the *clpX* gene area confirms transposon insertion. Hence, it confirmed *clpX* as the disrupted gene by the insertion of transposons. A PCR was conducted to verify this insertion further. Figure 4.7 B shows the PCR products amplify in the *clpX* region. Once the Tn5 is inserted, the DNA fragment should be longer (1591 bp) than a non- disrupted *clpX* (1539 bp). According to the gel image, samples 3,4,5,6 migrate slowly compared to samples 1,2,7 and control (BW25113 WT). These products were sent for sequencing, and it confirmed the presence of Tn5-*clpX*. The samples 1,2,7 sequencing results showed an intact *clpX*.

Further analysis was performed to determine which genes disruption is responsible for the higher expression and MIC values of samples 1,2 and 7. For that purpose, we designed primers to amplify *clpP* and *sspB* regions. These have been identified to have

important roles in AcrB-ssrA degradation. However, the agarose gel image analysis exhibited intact *clpP* and *sspB* regions (Figure 4.7 C).
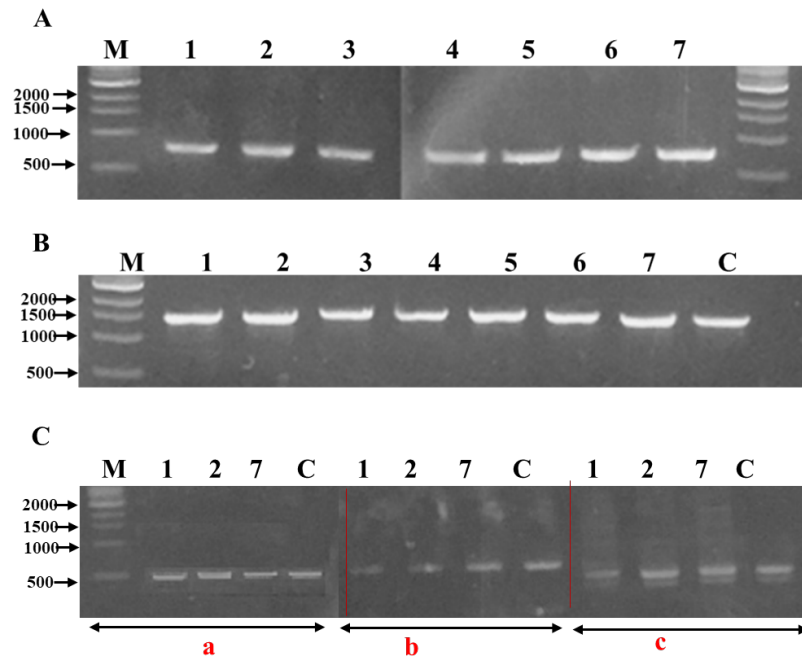
 Figure 4.7 Agarose gel electrophoresis analysis of the PCR products.
A) Confirmation of the presence of Tn5-Kanamycin cassette. B) Confirmation of *clpX*-Tn5 insertion. Sample 3,4,5,6 has slow migration. C) Analysis of samples 1.2 and 7. a) analysis of *sspB* region b) Presence of IS4 kanamycin cassette c) Analysis of *clpP* region

Further analysis is required to identify the disrupted genes that increase the expression in samples 1,2 and 7. However, due to the time and resource limitation, this project was ended at this point.

4.4   Conclusion

Transposons library creation is one of the most versatile tools in genetic studies. It provides efficient and robust genetic mutation analysis to identify novel genes for a particular function, virulence genes, and non-essential genes. The availability of high throughput sequencing methods such as NGS has made the use of transposons much more reliable and efficient. Our purpose was to identify novel gene/genes that have an essential role in the ssrA tagged AcrB degradation. In the long term, identifying genes important for the AcrB degradation process would provide new pathways in studying possible inhibitors/drugs to

reduce the drug efflux through the AcrAB-Tolc efflux pump. Even though the transposons library formation in this experiment did not identify novel genes, it identified an already known gene *clpX*. The observed increase in AcrB expression after disruption by transposon validates the effectiveness of the strategy. Unfortunately, the size of the library created in the current study limited the success of the search. Efficient and more reliable identification of novel genes would require the creation of a more extensive transposons library. The construction of a large library of mutants is crucial in transposons studies. Multiple insertions can be detected in every possible locus in a large, complicated library. The higher the insertion density, the more precise the identification of region-of-interest boundaries. If the library's density is too low, certain genes may go undetected.

CHAPTER 5.   Discussion and future work

The RND family efflux pump AcrAB-TolC in *E. coli* and its homologs in other Gram-negative bacteria play significant roles in conferring multidrug resistance to the cells. The pump component structures have been investigated through crystallography and cryo-EM methods. Even though this structural knowledge has led to the elucidation of the substrate efflux mechanisms and pump assembly models, there are still several unanswered questions about the AcrAB-Tolc pump system. In this study, our focus was to address three major aspects regarding the inner membrane protein of the efflux complex, which is responsible for the recognition and binding of compounds before their transportation out of the cell. We have studied the conformational changes in functional rotation, the pump assembly process, and AcrB-ssrA degradation.

In chapter two, we focused on understanding the dynamics of AcrB during functional rotation in the process of drug efflux[131]. For this purpose, we introduced six inter-subunit disulfide bonds into the periplasmic domain of AcrB using site-directed mutagenesis. The goal was to study the importance of the relative flexibility at the inter-subunit interface. We utilized MIC, Western blot analysis, and EtBr efflux assay. The formation of disulfide bond-linked AcrB oligomers, which were reduced into monomers under reducing conditions, was analyzed through Western blot. We evaluated the impact of mutation and formation of disulfide bond on efflux through comparison of the minimum inhibitory concentration (MIC) of an AcrB knockout strain expressing different mutants.

Furthermore, ethidium bromide accumulation assay was used to determine if the reduction of activity in a double mutant is due to restriction on conformational changes by the disulfide bond formation. We used dithiothreitol (DTT) as the reducing agent. In two cases, the activities of the double Cys mutants were partially restored by DTT reduction, confirming the importance of relative movement in the respective location for function. Nile red assay is another efflux quantification method that could have used for this study[176].

To extend this study, identifying more potential disulfide bond forming locations and studying their impact would be necessary. Ultimately, these findings provide new insights into the dynamics of the AcrAB-TolC efflux pump in *E. Coli*

Chapter three discussed the effect of over-expressing functionally defective pump components in wild-type *E. coli* cells to probe the pump assembly process[153]. In this study, we utilized the "dominant-negative" effect concept. Based on previous studies, the incorporation of a defective component to the pump is expected to reduce the efflux efficiency of the complex. When considering pump components separately, mutations in AcrB have been reported to disrupt efflux through different mechanisms. We examined proton translocation pathway and substrate binding pathway mutants and found that none demonstrated the expected dominant-negative effect. Our current data reveals that the AcrB-TolC complex assembly appears to have a proof-read mechanism that effectively eliminated the formation of a futile pump complex. We used MIC and expression analysis through Western blot as basic study methods. However, to investigate the efflux efficiency of the defective pump components, incorporating Nile red assay would be beneficial. Moreover, further studies of the pump assembly can perform regarding other elements in the efflux pump. Thorough investigation would provide a better picture about the pump assembly process.

The next question we wanted to answer was regarding the ArB degradation. A previous study from our group revealed that AcrB tagged by ssrA at the C-terminus facilitated degradation of the protein by ClpXP proteases[113]. In this project, we focused on exploring other protein degradation mechanisms or proteases involve in AcrB-ssrA degradation. For this purpose, we used transposons as the primary tool. We hypothesize that the increased activity of AcrB-ssrA protein is due to a mutation or inactivation of a gene involved in the degradation of AcrB-ssrA. Through gene sequence analysis, we identified *clpX* as the gene location disrupted by transposons insertion. Since *clpX* is an already recognized and widely studied protease system, this is not a novel finding. However, this finding validates our transposons library creation and screening methods.

It is essential to have an extensive transposons library. It would provide more flexibility and a wide range of gene disruptions to explore. In future work, creating a transposons library with many mutants should be the first step in this project. One of the significant challenges in this project was the identification of transposons inserted location. Initially, we used several sequence analysis methods, such as Random Amplification of Transposons Ends (RATE), arbitrary PCR method, invert PCR methods mentioned in the

previous literature[177-179]. However, these methods did not provide good sequencing results, which led us to use the next-generation sequencing (NGS) method. NGS is an expensive method; hence, in continuing this project, one of the primary focuses should be a more reliable, inexpensive, and effective transposons location identification method.

The following steps after identifying a specific gene include a complete analysis of the effects of the gene. The primary focus will be on verifying the potential role of the identified protein in membrane protein degradation, using molecular cloning, protein expression, and purification methods. Utilizing this information to determine its structure and potential function using available literature and genomic sequence can be the next step. The potential function information will be helpful in experimentally testing possible hypotheses. Moreover, investigating its role in the ssrA-facilitated degradation of other model proteins would provide greater insight into its function.

BIBLIOGRAPHY

[1] De Flora, S., Quaglia, A., Bennicelli, C., and Vercelli, M. (2005) The epidemiological revolution of the 20th century, *The FASEB Journal 19*, 892-897.

[2] Threats, I. o. M. F. o. M. (2009) 5: Infectious disease emergence: Past, present, and future, In *Microbial evolution and co-adaptation: A tribute to the life and scientific legacies of Joshua Lederberg: Workshop summary*.

[3] Spring, M. (1975) A brief survey of the history of the antimicrobial agents, *Bulletin of the New York Academy of Medicine 51*, 1013.

[4] Clardy, J., Fischbach, M. A., and Currie, C. R. (2009) The natural history of antibiotics, *Current biology 19*, R437-R441.

[5] Davies, J., and Davies, D. (2010) Origins and evolution of antibiotic resistance, *Microbiology and molecular biology reviews 74*, 417-433.

[6] Aminov, R. (2017) History of antimicrobial drug discovery: Major classes and health impact, *Biochemical pharmacology 133*, 4-19.

[7] Diggins, F. W. (1999) The true history of the discovery of penicillin, with refutation of the misinformation in the literature, *British journal of biomedical science 56*, 83.

[8] Hodgkin, D. C. T. (1949) The X-ray analysis of the structure of penicillin, *Adv. Sci. 6*, 85–89.

[9] Adedeji, W. (2016) The treasure called antibiotics, *Annals of Ibadan postgraduate medicine 14*, 56.

[10] Aslam, B., Wang, W., Arshad, M. I., Khurshid, M., Muzammil, S., Rasool, M. H., Nisar, M. A., Alvi, R. F., Aslam, M. A., and Qamar, M. U. (2018) Antibiotic resistance: a rundown of a global crisis, *Infection and drug resistance 11*, 1645.

[11] Rossolini, G. M., Arena, F., Pecile, P., and Pollini, S. (2014) Update on the antibiotic resistance crisis, *Current opinion in pharmacology 18*, 56-60.

[12] T.P. Van Boeckel, S. G., A. Ashok, Q. Caudron, B.T. Grenfell, S.A. Levin, R. Laxminarayan, . (2014) Global antibiotic consumption 2000 to 2010: an analysis of national pharmaceutical sales data, , *Lancet Infect. Dis. 14*, 742-750.

[13] Saga, T., and Yamaguchi, K. (2009) History of antimicrobial agents and resistant bacteria, *Jmaj 52*, 103-108.

[14] O'Neil, J. (2014) Antimicrobial resistance : tackling a crisis for the future health and wealth of nations

[15] Organization, W. H. (2000) Antimicrobial resistance, *Weekly Epidemiological Record= Relevé épidémiologique hebdomadaire 75*, 336-336.

[16] CDC. Antibiotics/Antimicrobial Resistance. https://www.cdc.gov/drugresistance . [Accessed on May 22.

[17] Spellberg, B., Bartlett, J. G., and Gilbert, D. N. (2013) The future of antibiotics and resistance, *New England Journal of Medicine 368*, 299-302.

[18] Ma, D., Cook, D. N., Hearst, J. E., and Nikaido, H. (1994) Efflux pumps and drug resistance in gram-negative bacteria, *Trends in microbiology 2*, 489-493.

[19] Coates A, H. Y., Bax R, Page C. (2002) The future challenges facing the development of new Antimicrobial drugs. , *Nat Rev Drug Discov 1*, 895-910.

[20] Ling, L. L., Schneider, T., Peoples, A. J., Spoering, A. L., Engels, I., Conlon, B. P., Mueller, A., Schäberle, T. F., Hughes, D. E., and Epstein, S. (2015) A new antibiotic kills pathogens without detectable resistance, *Nature 517*, 455-459.

[21] Moellering Jr, R. C. (2011) Discovering new antimicrobial agents, *International journal of antimicrobial agents 37*, 2-9.

[22] Fields, F. R., Lee, S. W., and McConnell, M. J. (2017) Using bacterial genomes and essential genes for the development of new antibiotics, *Biochemical pharmacology 134*, 74-86.

[23] Brown, E. D., and Wright, G. D. (2005) New targets and screening approaches in antimicrobial drug discovery, *Chemical reviews 105*, 759-774.

[24] Land, M., Hauser, L., Jun, S.-R., Nookaew, I., Leuze, M. R., Ahn, T.-H., Karpinets, T., Lund, O., Kora, G., and Wassenaar, T. (2015) Insights from 20 years of bacterial genome sequencing, *Functional & integrative genomics 15*, 141-161.

[25] Fleischmann, R. D., Adams, M. D., White, O., Clayton, R. A., Kirkness, E. F., Kerlavage, A. R., Bult, C. J., Tomb, J.-F., Dougherty, B. A., and Merrick, J. M. (1995) Whole-genome random sequencing and assembly of Haemophilus influenzae Rd, *Science 269*, 496-512.

[26] Payne, D. J., Gwynn, M. N., Holmes, D. J., and Pompliano, D. L. (2007) Drugs for bad bugs: confronting the challenges of antibacterial discovery, *Nature reviews Drug discovery 6*, 29-40.

[27] R. Bax, S. G. (2015) Antibiotics: the changing regulatory and pharmaceutical industry paradigm, *J. Antimicrob. Chemother. 70*, 1281–1284.

[28] Worthington, R. J., and Melander, C. (2013) Overcoming resistance to β-lactam antibiotics, *The Journal of organic chemistry 78*, 4207-4213.

[29] Fisher, J. F., Meroueh, S. O., and Mobashery, S. (2005) Bacterial resistance to β-lactam antibiotics: compelling opportunism, compelling opportunity, *Chemical reviews 105*, 395-424.

[30] Elander, R. (2003) Industrial production of β-lactam antibiotics, *Applied microbiology and biotechnology 61*, 385-392.

[31] Outterson, K., Rex, J.H., Jinks, T., Jackson, P., Hallinan, J., Karp, S., Hung, D.T., Franceschi, F., Merkeley, T., Houchens, C. and Dixon, D.M.,. (2016) Accelerating global innovation to address antibacterial resistance: introducing CARB-X. , *Nature Reviews Drug Discovery, 15*, 589-590.

[32] Kümmerer, K. (2003) Significance of antibiotics in the environment, *Journal of Antimicrobial Chemotherapy 52*, 5-7.

[33] Haynes, K. M., Abdali, N., Jhawar, V., Zgurskaya, H. I., Parks, J. M., Green, A. T., Baudry, J., Rybenkov, V. V., Smith, J. C., and Walker, J. K. (2017) Identification and Structure-Activity Relationships of Novel Compounds that Potentiate the Activities of Antibiotics in Escherichia coli, *J Med Chem 60*, 6205-6219.

[34] Paterson, D. L. (2008) Impact of antibiotic resistance in gram-negative bacilli on empirical and definitive antibiotic therapy, *Clinical infectious diseases : an official publication of the Infectious Diseases Society of America 47 Suppl 1*, S14-20.

[35] Tanwar, J., Das, S., Fatima, Z., and Hameed, S. (2014) Multidrug resistance: an emerging crisis, *Interdisciplinary perspectives on infectious diseases 2014*.

[36] Prevention, C. f. D. C. a. (2013) Threat Report 2013: Antibiotic/ Antimicrobial Resistance, .

[37] Jabes, D. (2011) The antibiotic R&D pipeline: an update, *Current opinion in microbiology 14*, 564-569.

[38] Hancock, R. E. (1997) Peptide antibiotics, *The lancet 349*, 418-422.

[39] https://grandroundsinurology.com/multi-drug-resistance-bacteria-recent-trends-in-uropathogens/.

[40] Bockstael, K., and Van Aerschot, A. (2009) Antimicrobial resistance in bacteria, *Central European Journal of Medicine 4*, 141-155.

[41] Schindler, B. D., and Kaatz, G. W. (2016) Multidrug efflux pumps of Gram-positive bacteria, *Drug resistance updates : reviews and commentaries in antimicrobial and anticancer chemotherapy 27*, 1-13.

[42] Atzori, A., Malviya, V. N., Malloci, G., Dreier, J., Pos, K. M., Vargiu, A. V., and Ruggerone, P. (2019) Identification and characterization of carbapenem binding sites within the RND-transporter AcrB, *Biochimica et biophysica acta. Biomembranes 1861*, 62-74.

[43] Morris, S., and Cerceo, E. (2020) Trends, epidemiology, and management of multi-drug resistant gram-negative bacterial infections in the hospitalized setting, *Antibiotics 9*, 196.

[44] Du, D., Wang-Kan, X., Neuberger, A., van Veen, H.W., Pos, K.M., Piddock, L.J. and Luisi, B.F. (2018) Multidrug efflux pumps: structure, function and regulation. , *Nature Reviews Microbiology 16*, 523-539.

[45] Yen, M. R., Chen, J. S., Marquez, J. L., Sun, E. I., and Saier, M. H. (2010) Multidrug resistance: phylogenetic characterization of superfamilies of secondary carriers that include drug exporters, In *Membrane Transporters in Drug Discovery and Development*, pp 47-64, Springer.

[46] Zwama, M., and, and Yamaguchi, A. (2018) Molecular mechanisms of AcrB-mediated multidrug export,, *Res Microbiol 169*, 372-383.

[47] Poole, K. (2004) Efflux-mediated multiresistance in Gram-negative bacteria, *Clinical Microbiology and infection 10*, 12-26.

[48] Fitzpatrick, A. W., Llabrés, S., Neuberger, A., Blaza, J. N., Bai, X.-c., Okada, U., Murakami, S., Van Veen, H. W., Zachariae, U., and Scheres, S. H. (2017) Structure of the MacAB–TolC ABC-type tripartite multidrug efflux pump, *Nature microbiology 2*, 1-8.

[49] Kim, J.-S., Jeong, H., Song, S., Kim, H.-Y., Lee, K., Hyun, J., and Ha, N.-C. (2015) Structure of the tripartite multidrug efflux pump AcrAB-TolC suggests an alternative assembly mode, *Molecules and cells 38*, 180.

[50] Nikaido, H., and Zgurskaya, H. I. (2001) AcrAB and related multidrug efflux pumps of Escherichia coli, *Journal of molecular microbiology and biotechnology 3*, 215-218.

[51] Du, D., van Veen, H. W., Murakami, S., Pos, K. M., and Luisi, B. F. (2015) Structure, mechanism and cooperation of bacterial multidrug transporters, *Current opinion in structural biology 33*, 76-91.

[52] Nishino, K., Nikaido, E., and Yamaguchi, A. (2009) Regulation and physiological function of multidrug efflux pumps in Escherichia coli and Salmonella, *Biochimica et Biophysica Acta (BBA)-Proteins and Proteomics 1794*, 834-843.

[53] Murakami, S., Nakashima, R., Yamashita, E., Matsumoto, T., and Yamaguchi, A. (2006) Crystal structures of a multidrug transporter reveal a functionally rotating mechanism, *Nature 443*, 173-179.

[54] Seeger, M. A., Diederichs, K., Eicher, T., Brandstatter, L., Schiefner, A., Verrey, F., and Pos, K. M. (2008) The AcrB efflux pump: conformational cycling and peristalsis lead to multidrug resistance, *Current drug targets 9*, 729-749.

[55] Seeger, M. A., Schiefner, A., Eicher, T., Verrey, F., Diederichs, K., and Pos, K. M. (2006) Structural asymmetry of AcrB trimer suggests a peristaltic pump mechanism, *Science 313*, 1295-1298.

[56] Higgins, C. F. (2007) Multiple molecular mechanisms for multidrug resistance transporters, *Nature 446*, 749-757.

[57] Yamaguchi, A., Nakashima, R., and Sakurai, K. (2015) Structural basis of RND-type multidrug exporters, *Frontiers in microbiology 6*, 327.

[58] Zgurskaya, H. I., Weeks, J. W., Ntreh, A. T., Nickels, L. M., and Wolloscheck, D. (2015) Mechanism of coupling drug transport reactions located in two different membranes, *Frontiers in microbiology 6*, 100-100.

[59] Zgurskaya, H. I., and Nikaido, H. (1999) AcrA is a highly asymmetric protein capable of spanning the periplasm, *Journal of molecular biology 285*, 409-420.

[60] Yen, M. R., Peabody, C. R., Partovi, S. M., Zhai, Y., Tseng, Y. H., and Saier, M. H. (2002) Protein-translocating outer membrane porins of Gram-negative bacteria, *Biochimica et biophysica acta 1562*, 6-31.

[61] Lobedanz, S., Bokma, E., Symmons, M. F., Koronakis, E., Hughes, C., and Koronakis, V. (2007) A periplasmic coiled-coil interface underlying TolC recruitment and the assembly of bacterial drug efflux pumps, *Proceedings of the National Academy of Sciences of the United States of America 104*, 4612-4617.

[62] Mikolosko, J., Bobyk, K., Zgurskaya, H. I., and Ghosh, P. (2006) Conformational flexibility in the multidrug efflux system protein AcrA, *Structure (London, England : 1993) 14*, 577-587.

[63] Murakami, S., Nakashima, R., Yamashita, E., and Yamaguchi, A. (2002) Crystal structure of bacterial multidrug efflux transporter AcrB, *Nature 419*, 587-593.

[64] Koronakis, V., Sharff, A., Koronakis, E., Luisi, B., and Hughes, C. (2000) Crystal structure of the bacterial membrane protein TolC central to multidrug efflux and protein export, *Nature 405*, 914-919.

[65] Wang, Z., Fan, G., Hryc, C. F., Blaza, J. N., Serysheva, II, Schmid, M. F., Chiu, W., Luisi, B. F., and Du, D. (2017) An allosteric transport mechanism for the AcrAB-TolC multidrug efflux pump, *Elife 6*.

[66] Janganan, T. K., Bavro, V. N., Zhang, L., Matak-Vinkovic, D., Barrera, N. P., Venien-Bryan, C., Robinson, C. V., Borges-Walmsley, M. I., and Walmsley, A. R. (2011) Evidence for the assembly of a bacterial tripartite multidrug pump with a stoichiometry of 3:6:3, *The Journal of biological chemistry 286*, 26900-26912.

[67] Stegmeier, J. F., Polleichtner, G., Brandes, N., Hotz, C., and Andersen, C. (2006) Importance of the adaptor (membrane fusion) protein hairpin domain for the functionality of multidrug efflux pumps, *Biochemistry 45*, 10303-10312.

[68] Yum, S., Xu, Y., Piao, S., Sim, S. H., Kim, H. M., Jo, W. S., Kim, K. J., Kweon, H. S., Jeong, M. H., Jeon, H., Lee, K., and Ha, N. C. (2009) Crystal structure of the

periplasmic component of a tripartite macrolide-specific efflux pump, *Journal of molecular biology 387*, 1286-1297.

[69] Nikaido, H. (2011) Structure and mechanism of RND-type multidrug efflux pumps, *Advances in enzymology and related areas of molecular biology 77*, 1-60.

[70] Du, D., Wang, Z., James, N. R., Voss, J. E., Klimont, E., Ohene-Agyei, T., Venter, H., Chiu, W., and Luisi, B. F. (2014) Structure of the AcrAB-TolC multidrug efflux pump, *Nature 509*, 512-515.

[71] Symmons, M. F., Bokma, E., Koronakis, E., Hughes, C., and Koronakis, V. (2009) The assembled structure of a complete tripartite bacterial multidrug efflux pump, *Proceedings of the National Academy of Sciences 106*, 7173-7178.

[72] Marshall, R. L., and Bavro, V. N. (2020) Mutations in the TolC periplasmic domain affect substrate specificity of the AcrAB-TolC pump, *Frontiers in molecular biosciences 7*, 166.

[73] Koronakis, V., Eswaran, J., and Hughes, C. (2004) Structure and function of TolC: the bacterial exit duct for proteins and drugs, *Annual review of biochemistry 73*, 467-489.

[74] Kobylka, J., Kuth, M. S., Muller, R. T., Geertsma, E. R., and Pos, K. M. (2020) AcrB: a mean, keen, drug efflux machine, *Ann N Y Acad Sci 1459*, 38-68.

[75] Misra, R., and Bavro, V. N. (2009) Assembly and transport mechanism of tripartite drug efflux systems, *Biochimica et Biophysica Acta (BBA)-Proteins and Proteomics 1794*, 817-825.

[76] Husain, F., Humbard, M., and Misra, R. (2004) Interaction between the TolC and AcrA proteins of a multidrug efflux system of Escherichia coli, *Journal of bacteriology 186*, 8533-8536.

[77] Tikhonova, E. B., and Zgurskaya, H. I. (2004) AcrA, AcrB, and TolC of Escherichia coli Form a Stable Intermembrane Multidrug Efflux Complex, *The Journal of biological chemistry 279*, 32116-32124.

[78] Lomovskaya, O., Warren, M. S., Lee, A., Galazzo, J., Fronko, R., Lee, M., Blais, J., Cho, D., Chamberland, S., Renau, T., Leger, R., Hecker, S., Watkins, W., Hoshino, K., Ishida, H., and Lee, V. J. (2001) Identification and characterization of inhibitors of multidrug resistance efflux pumps in Pseudomonas aeruginosa: novel agents for combination therapy, *Antimicrobial agents and chemotherapy 45*, 105-116.

[79] Nakamura, H. (1965) Gene-Controlled Resistance to Acriflavine and Other Basic Dyes in Escherichia coli, *Journal of bacteriology 90*, 8-14.

[80] Nakamura, H. (1968) Genetic determination of resistance to acriflavine, phenethyl alcohol, and sodium dodecyl sulfate in Escherichia coli, *Journal of bacteriology 96*, 987-996.

[81] Das, D., Xu, Q. S., Lee, J. Y., Ankoudinova, I., Huang, C., Lou, Y., DeGiovanni, A., Kim, R., and Kim, S.-H. (2007) Crystal structure of the multidrug efflux transporter AcrB at 3.1 Å resolution reveals the N-terminal region with conserved amino acids, *Journal of structural biology 158*, 494-502.

[82] Murakami, S. (2008) Multidrug efflux transporter, AcrB—the pumping mechanism, *Current opinion in structural biology 18*, 459-465.

[83] Pos, K. M., Schiefner, A., Seeger, M. A., and Diederichs, K. (2004) Crystallographic analysis of AcrB, *FEBS letters 564*, 333-339.

[84] Sennhauser, G., Amstutz, P., Briand, C., Storchenegger, O., and Grutter, M. G. (2007) Drug export pathway of multidrug exporter AcrB revealed by DARPin inhibitors, *PLoS Biol 5*, e7.

[85] Tornroth-Horsefield, S., Gourdon, P., Horsefield, R., Brive, L., Yamamoto, N., Mori, H., Snijder, A., and Neutze, R. (2007) Crystal structure of AcrB in complex with a single transmembrane subunit reveals another twist, *Structure (London, England : 1993) 15*, 1663-1673.

[86] Edward, W. Y., Aires, J. R., McDermott, G., and Nikaido, H. (2005) A periplasmic drug-binding site of the AcrB multidrug efflux pump: a crystallographic and site-directed mutagenesis study, *Journal of bacteriology 187*, 6804-6815.

[87] Eicher, T., Seeger, M. A., Anselmi, C., Zhou, W., Brandstätter, L., Verrey, F., Diederichs, K., Faraldo-Gómez, J. D., and Pos, K. M. (2014) Coupling of remote alternating-access transport mechanisms for protons and substrates in the multidrug efflux pump AcrB, *Elife 3*, e03145.

[88] Zhang, X. C., Liu, M., and Han, L. (2017) Energy coupling mechanisms of AcrB-like RND transporters, *Biophys Rep 3*, 73-84.

[89] Ruggerone, P., Murakami, S., Pos, K. M., and Vargiu, A. V. (2013) RND efflux pumps: structural information translated into function and inhibition mechanisms, *Curr Top Med Chem 13*, 3079-3100.

[90] Müller, R. T., Travers, T., Cha, H.-j., Phillips, J. L., Gnanakaran, S., and Pos, K. M. (2017) Switch loop flexibility affects substrate transport of the AcrB efflux pump, *Journal of molecular biology 429*, 3863-3874.

[91] Nakashima, R., Sakurai, K., Yamasaki, S., Nishino, K., and Yamaguchi, A. (2011) Structures of the multidrug exporter AcrB reveal a proximal multisite drug-binding pocket, *Nature 480*, 565-569.

[92] Takatsuka, Y., Chen, C., and Nikaido, H. (2010) Mechanism of recognition of compounds of diverse structures by the multidrug efflux pump AcrB of Escherichia coli, *Proceedings of the National Academy of Sciences 107*, 6559-6565.

[93] Kobayashi, N., Tamura, N., van Veen, H. W., Yamaguchi, A., and Murakami, S. (2014) β-Lactam selectivity of multidrug transporters AcrB and AcrD resides in the proximal binding pocket, *Journal of Biological Chemistry 289*, 10680-10690.

[94] Zwama, M., Yamasaki, S., Nakashima, R., Sakurai, K., Nishino, K., and Yamaguchi, A. (2018) Multiple entry pathways within the efflux transporter AcrB contribute to multidrug recognition, *Nat Commun 9*, 124.

[95] Oswald, C., Tam, H.-K., and Pos, K. M. (2016) Transport of lipophilic carboxylates is mediated by transmembrane helix 2 in multidrug transporter AcrB, *Nature communications 7*, 1-10.

[96] Schulz, R., Vargiu, A. V., Collu, F., Kleinekathöfer, U., and Ruggerone, P. (2010) Functional rotation of the transporter AcrB: insights into drug extrusion from simulations, *PLoS computational biology 6*.

[97] Takatsuka, Y., and Nikaido, H. (2007) Site-directed disulfide cross-linking shows that cleft flexibility in the periplasmic domain is needed for the multidrug efflux pump AcrB of Escherichia coli, *Journal of bacteriology 189*, 8677-8684.

[98] Takatsuka, Y., and Nikaido, H. (2009) Covalently linked trimer of the AcrB multidrug efflux pump provides support for the functional rotating mechanism, *Journal of bacteriology 191*, 1729-1737.

[99] Vargiu, A. V., Ramaswamy, V. K., Malvacio, I., Malloci, G., Kleinekathöfer, U., and Ruggerone, P. (2018) Water-mediated interactions enable smooth substrate transport in a bacterial efflux pump, *Biochimica et Biophysica Acta (BBA)-General Subjects 1862*, 836-845.

[100] Bohnert, J. A., Schuster, S., Seeger, M. A., Fähnrich, E., Pos, K. M., and Kern, W. V. (2008) Site-directed mutagenesis reveals putative substrate binding residues in the Escherichia coli RND efflux pump AcrB, *Journal of bacteriology 190*, 8225-8229.

[101] Fischer, N., Raunest, M., Schmidt, T. H., Koch, D. C., and Kandt, C. (2014) Efflux pump-mediated antibiotics resistance: insights from computational structural biology, *Interdisciplinary Sciences: Computational Life Sciences 6*, 1-12.

[102] Flynn, G. C., Pohl, J., Flocco, M. T., and Rothman, J. E. (1991) Peptide-binding specificity of the molecular chaperone BiP, *Nature 353*, 726-730.

[103] Rodriguez Aliaga, P. (2016) A Finely Tuned Molecular Motor: Mechanochemistry and Power Efficiency in the AAA+ Protease Machine ClpXP, UC Berkeley.

[104] Baker, T. A., and Sauer, R. T. (2012) ClpXP, an ATP-powered unfolding and protein-degradation machine, *Biochimica et Biophysica Acta (BBA)-Molecular Cell Research 1823*, 15-28.

[105] Sauer, R. T., Bolon, D. N., Burton, B. M., Burton, R. E., Flynn, J. M., Grant, R. A., Hersch, G. L., Joshi, S. A., Kenniston, J. A., and Levchenko, I. (2004) Sculpting the proteome with AAA+ proteases and disassembly machines, *Cell 119*, 9-18.

[106] Glynn, S. E., Martin, A., Nager, A. R., Baker, T. A., and Sauer, R. T. (2009) Structures of asymmetric ClpX hexamers reveal nucleotide-dependent motions in a AAA+ protein-unfolding machine, *Cell 139*, 744-756.

[107] Flynn, J. M., Neher, S. B., Kim, Y.-I., Sauer, R. T., and Baker, T. A. (2003) Proteomic discovery of cellular substrates of the ClpXP protease reveals five classes of ClpX-recognition signals, *Molecular cell 11*, 671-683.

[108] Sekar, K., Gentile, A. M., Bostick, J. W., and Tyo, K. E. (2016) N-terminal-based targeted, inducible protein degradation in Escherichia coli, *PloS one 11*, e0149746.

[109] Fritze, J., Zhang, M., Luo, Q., and Lu, X. (2020) An overview of the bacterial SsrA system modulating intracellular protein levels and activities, *Applied microbiology and biotechnology 104*, 5229-5241.

[110] Levchenko, I., Grant, R. A., Wah, D. A., Sauer, R. T., and Baker, T. A. (2003) Structure of a delivery protein for an AAA+ protease in complex with a peptide degradation tag, *Molecular cell 12*, 365-372.

[111] McGinness, K. E., Baker, T. A., and Sauer, R. T. (2006) Engineering controllable protein degradation, *Molecular cell 22*, 701-707.

[112] Horwich, A. L., Weber-Ban, E. U., and Finley, D. (1999) Chaperone rings in protein folding and degradation, *Proceedings of the National Academy of Sciences 96*, 11033-11040.

[113] Chai, Q., Wang, Z., Webb, S. R., Dutch, R. E., and Wei, Y. (2016) The ssrA-tag facilitated degradation of an integral membrane protein, *Biochemistry 55*, 2301-2304.

[114] Venter, H., Mowla, R., Ohene-Agyei, T., and Ma, S. (2015) RND-type drug efflux pumps from Gram-negative bacteria: molecular mechanism and inhibition, *Frontiers in microbiology 6*, 377.

[115] Brookfield, J. F. (2005) The ecology of the genome—mobile DNA elements and their hosts, *Nature Reviews Genetics 6*, 128-136.

[116] Muñoz-López, M., and García-Pérez, J. L. (2010) DNA transposons: nature and applications in genomics, *Current genomics 11*, 115-128.

[117] De la Cruz, F., and Davies, J. (2000) Horizontal gene transfer and the origin of species: lessons from bacteria, *Trends in microbiology 8*, 128-133.

[118] Feschotte, C., and Pritham, E. J. (2007) DNA transposons and the evolution of eukaryotic genomes, *Annu. Rev. Genet. 41*, 331-368.

[119] Devine, S. E., and Boeke, J. D. (1994) Efficient integration of artificial transposons into plasmid targets in vitro: a useful tool for DNA mapping, sequencing and genetic analysis, *Nucleic Acids Research 22*, 3765-3772.

[120] Hyde, F. EZ-Tn5™ Transposon Tools: How Can Transposons Accelerate Your Genomics Research?

[121] De Lorenzo, V., and Timmis, K. N. (1994) [31] Analysis and construction of stable phenotypes in Gram-negative bacteria with Tn5-and Tn10-derived minitransposons, *Methods in enzymology 235*, 386-405.

[122] Warnke-Sommer, J., and Ali, H. (2016) Graph mining for next generation sequencing: leveraging the assembly graph for biological insights, *BMC genomics 17*, 1-20.

[123] Tait, R. C., Close, T. J., Lundquist, R. C., Hagiya, M., Rodriguez, R. L., and Kado, C. I. (1983) Construction and Characterization of a Versatile Broad Host Range DNA Cloning System for Gram–Negative Bacteria, *Bio/Technology 1*, 269-275.

[124] Goryshin, I. Y., Jendrisak, J., Hoffman, L. M., Meis, R., and Reznikoff, W. S. (2000) Insertional transposon mutagenesis by electroporation of released Tn5 transposition complexes, *Nature biotechnology 18*, 97-100.

[125] Gallagher, L. A., Ramage, E., Jacobs, M. A., Kaul, R., Brittnacher, M., and Manoil, C. (2007) A comprehensive transposon mutant library of Francisella novicida, a bioweapon surrogate, *Proceedings of the National Academy of Sciences 104*, 1009-1014.

[126] Fitzgerald, G. F., and Gasson, M. J. (1988) In vivo gene transfer systems and transposons, *Biochimie 70*, 489-502.

[127] Kirby, J. R. (2007) In Vivo Mutagenesis Using EZ-Tn5™, *Methods in enzymology 421*, 17-21.

[128] Vidal, J. E., Chen, J., Li, J., and McClane, B. (2009) Use of an EZ-Tn5-based random mutagenesis system to identify a novel toxin regulatory Locus in Clostridium perfringens, *Strain 13*.

[129] Goryshin, I. Y., and Reznikoff, W. S. (1998) Tn5 in vitro transposition, *Journal of Biological Chemistry 273*, 7367-7374.

[130] Kazazian, H. H. (2004) Mobile elements: drivers of genome evolution, *science 303*, 1626-1632.

[131] Rajapaksha, P., Pandeya, A., and Wei, Y. (2020) Probing the Dynamics of AcrB Through Disulfide Bond Formation, *ACS omega 5*, 21844-21852.

[132] Nikaido, H. (1998) Multiple antibiotic resistance and efflux, *Current opinion in microbiology 1*, 516-523.

[133] Zgurskaya, H. I., and Nikaido, H. (2000) Multidrug resistance mechanisms: drug efflux across two membranes, *Molecular microbiology 37*, 219-225.

[134] Sulavik, M. C., Houseweart, C., Cramer, C., Jiwani, N., Murgolo, N., Greene, J., DiDomenico, B., Shaw, K. J., Miller, G. H., and Hare, R. (2001) Antibiotic susceptibility profiles ofEscherichia coli strains lacking multidrug efflux pump genes, *Antimicrobial agents and chemotherapy 45*, 1126-1136.

[135] Eswaran, J., Koronakis, E., Higgins, M. K., Hughes, C., and Koronakis, V. (2004) Three's company: component structures bring a closer view of tripartite drug efflux pumps, *Current opinion in structural biology 14*, 741-747.

[136] Nikaido, H. (1996) Multidrug efflux pumps of gram-negative bacteria, *Journal of bacteriology 178*, 5853.

[137] Daury, L., Orange, F., Taveau, J.-C., Verchère, A., Monlezun, L., Gounou, C., Marreddy, R. K., Picard, M., Broutin, I., and Pos, K. M. (2016) Tripartite assembly of RND multidrug efflux pumps, *Nature communications 7*, 1-8.

[138] Shi, X., Chen, M., Yu, Z., Bell, J. M., Wang, H., Forrester, I., Villarreal, H., Jakana, J., Du, D., and Luisi, B. F. (2019) In situ structure and assembly of the multidrug efflux pump AcrAB-TolC, *Nature communications 10*, 1-6.

[139] Li, X.-Z., Plésiat, P., and Nikaido, H. (2015) The challenge of efflux-mediated antibiotic resistance in Gram-negative bacteria, *Clinical microbiology reviews 28*, 337-418.

[140] Takatsuka, Y., and Nikaido, H. (2010) Site-directed disulfide cross-linking to probe conformational changes of a transporter during its functional cycle: Escherichia coli AcrB multidrug exporter as an example, In *In Vitro Mutagenesis Protocols*, pp 343-354, Springer.

[141] Lu, W., Zhong, M. a., and Wei, Y. (2011) A reporter platform for the monitoring of in vivo conformational changes in AcrB, *Protein and peptide letters 18*, 863-871.

[142] Lu, W., Zhong, M., Chai, Q., Wang, Z., Yu, L., and Wei, Y. (2014) Functional relevance of AcrB trimerization in pump assembly and substrate binding, *PLoS One 9*.

[143] Wang, Z., Ye, C., Zhang, X., and Wei, Y. (2015) Cysteine residue is not essential for CPM protein thermal-stability assay, *Analytical and bioanalytical chemistry 407*, 3683-3691.

[144] Humphries, R. M., Ambler, J., Mitchell, S. L., Castanheira, M., Dingle, T., Hindler, J. A., Koeth, L., and Sei, K. (2018) CLSI methods development and standardization working group best practices for evaluation of antimicrobial susceptibility tests, *Journal of clinical microbiology 56*.

[145] Lu, W., Zhong, M., and Wei, Y. (2011) Folding of AcrB subunit precedes trimerization, *Journal of molecular biology 411*, 264-274.

[146] Paixão, L., Rodrigues, L., Couto, I., Martins, M., Fernandes, P., De Carvalho, C. C., Monteiro, G. A., Sansonetty, F., Amaral, L., and Viveiros, M. (2009) Fluorometric determination of ethidium bromide efflux kinetics in Escherichia coli, *Journal of Biological Engineering 3*, 18.

[147] Craig, D. B., and Dombkowski, A. A. (2013) Disulfide by Design 2.0: a web-based tool for disulfide engineering in proteins, *BMC bioinformatics 14*, 346.

[148] Murakami, S., Tamura, N., Saito, A., Hirata, T., and Yamaguchi, A. (2004) Extramembrane central pore of multidrug exporter AcrB in Escherichia coli plays an important role in drug transport, *Journal of Biological Chemistry 279*, 3743-3748.

[149] Yu, L., Lu, W., and Wei, Y. (2011) AcrB trimer stability and efflux activity, insight from mutagenesis studies, *PLoS One 6*.

[150] Schindelin, J., Arganda-Carreras, I., Frise, E., Kaynig, V., Longair, M., Pietzsch, T., Preibisch, S., Rueden, C., Saalfeld, S., Schmid, B., Tinevez, J.-Y., White, D. J., Hartenstein, V., Eliceiri, K., Tomancak, P., and Cardona, A. (2012) Fiji: an open-source platform for biological-image analysis, *Nature Methods 9*, 676-682.

[151] Seeger, M. A., Von Ballmoos, C., Eicher, T., Brandstätter, L., Verrey, F., Diederichs, K., and Pos, K. M. (2008) Engineered disulfide bonds support the functional rotation mechanism of multidrug efflux pump AcrB, *Nature structural & molecular biology 15*, 199.

[152] Parmar, M., Rawson, S., Scarff, C. A., Goldman, A., Dafforn, T. R., Muench, S. P., and Postis, V. L. (2018) Using a SMALP platform to determine a sub-nm single particle cryo-EM membrane protein structure, *Biochimica et Biophysica Acta (BBA)-Biomembranes 1860*, 378-383.

[153] Rajapaksha, P., Ojo, I., Yang, L., Pandeya, A., Abeywansha, T., and Wei, Y. (2021) Insight into the AcrAB-TolC Complex Assembly Process Learned from Competition Studies, *Antibiotics 10*, 830.

[154] Krishnamoorthy, G., Tikhonova, E. B., Dhamdhere, G., and Zgurskaya, H. I. (2013) On the role of TolC in multidrug efflux: the function and assembly of AcrAB-TolC tolerate significant depletion of intracellular TolC protein, *Mol Microbiol 87*, 982-997.

[155] Lu, W., Chai, Q., Zhong, M., Yu, L., Fang, J., Wang, T., Li, H., Zhu, H., and Wei, Y. (2012) Assembling of AcrB trimer in cell membrane, *Journal of molecular biology 423*, 123-134.

[156] Li, C., Wen, A., Shen, B., Lu, J., Huang, Y., and Chang, Y. (2011) FastCloning: a highly simplified, purification-free, sequence-and ligation-independent PCR cloning method, *BMC biotechnology 11*, 1-10.

[157] Eicher, T., Cha, H.-j., Seeger, M. A., Brandstätter, L., El-Delik, J., Bohnert, J. A., Kern, W. V., Verrey, F., Grütter, M. G., and Diederichs, K. (2012) Transport of drugs by the multidrug transporter AcrB involves an access and a deep binding pocket that are separated by a switch-loop, *Proceedings of the National Academy of Sciences 109*, 5687-5692.

[158] Su, C.-C., Li, M., Gu, R., Takatsuka, Y., McDermott, G., Nikaido, H., and Edward, W. Y. (2006) Conformation of the AcrB multidrug efflux pump in mutants of the putative proton relay pathway, *Journal of bacteriology 188*, 7290-7296.

[159] Murakami, S., and Yamaguchi, A. (2003) Multidrug-exporting secondary transporters, *Current opinion in structural biology 13*, 443-452.

[160] Guan, L., and Nakae, T. (2001) Identification of Essential Charged Residues in Transmembrane Segments of the Multidrug Transporter MexB ofPseudomonas aeruginosa, *Journal of bacteriology 183*, 1734-1739.

[161] Liu, M., and Zhang, X. C. (2017) Energy-coupling mechanism of the multidrug resistance transporter AcrB: Evidence for membrane potential-driving hypothesis through mutagenic analysis, *Protein & cell 8*, 623-627.

[162] Matsunaga, Y., Yamane, T., Terada, T., Moritsugu, K., Fujisaki, H., Murakami, S., Ikeguchi, M., and Kidera, A. (2018) Energetics and conformational pathways of functional rotation in the multidrug transporter AcrB, *Elife 7*, e31715.

[163] Kinana, A. D., Vargiu, A. V., and Nikaido, H. (2016) Effect of site-directed mutations in multidrug efflux pump AcrB examined by quantitative efflux assays, *Biochemical and biophysical research communications 480*, 552-557.

[164] Torres, V. J., McClain, M. S., and Cover, T. L. (2006) Mapping of a domain required for protein-protein interactions and inhibitory activity of a Helicobacter pylori dominant-negative VacA mutant protein, *Infection and immunity 74*, 2093-2101.

[165] Valente, L., and Nishikura, K. (2007) RNA binding-independent dimerization of adenosine deaminases acting on RNA and dominant negative effects of nonfunctional subunits on dimer functions, *Journal of Biological Chemistry 282*, 16054-16061.

[166] Chevrier, L., De Brevern, A., Hernandez, E., Leprince, J., Vaudry, H., Guedj, A. M., and De Roux, N. (2013) PRR repeats in the intracellular domain of KISS1R are important for its export to cell membrane, *Molecular Endocrinology 27*, 1004-1014.

[167] Mantovani, R., Li, X.-Y., Pessara, U., Van Huisjduijnen, R. H., Benoist, C., and Mathis, D. (1994) Dominant negative analogs of NF-YA, *Journal of Biological Chemistry 269*, 20340-20346.

[168] Zgurskaya, H. I., and Nikaido, H. (2000) Cross-linked complex between oligomeric periplasmic lipoprotein AcrA and the inner-membrane-associated multidrug efflux pump AcrB from Escherichia coli, *Journal of bacteriology 182*, 4264-4267.

[169] Hazel, A. J., Abdali, N., Leus, I. V., Parks, J. M., Smith, J. C., Zgurskaya, H. I., and Gumbart, J. C. (2019) Conformational dynamics of AcrA govern multidrug efflux pump assembly, *ACS infectious diseases 5*, 1926-1935.

[170] Svensson, L., Poljakovic, M., Säve, S., Gilberthorpe, N., Schön, T., Strid, S., Corker, H., Poole, R. K., and Persson, K. (2010) Role of flavohemoglobin in combating nitrosative stress in uropathogenic Escherichia coli–implications for urinary tract infection, *Microbial pathogenesis 49*, 59-66.

[171] Andersen, J. L., He, G.-X., Kakarla, P., KC, R., Kumar, S., Lakra, W. S., Mukherjee, M. M., Ranaweera, I., Shrestha, U., and Tran, T. (2015) Multidrug efflux pumps from Enterobacteriaceae, Vibrio cholerae and Staphylococcus aureus bacterial food pathogens, *International journal of environmental research and public health 12*, 1487-1547.

[172] Edward, W. Y., Aires, J. R., and Nikaido, H. (2003) AcrB multidrug efflux pump of Escherichia coli: composite substrate-binding cavity of exceptional flexibility generates its extremely wide substrate specificity, *Journal of bacteriology 185*, 5657-5664.

[173] Maurizi, M., Clark, W. P., Kim, S.-H., and Gottesman, S. (1990) Clp P represents a unique family of serine proteases, *Journal of Biological Chemistry 265*, 12546-12552.

[174] Roche, E. D., and Sauer, R. T. (1999) SsrA-mediated peptide tagging caused by rare codons and tRNA scarcity, *The EMBO Journal 18*, 4579-4589.

[175] Farrell, C. M., Grossman, A. D., and Sauer, R. T. (2005) Cytoplasmic degradation of ssrA-tagged proteins, *Molecular microbiology 57*, 1750-1761.

[176] Husain, F., and Nikaido, H. (2010) Substrate path in the AcrB multidrug efflux pump of Escherichia coli, *Molecular microbiology 78*, 320-330.

[177] Hawkey, J., Hamidian, M., Wick, R. R., Edwards, D. J., Billman-Jacobe, H., Hall, R. M., and Holt, K. E. (2015) ISMapper: identifying transposase insertion sites in bacterial genomes from short read sequence data, *BMC genomics 16*, 1-11.

[178] Ducey, T. F., and Dyer, D. W. (2002) Rapid identification of EZ:: TN™ transposon insertion sites in the genome of Neisseria gonorrhoeae, In *Epicentre Forum*, pp 6-7.

[179] Singer, T., and Burke, E. (2003) High-throughput TAIL-PCR as a tool to identify DNA flanking insertions, In *Plant Functional Genomics*, pp 241-271, Springer.

VITA

Personal information

Name	Prasangi Irosha Rajapaksha
Nationality	Sri Lanka

Educational Background

2015-2016   M.S in Animal Science- Regenerative Bioscience
              University of Georgia, USA

2009-2014   B.S. in Molecular Biology and Biotechnology
              University of Peradeniya, Sri Lanka

Publications

1) **Rajapaksha, P**., Ojo, I., Yang, L., Pandeya, A., Abeywansha, T., and Wei, Y. (2021) Insight into the AcrAB-TolC Complex Assembly Process Learned from Competition Studies, *Antibiotics 10*, 830.

2) **Prasangi Rajapaksha**, Ankit Pandeya, Yinan Wei, "Probing the dynamics of AcrB through disulfide bond formation." (2020) *ACS Omega* 5 (34), 21844-21852 DOI: 10.1021/acsomega.0c02921

3) Yu-Ming Tu, Woochul Song, Tingwei Ren, Yuexiao Shen, Ratul Chowdhury**, Prasangi Rajapaksha,** Tyler E. Culp, Alina Thokkadam, Drew Carson, Yuxuan Dai, Arwa Mukthar, Miaoci Zhang, Dibakar Bhattacharya, William A. Phillip, Enrique D. Gomez1, Robert J. Hickey, Yinan Wei, and Manish Kumar. "Rapid Fabrication of Precise, High-Throughput Filters from Membrane Protein Nanosheets" (2019)- *Nature Materials* 19, no. 3 (2020): 347-354

4) Thokkadam, Alina M., **Prasangi Rajapaksha**, Yu-Ming Tu, Manish Kumar, and Yinan Wei. "Purification of an Engineered Membrane Protein FhuA for Size-Dependent Separation." *Biophysical Journal* 116, no. 3 (2019): 346a.

5) Wagh, Priyesh, Xinyi Zhang, Ryan Blood, Peter M. Kekenes-Huskey, **Prasangi Rajapaksha**, Yinan Wei, and Isabel C. Escobar. "Increasing salt rejection of polybenzimidazole nanofiltration membranes via the addition of immobilized and aligned aquaporins." *Processes* 7, no. 2 (2019): 76.

6) Wang, Zhaoshuai, Wei Lu, **Prasangi Rajapaksha**, Thomas Wilkop, Yuguang Cai, and Yinan Wei. "Comparison of in vitro and in vivo oligomeric states of a wild type and mutant trimeric inner membrane multidrug transporter." *Biochemistry and Biophysics Reports* 16 (2018): 122- 129.

7) Liu, Hong-Xiang, **Prasangi Rajapaksha**, Zhonghou Wang, Naomi E. Kramer, and Brett J. Marshall. "An Update on the Sense of Taste in Chickens: A Better Developed System than Previously Appreciated." *Journal of nutrition & food sciences* 8, no. 2 (2018).

8) **Prasangi Rajapaksha***, Zhonghou Wang, Nandakumar Venkatesan; Jason Payne; Raymond Swetenburg; Kayvan Tehrani, Fuminori Kawabata; Luke Mortensen, Shoji Tabata; Steven Stice; Robert Beckstead, Hongxiang Liu "Labeling and analysis of chicken taste buds with molecular markers in the oral epithelial sheets" *Scientific Reports* 6 (2016).

9) Nandakumar Venkatesan*, **Prasangi Rajapaksha***; Jason Payne; Forrest Goodfellow; Zhonghou Wang; Fuminori Kawabata; Shoji Tabata; Steven Stice; Robert Beckstead, Hongxiang Liu "Distribution of α-Gustducin and Vimentin in premature and mature taste buds in chickens". *Biochemical and Biophysical Research Communications.* 479, no. 2 (2016): 305-311.

10) Chamikara M, Dissanayake R, Gerath D, Karannagoda N, Amarasekara S, **Rajapaksha P**, Tennakoon A (2016) Glossary in Sinhala Language ,Molecular Biology and Biotechnoloy- Volume . Editors: Sooriyapathirana S, Chamikara M, Dissanayake R, Rajapakse S. ISBN: 978- 95541753-2-7

11) **Rajapaksha P,** Lakmali MBD, Dunuwille SWMB, Janaththani P, Rajapakse S, Wijayagunawardane M, Kodithuwakku S, Sooriyapathirana SDSS. "A DNA fingerprinting scheme to establish the identity of semen samples of cattle breeds in artificial insemination programs of Sri Lanka." *Wayamba Journal of Animal Science – ISSN: 2012-578X; P947-P954, 2014.*

12) Chamikara MDM, Ishan M, Karunadasa SS, Perera MKDI, **Rajapaksha PI**, Lelwala RV, Kasthuriarachchi VDW, Jeyakumar DT, Weebadde CK and Sooriyapathirana SDSS. "Morphological and DNA marker analysis of fruit size and shape in selected accessions and commercial cultivars of *Capsicum* spp. in Sri Lanka." *International Journal of Multidisciplinary Studies* 2(1) (2014): 29-50

Awards and Honors

1) **Max Steckler Fellowship 2018,** Outstanding oral qualifier award for the performance in oral qualification exam

2) **Fast Start Award -2017,** for the overall academic progress in first year of the degree program. Awarded by Department of Chemistry, University of Kentucky**.**

3) **University Award for Academic Excellence- 2014,** for the meritable performances in BS program- Molecular Biology and Biotechnology. Awarded at 76th General Convocation - 2014, University of Peradeniya, Sri Lanka